# Work on Grippers for Assistive Tasks

Maya N. Keely

Thesis submitted to the Faculty of the
Virginia Polytechnic Institute and State University
in partial fulfillment of the requirements for the degree of

Master of Science
in
Mechanical Engineering

Dylan P. Losey, Chair
Michael D. Bartlett
Suyi Li

3/31/25
Blacksburg, Virginia

Keywords: HRI, Assistive Robotics, Soft Grippers

# Work on Grippers for Assistive Tasks

Maya N. Keely

(ABSTRACT)

For robot arms to perform everyday tasks in unstructured environments, these robots must be able to manipulate a diverse range of objects. Today's robots often grasp objects with either soft grippers or rigid end-effectors. However, purely rigid or purely soft grippers have fundamental limitations: soft grippers struggle with irregular, heavy objects, while rigid grippers often cannot grasp small, numerous items. Combining the capabilities of rigid and soft grippers while equipped to the end effector of a robot arm could provide a larger range of capabilities for everyday tasks.

For millions of adults with mobility limitations, eating meals is a daily challenge. A variety of robotic systems have been developed to address this societal need. These robots serve as a proxy for the human's arm: the user inputs the food they want to eat, and the robot autonomously picks up that food and brings it to the user's mouth. Unfortunately, end user adoption of robot-assisted feeding is limited, in part because existing devices are unable to seamlessly grasp, manipulate, and feed diverse foods. Recent works seek to address this issue by creating new algorithms for food acquisition and bite transfer. In parallel to these algorithmic developments, however, we hypothesize that mechanical intelligence will make it fundamentally easier for robot arms to feed humans.

In this paper we therefore introduce two end effector designs. One of which is called the RISO, a mechanics and controls approach for unifying traditional RIgid end effectors with a novel class of SOft adhesives. When grasping an object, RISOs can use either the rigid end effector

(pinching the item between non-deformable fingers) and/or the soft materials (attaching and releasing items with switchable adhesives). This enhances manipulation capabilities by combining and decoupling rigid and soft mechanisms. The second end effector design we propose is the Kiri-Spoon, a soft utensil specifically designed for robot-assisted feeding. Kiri-Spoon consists of a spoon-shaped kirigami structure: when actuated, the kirigami sheet deforms into a bowl of increasing curvature. Robot arms equipped with Kiri-Spoon can leverage the kirigami structure to wrap-around morsels during acquisition, contain those items as the robot moves, and then compliantly release the food into the user's mouth. Overall, Kiri-Spoon combines the familiar and comfortable shape of a standard, rigid spoon with the increased capabilities of soft robotic grippers. In this paper, we go on to outline the process used to develop these end effector designs. In addition, we show the experimental and user study results obtained suggest these grippers could improve the current capabilities of robot arms in assisting humans and performing everyday tasks.

# Work on Grippers for Assistive Tasks

Maya N. Keely

(GENERAL AUDIENCE ABSTRACT)

A robot arm is a device that often emulates the movements of a human arm. Having multiple links and joints with a mechanism at the endpoint to assist with manipulation, similar to a hand, called an end-effector. Robot arms are good at monotonous, repetititive tasks, however, for them to perform everyday tasks in unstructured environments, robots must be able to manipulate a diverse range of objects. Today's robots often grasp objects with either soft or rigid end-effectors. However, purely rigid or purely soft grippers have fundamental limitations: soft grippers struggle with irregular, heavy objects, while rigid grippers often cannot grasp small, numerous items. Combining the capabilities of rigid and soft grippers while equipped to the end effector of a robot arm could provide a larger range of capabilities for everyday tasks.

An everyday task that, for millions of adults with mobility limitations, proves to be a daily challenge is eating meals independently. A variety of robotic systems have been developed to address this societal need. These robots serve as a proxy for the human's arm: the user inputs the food they want to eat, and the robot picks up that food and brings it to the user's mouth. Unfortunately, real-world use of robot-assisted feeding is limited, in part because existing devices are unable to seamlessly grasp, manipulate, and feed diverse foods. Recent works seek to address this issue by improving the robotic feeding process. In parallel to these software developments, however, we hypothesize that mechanical advancements will make it fundamentally easier for robot arms to feed humans.

In this paper we therefore introduce two end effector designs. One of which is called the RISO, a mechanics and controls approach for unifying traditional RIgid end effectors with a novel class of SOft adhesives. When grasping an object, RISOs can use either the rigid end effector (pinching the item between non-deformable fingers) and/or the soft materials (attaching and releasing items with switchable adhesives). This enhances manipulation capabilities by combining and decoupling rigid and soft mechanisms. The second end effector design we propose is the Kiri-Spoon, a soft utensil specifically designed for robot-assisted feeding. Kiri-Spoon consists of a spoon-shaped kirigami structure: when actuated, the kirigami sheet deforms into a bowl of increasing curvature. Robot arms equipped with Kiri-Spoon can leverage the kirigami structure to wrap-around morsels during acquisition, contain those items as the robot moves, and then compliantly release the food into the user's mouth. Overall, Kiri-Spoon combines the familiar and comfortable shape of a standard, rigid spoon with the increased capabilities of soft robotic grippers. In this paper, we go on to outline the process used to develop these end effector designs. In addition, we show the experimental and user study results obtained suggest these grippers could improve the current capabilities of robot arms in assisting humans and performing everyday tasks.

# Contents

# List of Figures

# List of Tables

# List of Abbreviations

ADL Activity of Daily Living

RISO RIgid-SOft

# Chapter 1

# Introduction

### 1.0.1 Motivation

Across food processing, parts manufacturing, and assistive caregiving, there is a need for robot arms that can grasp and manipulate a diverse range of everyday objects [6, 76, 81, 107]. Industry-standard arms often use *rigid* grippers that pinch items between two or more non-deformable fingers [3, 14, 71, 74, 103]. However, these rigid grippers are not able to pick up and hold objects that are small, numerous, or irregularly shaped (e.g., a pile of candy). To address these shortcomings, recent works have developed a variety of *soft* grippers using mechanisms such as gecko-inspired adhesives [32, 37, 75, 84, 94], granular jamming [15, 104], electroadhesion [4, 17, 80], or responsive materials [8, 20, 39, 83, 85, 91, 100]. But soft grippers have a separate grasping domain, and are often unable to hold the large, heavy items that rigid end-effectors are able to pick up and carry (e.g., a bottle of syrup). When a robot arm leverages grippers that are either purely rigid or purely soft, it fundamentally limits the types of objects that robot can manipulate. We therefore seek to expand the range of graspable objects by combining rigid and compliant components within the robot's gripper. Recent works have started to develop grippers that integrate both elements [19, 29, 35, 38, 50, 53, 62, 67, 69]. However, within existing designs the rigid and soft capabilities are inherently *coupled*; e.g., robotic fingers that alternate between rigid links and soft joints. By contrast, our core insight is that we can *decouple* and *couple* the rigid and soft mechanisms by combining

traditional rigid end-effectors with soft adhesive sheets. This decoupling has the potential to fundamentally increase the range of robotic grasps: from purely rigid (e.g., manipulating a bottle of syrup) to purely soft (e.g., picking up a pile of candy) to a combination of rigid and soft (e.g., holding beads of multiple sizes).

Developing the RISO was my introduction into the possibilities of robotic manipulation when addressing the gaps in current end effector capabilities. Specifically, in assistive caregiving, many people rely on others for most activities they perform in daily life and current assistive devices that are supposed to provide independence, don't work as reliably as a caretaker. One specific Activity of Daily Living (ADL) proves to be specifically difficult to create a reliable robotic adaptation for: eating. Food is central to the human experience. Beyond its role in survival, health, and wellness, the ability to feed oneself fosters socialization, expresses identities, and marks significant moments [59]. Unfortunately, there are almost 2 million American adults living with disabilities who rely on a caregiver's assistance everyday in order to eat [92]. This reliance can lead to feelings of dependence among care recipients [40, 82], while also placing a significant workload on caregivers [26, 106]. Assistive robots have the potential to help these users. For example, wheelchair-mounted robot arms [6, 51] and table-mounted feeding devices [60, 63] could enable operators to control their own meals and achieve modified independence. Our work envisions robotic systems capable of picking up a bite of the user's desired food and safely transferring it to their mouth. To reach this future, existing work in robot-assisted feeding has focused on the algorithms the robot uses. This includes learning and vision strategies for how the robot detects and skewers foods [33, 55, 90], as well as control and motion planning for how the robot transfers that food item into the human's mouth [44, 64, 79]. All of these algorithmic features are necessary for a successful feeding system. But the *mechanical utensil* that the robot arm applies to pick up, carry, and deliver foods is also critical. At first glance, it might seem obvious

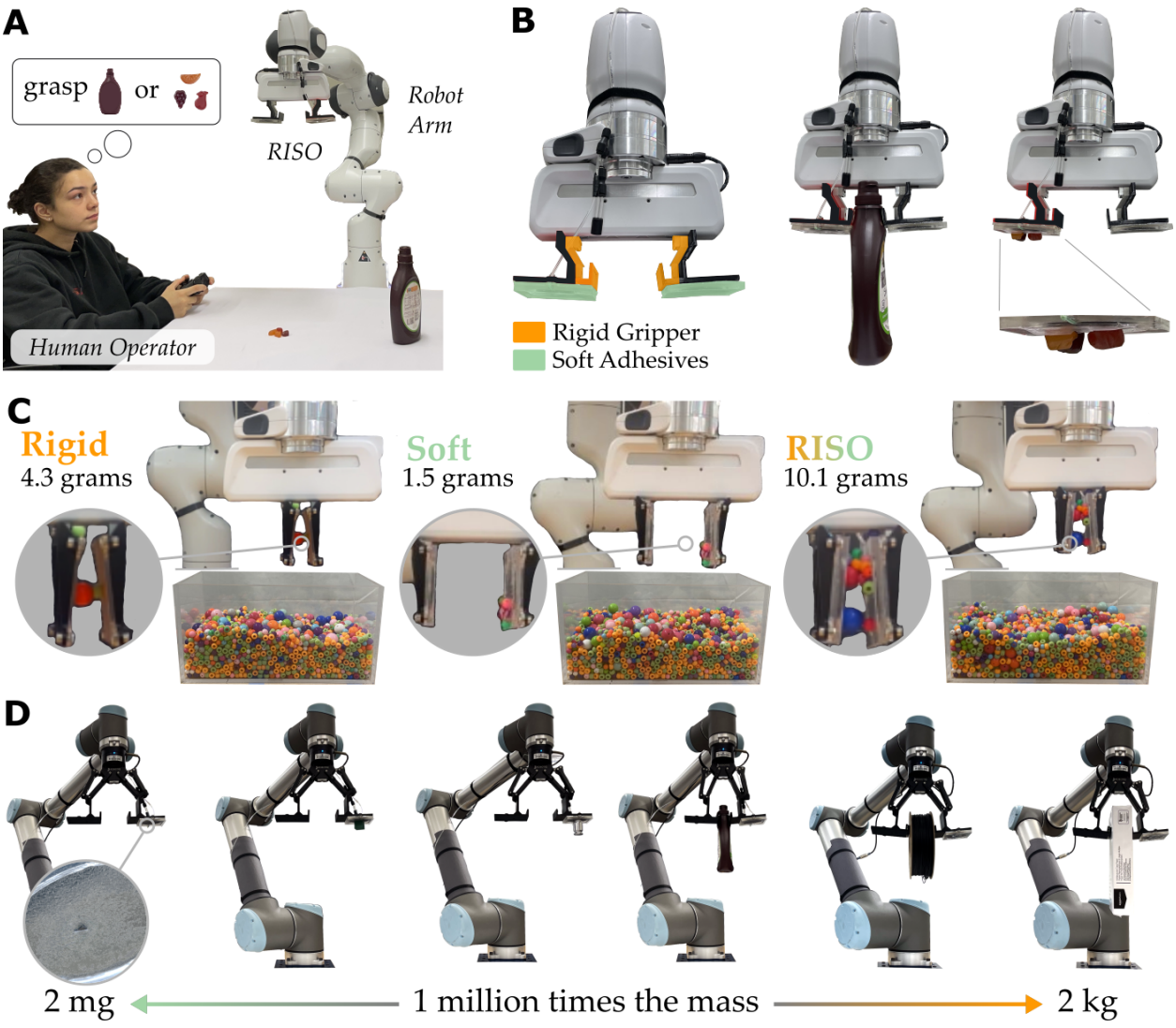


Figure 1.1: **RISO enhances grasping by combining and decoupling rigid and soft mechanisms.** (**A**) Human operators and robot arms can leverage RISOs to pick up, hold, and release objects. (**B**) RISOs are formed by mounting soft adhesive sheets to the surfaces of traditional rigid end-effectors. (**C**) When grasping an item RISO can use a fully rigid grasp (pinching the object between non-deformable fingers) a fully soft grasp (causing the object to adhere to its surface), or a combined rigid and soft grasp. (**D**) With this spectrum of grasps, RISO is able to pick up objects ranging from 2 mg items to 2.9 kg, a 1.5 million times change in mass.


Figure 1.2: Kiri-Spoon is a spoon-shaped kirigami utensil specifically designed for robot-assisted feeding. (Left) Robot arms equipped with Kiri-Spoon can robustly acquire foods from the plate, safely carry those morsels to the human, and then seamlessly transfer items into the user's mouth. (Right) It is challenging for robot arms to dexterously manipulate traditional utensils such as forks and spoons. By comparison, Kiri-Spoon makes the robot's task fundamentally easier by flexibly wrapping around the desired foods. This capability enables Kiri-Spoon to function as a fork (pinching foods) or as a spoon (scooping foods).

that robots should just leverage traditional utensils (e.g., forks and spoons). People have been using spoons for at least $3,000$ years [27]; these implements are optimized for humans, and prior works on assistive feeding have therefore equipped robots with familiar utensils. But are rigid forks and spoons really the best utensil for a *robot* to use? Answering this question involves a balance between the robot's capability and the human's comfort. From the robot's perspective, utilizing traditional utensils like forks and spoons requires precise and careful manipulation. To pick up a morsel the robot must dexterously coordinate the utensil's motion (e.g., skewering, scooping, twisting) in a way that is tailored to that specific food item. Next — after the food is grasped — the robot needs to smoothly regulate its motion and orientation to prevent the food from spilling during transit (i.e., sliding off the fork or slipping out of the spoon).

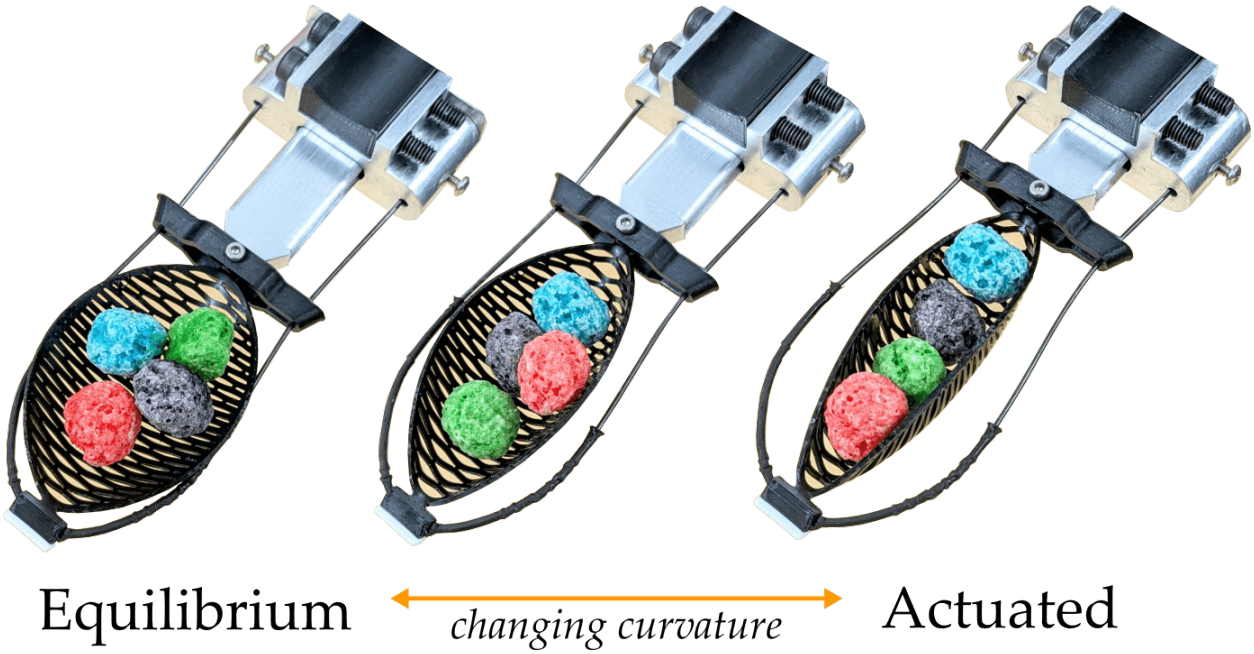


Figure 1.3: Actuating and releasing Kiri-Spoon. The core element of Kiri-Spoon is an elliptical kirigami sheet with discrete ribbons orthogonal to the applied forces. Retracting one end of Kiri-Spoon causes this 2D sheet to buckle and form a 3D bowl with increasing curvature, thereby encapsulating food items.

### 1.0.2 Background

We leverage our insight to create **RISOs**, robotic grippers that unify **RI**gid end-effectors with **SO**ft materials (see Figure 1.1A-B). RISOs are formed by mounting sheets of switchable adhesives onto the surfaces of rigid robotic fingers, and then controlling both the rigid and soft components during manipulation tasks. When the robot arm moves to pick up an item, it can (a) pinch the object between the fingers of the rigid gripper, (b) cause the object to stick to the soft surfaces, or (c) use a combination of the rigid pinch and soft adhesion to hold the object (see Figure 1.1C). In practice, RISO advances the range of robotic grasping by combining and decoupling purely rigid and purely soft grippers. For example, RISOs can grasp objects in real-time across a 1.5 million times range in mass — picking up, carrying, and releasing objects from 2 mg to 2.9 kg (see Figure 1.1D, S6, and S7). We first explored

the feasibility of RISO in preliminary work [58]. Similarly for the Kiri-Spoon, we wanted to develop a solution that addressed some of the current challenges. Recent soft grippers such as [29, 32, 49, 54, 81] enhance robot capabilities by robustly encapsulating, holding, or adhering to diverse food items in ways that traditional forks or spoons cannot achieve. But from the human's perspective, this increase in robot capability comes at the cost of convenience. Today's soft end-effectors are not utensils: users cannot easily or comfortably transfer foods from these grippers into their mouths. Instead, traditional utensils like forks or spoons are best suited for the human's needs — people seamlessly take bites of foods from these familiar implements. In this paper we propose to complement recent algorithmic advances in assistive robot arms by introducing a physical utensil specifically for robot-assisted feeding. To augment the robot's capabilities while accounting for the human's perspective, our hypothesis is that:

*Utensils for assistive robots should combine*
*the enhanced* functionality *of soft grippers with*
*the comfortable* form factor *of traditional utensils.*

Based on this hypothesis we introduce **Kiri-Spoon**: a **spoon**-like utensil featuring a soft **kiri**gami base (see Figure 1.2). In its equilibrium state the Kiri-Spoon maintains the same size and shape as a traditional spoon, allowing users to take natural bites of food. But when actuated, the Kiri-Spoon rapidly increases curvature, creating a bowl that robustly holds foods within its compliant manifold (see Figure 1.3). Across bite acquisition, carrying, and transfer, Kiri-Spoon offers a *mechanical advantage* to the process of robot-assisted feeding. During acquisition, robot arms no longer need to make fine-grained skewering, scooping, or twisting motions: once the Kiri-Spoon is in contact with the desired morsel, we can simply actuate the utensil to grasp that item. Similarly, when carrying the acquired foods, the robot does not have to maintain a steady speed or specific orientation: the actuated Kiri-Spoon

encloses items so that they cannot easily slide or fall during transit. Finally — after bringing the food to the human — the system reverts to a typical spoon form factor for human-friendly bite transfer. Overall, this paper introduces, characterizes, and evaluates the first utensil specifically designed for robot-assisted feeding. We make the following contributions[1]:

### 1.0.3 Contributions

**RISO**

**Characterizing gripper capabilities** Functionally, our soft materials take the form of flat silicone sheets that we can rapidly control to switch between grasping and releasing in less than 0.1 seconds. We characterize the gripping force applied by these structures as a function of the grasped object's radius, curvature, roughness, and porosity. We find that the soft materials combine both adhesion (i.e., using surface forces to attach to the object) and wrapping (i.e., constricting around the object), achieving forces reaching 50 N in idealized testing conditions.

**Integrating RISOs with robot arms and human users** We recognize that increased gripping capability is not meaningful if robot arms and human operators cannot harness RISOs. Accordingly, we develop control strategies with varying levels of autonomy to make it easier for robots and humans to utilize RISOs. In particular, we present a shared autonomy approach that (a) uses the human's joystick inputs to infer their desired object and grasp type, and then (b) autonomously aligns the RISO to complete the intended grasp. We show

[1]Note that a preliminary version of this work was published at the IEEE/RSJ Int. Conf. on Intelligent Robots and Systems [50]. This paper is significantly different because here we redesign Kiri-Spoon alongside stakeholders, derive a detailed mechanics model, and then conduct multiple new experiments. These new experiments include autonomously acquiring diverse foods, evaluations with stakeholders, as well as comparing the effects of algorithmic and mechanical intelligence.

that this shared autonomy method reduces the number of human inputs needed to complete manipulation tasks.

**Comparing to existing grippers** We perform grasping experiments with robot arms and human operators to compare RISOs, an industrial soft gripper, and a granular jamming gripper. Across both autonomous and human controlled conditions, we observe that robots equipped with RISOs are able to pick up, hold, and release a more diverse range of everyday objects. User responses to Likert scale surveys indicate that our participants subjectively rated the RISO gripper as easier to user and more preferable than the tested state-of-the-art alternatives.

**Demonstrating practical applications** We finally showcase our system's practical abilities in assistive scenarios by controlling a robot arm and RISO gripper to make pizza. Here the human teleoperates the arm and RISO to manipulate larger food objects (e.g., placing the crust, spreading the sauce) and arrange smaller food items (e.g., pepperoni, pepper, and olive toppings). When viewed together, our results suggest that RISOs provide an exceptional gripping range in both capacity and object diversity, clearly distinguishing our framework from the baselines. These advances provide a path forward for robotic grippers, particularly within unstructured environments where manipulation of diverse and unexpected items is essential. See videos of our RISOs and experiments here: https://youtu.be/du085R0gPFI

## Kiri-Spoon

**Designing Kiri-Spoon** We start by introducing Kiri-Spoon. Our design process follows an iterative approach led by stakeholders — including both caregivers and end-users. Through interviews with occupational therapists and trials with people that have physical

disabilities, we mutually arrive at Kiri-Spoon. At its heart, the key component of Kiri-Spoon is a soft, elliptical sheet of plastic with parallel cuts (i.e., a 2D kirigami sheet). When this kirigami structure is pulled on both ends it deforms into a 3D bowl with increasing curvature; when released, it returns to a flat spoon shape.

**Modeling the Mechanics and Geometry** We next derive physics models to capture the relationship between applied forces and kirigami geometry. To reach these models we separately analyze each interdependent component of the kirigami system: i) the boundary ribbon that surrounds the edge of our spoon, ii) the discrete ribbons that form the center of our spoon, and iii) the mesh ribbons that create our connected base. We then combine these terms to predict the amount of tensile force needed to cause the Kiri-Spoon to wrap around food items. Our validation tests show that the resulting model is an accurate lower bound across Kiri-Spoon designs with varying materials, thickness, and size.

**Equipping Assistive Robots with Kiri-Spoon** Our work is motivated in part by the need to develop a utensil for assistive robot arms. Accordingly, we next quantify how effectively robots can leverage our proposed utensil as compared to traditional forks and spoons. We perform these experiments in ideal conditions where the robot arm uses each utensil to autonomously pick up a diverse set of known foods (e.g., carrots, tofu, soup, and cereal). Importantly, we show that robots can employ Kiri-Spoons both as a fork (pinching carrots or tofu) and as a spoon (scooping soup or cereal). We also identify the types of foods that are the failure cases for our Kiri-Spoon — large, flat morsels such as bread or lettuce.

**Evaluating across Users with Disabilities** Our work is also motivated by the need to make a utensil that stakeholders actually want to use. To explore how stakeholders perceive our final system, we attached Kiri-Spoon to a commercially available feeding device [63]. We

then brought this assistive device to a local center for adults living with physical disabilities. A caregiver and four participants tested the system with a standard spoon and with our proposed Kiri-Spoon. Overall, the participants subjectively rated Kiri-Spoon to be about as comfortable as a traditional spoon. In addition, their objective results and subjective responses show that Kiri-Spoon led to a higher success rate: foods were transferred from the table to the human's mouth more frequently with the Kiri-Spoon.

**Combining Mechanical and Algorithmic Advances** We conclude this paper by exploring how both mechanical and algorithmic components contribute to the effectiveness of robot-assisted feeding. We conduct a study along two axes: (a) the utensil the robot manipulates, and (b) the algorithm the robot uses to manipulate that utensil. Sixteen users without disabilities operate an assistive robot to grasp, carry, and then eat multiple foods. At one extreme, we equip the robot with standard forks and spoons, and the human manually teleoperates the robot throughout the entire eating process. At the other extreme, the robot leverages Kiri-Spoon and state-of-the-art assistive algorithms to detect, acquire, and then carry the desired foods to the user. We demonstrate that the combination of Kiri-Spoon and recent algorithmic advances leads to a more effective system than alternatives which improve only the hardware or only the software.

# Chapter 2

# Related Works

## 2.1 Related Work

### 2.1.1 History of Robot-Assisted Feeding

For people living with physical disabilities who currently rely on caregivers for meals, assistive technology offers an empowering tool towards increased independence [6, 60, 98]. Accordingly, robot-assisted feeding has a rich history. In general, assistive feeding devices autonomously pick up morels of food, carry that food to the human, and then hold the food in place while the user takes a bite. The human operator typically has control over which types of foods — and how much of those foods — the robot feeds to them. The first systems were introduced in the 1970s and 1980s, including the Morewood Spoon Lifter [86], the Robotic Arm/Worktable System for self-feeding [78], and Handy-1 [96]. These devices were extensively evaluated through user studies involving individuals with mobility limitations [70], paving the way for commercial feeding robots in the 1990s and early 2000s. Notable examples include the Winsford Feeder, My Spoon, Neater Eater, Bestic Arm, Meal Buddy, and Obi [61].

The resulting devices leverage traditional utensils — i.e., forks and spoons — to acquire, hold, and then transfer morsels to the human. In practice, however, they often either (a) struggle to pick up foods from plates and bowls, or (b) unintentionally spill food while carrying it

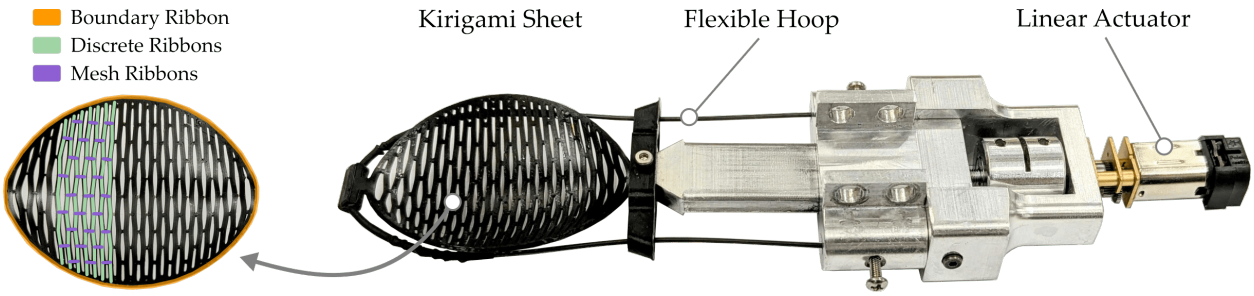


Figure 2.1: Design of Kiri-Spoon. (Left) A kirigami sheet is used to grasp, hold, and release food items. This sheet is composed of multiple ribbons: a boundary ribbon that surrounds the sheet, discrete ribbons that form the base of the spoon, and mesh ribbons that interconnect the discrete ribbons. (Right) The kirigami sheet is supported on one end by a flexible hoop. The other end is extended or retracted by a 1-DoF linear actuator. During eating, users interact with the flexible hoop and kirigami sheet.

to the user. This fundamentally limits the effectiveness and convenience of today's assistive eating technology. Overall, the lack of proficiency, comfort, and adaptability has contributed to limited adoption of robot-assisted feeding: out of all the devices mentioned above, only Neater Eater and Obi [63] remain commercially available (but not widely used).

### 2.1.2 Autonomous Algorithms for Feeding

To address these fundamental shortcomings, recent research has focused on developing autonomous algorithms for food acquisition and transfer. For example, approaches such as [25, 33, 55, 87, 90] study how a robot arm should manipulate a single utensil (e.g., a fork or spoon) to effectively pick up food items from a plate. These works highlight that humans typically employ a few basic motions during food acquisition with traditional Western utensils: stabbing, scooping, or twirling. Robots adapt these motion patterns to specific food items by reasoning over real-time visual and haptic data. In scenarios where acquiring the desired food involves multiple steps — such as pushing meatballs aside in order to access pasta noodles underneath — learning-based approaches have been proposed to tackle

complex, long-horizon manipulation tasks [12, 34, 36, 45, 88].

Once the robot acquires the desired food item, it must safely and comfortably transfer that food to the human's mouth. Research on bite transfer seeks to coordinate the robot's utensil throughout this process. This includes deciding when to feed the user [64], bringing the food item to the user's mouth so they can lean forward to take a bite [11, 24, 30, 73], or placing food items inside the user's mouth if necessary [44, 66, 79]. Existing works leverage visual data from the robot's in-hand camera to perceive the user's mouth, motion planning to control the arm, and haptic sensing to transfer food without applying unsafe forces. Some systems also rely on the user to partially guide the robot arm; for example, operators can leverage natural language or teleoperation inputs to correct the robot's motion throughout food acquisition and bite transfer [18, 48, 57, 65, 72].

In summary, state-of-the-art research focuses on algorithms for autonomously picking up and transferring food items. But within these works the robot uses traditional forks and spoons — and this inherently makes it more complicated for the robot to acquire and transfer foods. Instead of forcing robot arms to dexterously manipulate rigid utensils that were originally designed for humans, we will focus on creating a utensil specifically for robot-assisted feeding.

### 2.1.3 Soft Grippers for Food Manipulation

Looking outside the domain of assistive eating, there are a variety of robotic grippers already built for food processing and handling [102]. These grippers enhance the robot's ability to pick up and hold different food items by introducing new grasping mechanisms. For example, today's robots can leverage shape-changing structures to enclose morsels within a soft end-effector [15, 29, 81, 101]. Alternatively, other grippers utilize adhesive materials to cause foods to stick to the robot's surface [32, 39, 49], or create vacuums that maintain a

suction pressure on the desired morsel [37, 54]. Each of these grasping mechanisms provides advantages during acquisition: robots equipped with soft grippers can pick up, hold, and manipulate diverse food items more effectively than when using traditional rigid utensils.

However, state-of-the-art soft grippers are not designed for assistive eating applications, making it challenging to transfer food from the robot's gripper to the user's mouth. For instance, the food handling mechanisms proposed by [29], [49], and [101] would require the robot to drop morsels directly onto the user, which is impractical for feeding. Overall, food-handling grippers differ too greatly from traditional utensils for comfortable human use. At the other extreme, some works introduce minor modifications to traditional utensils. For example, [87], [79], and [45] add active degrees of freedom to a fork, while [23] incorporates passive degrees-of-freedom into a spoon for improved balance. Although these modified utensils are more user-friendly — allowing the user to take a bite directly — they lack the advanced capabilities of food-handling grippers, limiting their functionality and leading to the same challenges faced with traditional utensils (e.g., food slipping from the utensil).

Kiri-Spoon lies between these two mechanical extremes: it bridges the gap between the functionality of soft, shape-changing grippers and the familiar form of a traditional spoon. Our design achieves this balance by leveraging kirigami structures. While kirigami has been incorporated into previous grippers [16, 105], it has not yet been utilized for robot-assisted feeding. We aim to advance the state-of-the-art by designing, characterizing, and testing a human-friendly utensil tailored for robot-assisted feeding applications.

# Chapter 3

# RISO

## 3.1 Materials and Methods

Here we present our mechanics and control approach for RISO grippers. In Section 3.1.1 we explain the physics behind the soft adhesives, as well as their fabrication process. We then form RISOs by mounting sheets of these pneumatically-actuated soft materials onto the surfaces of rigid end-effectors. This combination of a rigid gripper and adhesives sheets introduces new control variables: e.g., deciding whether to use the soft adhesives or rigid grippers to pick up an object. In Section 3.1.2 we partially automate these decisions and make it easier for humans and robot to control RISOs by developing a share autonomy approach for RISO grippers.

### 3.1.1 Creating RISO Grippers

To understand the adhesive capacity of the soft gripper, we start with the underlying physical relationship between adhesive force $F_c$, contact area, and gripper compliance [9, 22]:

$$F_c \sim \sqrt{G_c}\sqrt{\frac{A}{C}} \tag{3.1}$$

Here $A$ is the contact area between the soft gripper and the target object, $C$ is the gripper's compliance in the loading direction, and $G_c$ captures the fracture energy of the interface. In practice, $G_c$ can treated as the energy per unit area that needs to be applied to separate the interface between gripper and object. In the case of reversible adhesives that do not rely on covalent chemical bonds[7, 10, 52], higher $G_c$ can be achieved through viscoelastic dissipation or other lossy processes at the interface.

For object manipulation, it is essential to be able to pick up and then subsequently release diverse objects. One challenge with soft grippers that utilize adhesion is to make an adhesive strong enough to pick up an object but weak enough so that the object can be released. In order to pick up a wide range of objects, from small, delicate items to large, heavy objects, adhesives have to achieve strong and releasable adhesion within the same material. So the range of mass that a gripper can manipulate becomes a key metric. Therefore, of particular interest for adhesive-based object manipulation is the ability to dramatically increase $F_c$ when gripping an object, and then rapidly decrease $F_c$ when releasing that object. To maximize $F_c$, 3.1 demonstrates that $A$ should be increased, $C$ should be decreased, and $G_c$ should be high. Typically, to achieve high contact area $A$ between the gripper surface and the surface of the object, the gripper should be as *soft* as possible. However, to minimize compliance $C$, the gripper also needs to be as *stiff* as possible. To accommodate these contrasting design directions, we focus on the overall $A/C$ ratio between contact area and compliance. We propose an adhesive design that is soft during initial contact between gripper and object (increasing contact area $A$), and then becomes rigid while maintaining that same contact area (decreasing the compliance $C$). Accordingly, to achieve a large $A/C$ ratio, it is desirable for the adhesive to be *tunable* so that the compliance can be changed during contact to first increase $A$ and then decrease $C$.

We apply these principles to create the soft adhesive for RISO grippers. This adhesive

consists of a tunable elastomeric membrane on a foam foundation (see Figure S1 for fabrication details). We actively control the membrane through pneumatic pressure (see Figure S2), allowing for three primary states: neutral pressure where the membrane is flat, positive pressure when the membrane inflates, and negative pressure where the membrane is constricted (decreased compliance). Grasping and releasing items is achieved by switching between these states.

**Release** To release an item we want to minimize $F_c$. Our soft adhesive achieves this by switching from negative pressure to positive pressure and inflating the membrane (Figure S3). This inflation causes the contact area to decrease, minimizing the ratio $A/C$.

**Neutral to Negative** To increase $F_c$ and adhere to an object, our soft gripper can use two different processes. The first is *neutral to negative*, where the membrane is initially at atmospheric pressure. We start the grasp by bringing the membrane into contact with the object, and then apply a negative pneumatic pressure to increase the stiffness of the membrane and foundation. This decreases $C$ while having a negligible effect on contact area $A$, increasing gripper force $F_c$ (see Figure 3.1A).

**Positive to Negative** To further increase the grasping force, we can alternatively start the membrane at a positive pressure (i.e., the membrane is initially inflated). Here the membrane is first inflated into a hemispherical shape and then pressed into the object to be grasped. This causes the object to embed into the inflated membrane and maximizes $A$ by creating both side and normal contacts. The pressure inside the membrane is then decreased, causing the membrane to tightly constrict around the object. This minimizes $C$ during the loading phase while also activating debonding mechanisms that can increase $G_c$ (see Figure 3.1B).

To create RISOs, these soft adhesive sheets are mounted onto the surfaces of rigid robotic grippers. Our approach is not tied to any specific rigid base; RISOs can be formed by attaching the adhesive sheets to variety of commercially available robotic grippers. In our experiments we test a rigid Robotiq gripper [3] as well as a Franka gripper [**?** ]. The placement of the adhesive sheets is also modular: they can be put on the base of the gripper (Figure 1.1B) or parallel to the gripper fingers (Figure 1.1C). This mechanical combination and decoupling provides the fundamental advantage of our design: we can have purely rigid, purely soft, or combined rigid/soft grasps depending on where the soft adhesives are mounted. However, the combination also introduces control challenges: standard control schemes for the rigid gripper may not be sufficient when the robot needs to coordinate grasps using both the rigid and soft mechanisms.

### 3.1.2 Controlling RISO Grippers

RISO has the potential to enhance grasping capabilities by combining and decoupling rigid and soft mechanisms. But to harness these capabilities, we must integrate RISOs with robot arms and human operators. The key challenge here is that RISOs introduce new low-level variables (e.g., the pressure of the soft adhesives) and high-level decisions (e.g., choosing to grasp an object with the soft materials, the rigid gripper, or both). Below we formulate this controls problem for RISO grippers. We then introduce solutions with varying levels of automation: from fully automated, to fully human controlled, to a shared autonomy approach between the human and robot.

**Formulating the Control Problem** We consider settings where a RISO gripper is the end-effector of a robot arm. Let $s \in \mathcal{S}$ be the system state, where $s$ includes the joint position of the robot arm $s_{robot}$, the pose of the rigid gripper $s_{\text{rigid}}$, and the pose of $n$ soft

adhesives $s_{\text{soft}_1}, \ldots, s_{\text{soft}_n}$. To pick up and manipulate objects, the robot arm must move the RISO so that either the rigid gripper $s_{\text{rigid}}$ or one of the soft adhesives $s_{\text{soft}_i}$ is in contact with the desired item. We use $o \in \mathcal{O}$ to denote the position of objects in the environment; our robot arm observes each object $o$ by using a mounted RGB-D camera and the Yolo-v5 object detection algorithm [47].

There are two inputs used to move the robot arm and actuate the RISO gripper. First, the robot can take autonomous actions $a_{\mathcal{R}} \in \mathcal{A}$ to change its own joint velocity. Second — if a human operator is present — this human can teleoperate the robot arm and RISO gripper with a joystick (see Figure 1.1A). The direction the user presses on the joystick sends a corresponding joint velocity command $a_{\mathcal{H}} \in \mathcal{A}$ to the robot. The objective for the system is to reach for and manipulate objects. Let $o^* \in \mathcal{O}$ be the target object, and let $g^* \in \mathcal{G}$ be the target grasp type. For example, if the human wants to pick up small, numerous candies, then $g^*$ could be the soft adhesive; alternatively, if the robot arm it trying to pick up a bottle of syrup, then $g^*$ should be the rigid gripper. Our controls problem is identifying an efficient sequence of autonomous robot actions and/or human inputs that will cause the robot to pick up object $o^* \in \mathcal{O}$ using the RISO grasp type $g^* \in \mathcal{G}$.

**Shared Autonomy for RISO Grippers** We developed three control strategies for RISO grippers along a spectrum of autonomy. At one extreme is fully **autonomous** control: here the robot arm acts in isolation without any human guidance. The robot leverages its RGB-D camera to detect objects in the workspace, and then autonomously moves the arm with actions $a_{\mathcal{R}}$ to align RISO with the closest object. RISO determines whether to attempt grasps using the rigid mechanism or soft adhesives based on the perceived size of the object — for objects with a height greater than 75 mm RISO uses the rigid gripper. At the other extreme of the spectrum is fully **human** control: in this condition humans use a joystick to

teleoperate the robot arm and RISO gripper throughout the task. The robot simply executes the human's commanded actions $a_{\mathcal{H}}$ to move its end-effector. When attempting to perform a soft grasp, humans must teleoperate the RISO to directly adjust low-level variables including the normal force and gripper pressure (i.e., how hard the gripper presses down on the object and the pressure of the gripper's pneumatic components).

Between these robot and human extremes we propose a **shared autonomy** framework for RISO grippers. This approach is designed to integrate the human, robot, and RISO while reducing the human's workload. Intuitively, under our approach the robot (a) infers the desired object $o^*$ and grasp $g^*$ from the human's inputs, and then (b) partially automates the process of reaching for and grasping that item. To estimate the human's desired object and grasp given the previous states $s^{0:t}$ and human actions $a_{\mathcal{H}}^{0:t}$, the robot leverages Bayesian inference:

$$P(o, g \mid s^{0:t}, a_{\mathcal{H}}^{0:t}) = b^{t+1}(o, g) \propto P(a_{\mathcal{H}}^{t} \mid s^{t}, o, g) \cdot b^{t}(o, g) \tag{3.2}$$

where $P(a_{\mathcal{H}}^{t} \mid s^{t}, o, g)$ models the human as a noisily-rational agent [46], and belief $b(o, g)$ is the joint probability that the human wants to reach object $o$ with grasp $g$. For instance, if the human teleoperates the robot to move RISO's soft adhesive towards a pile of candies, then $b(o, g)$ should report that the candies are the most likely object and the soft adhesives are the most likely grasp. The robot chooses actions $a_{\mathcal{R}}$ to assist the human in real time based on this inferred belief:

$$a_{\mathcal{R}} = \sum_{o \in \mathcal{O}} \sum_{g \in \mathcal{G}} (o - s_g) \cdot b(o, g) \tag{3.3}$$

In practice, 3.3 causes the robot arm to autonomously move towards likely objects while aligning the RISO gripper for the human's preferred grasp. This leads to a shared autonomy framework where the human is responsible for high-level decisions (e.g., which object to

grasp) and the robot assists with the low-level variables (e.g., moving the robot arm directly above the object, and automating the pressure changes for the soft adhesive). Our resulting shared autonomy approach is distinct from related works [42, 43, 57] because we not only need to infer the human's goal object, but also how the human wants to use the RISO to grasp that object.

## 3.2 Results

In this section we conduct experiments and user studies to explore the capabilities of RISO grippers. We start by exploring how adhesion and wrapping mechanisms contribute to the soft material's overall gripping force (Section 3.2.1), and then characterize gripping forces as a function of the target object's radius, curvature, roughness, and porosity (Section 3.2.2). Equipped with this understanding of the soft components, we next apply RISOs in systems with robot arms and human operators. In Section 3.2.3 we compare the range of objects that robots can grasp when using RISO grippers, industrial soft grippers, and a granular jamming gripper. We also conduct user studies to assess how easy it is for robots and humans to utilize RISOs with autonomous control, human control, and shared autonomy (Section 3.2.4). Put together, these four experiments characterize the soft components of RISOs, compare RISOs to state-of-the-art alternatives, and demonstrate how our controllers improve gripper performance and ease-of-use.

### 3.2.1 Measuring the Force Capacity of RISO's Soft Adhesives

We start by measuring the soft adhesive's force capacity when grasping a indenter (e.g., a target object) under controlled conditions. Figures 3.1C and 3.1D show the force profiles for

a 12.5 mm smooth indenter. To conduct these tests, the soft membrane was first brought into contact with the indenter, and then the membrane state was switched to a negative pressure. We finally pulled the soft gripper and indenter apart from one another until the two separated, enabling us to measure the total adhesive force $F_c$ (see Figure S4). Under the **positive to negative** condition the membrane was initially inflated (Figure 3.1B), while for the **neutral to negative** condition the membrane started at atmospheric pressure (Figure 3.1A).

Figure 3.1E extends our results across indenters of different radii. To provide a baseline for these results, we included a **positive to positive** condition where the membrane was always inflated. As expected, in this positive to positive case the adhesion was very low for all indenter radii; because the membrane never decreased its compliance, it was unable to achieve higher $F_c$ values. Next, we increased the adhesion force by switching between neutral and negative states. Here we observed higher $F_c$ as the indenter radii increased (i.e., as the contact area increased), and the soft gripper was able to reach a grasping force of 18 N for the 12.5 mm indenter. We finally repeated these same tests with the positive to negative condition. As before, the force capacity $F_c$ increased with the radius of the target object, but now the grasping forces were larger because of the combination of adhesive and wrapping mechanisms (Figure 3.1B). In the positive to negative condition the soft adhesive reached a maximum gripping force of 50 N for an indenter radius of 12.5 mm.

Based on the adhesive scaling analysis from 3.1, we plot $F_c$ vs. $\sqrt{A/C}$ in Figure 3.1F and find a good agreement between the physical model and experimental data. For the neutral to negative condition the slope gives a fracture energy of $G_c$= 4.2 J/m$^2$, which is in line with previous results[89]. By contrast, the positive to negative case produced a significantly larger fracture energy of $G_c$= 44.7 J/m$^2$. This suggests that the wrapping mechanism enhanced the capabilities of the soft adhesive by increasing $G_c$. We attribute this effect to the frictional

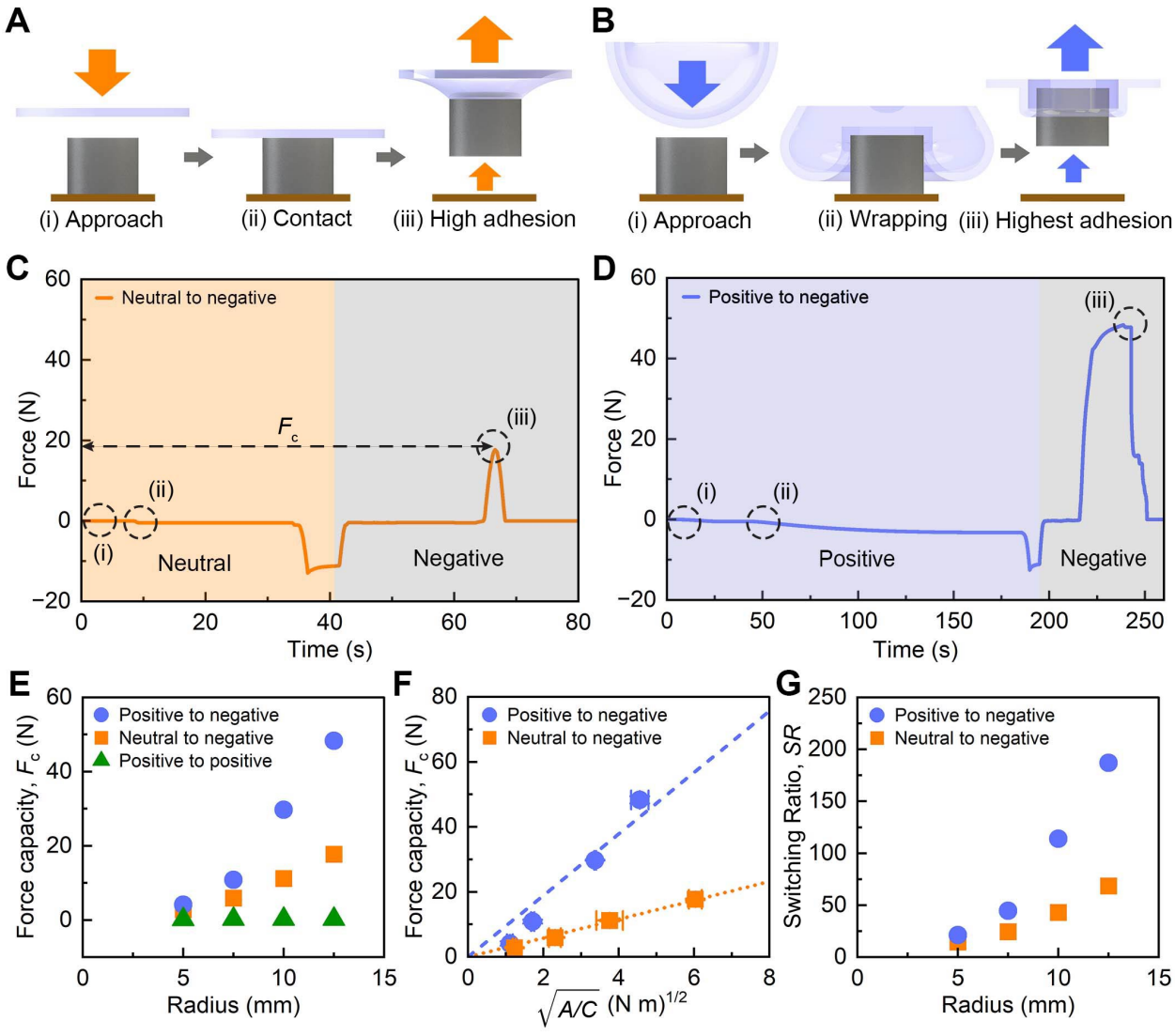


Figure 3.1: **Measuring the force capacity of RISO's soft adhesives.** (**A**) Soft grasps while switching the membrane from neutral to negative pressure. (**B**) Soft grasps while switching the membrane from positive to negative pressure. (**C**) Force profiles for neutral to negative and (**D**) positive to negative with a 12.5 mm smooth indenter (circles represent testing stages from **A** and **B**.) (**E**) Force capacity $F_c$ vs. indenter radius. (**F**) Force capacity $F_c$ vs. $\sqrt{A/C}$, where the points represent the experimental data and the lines represent the prediction from 3.1. Here $G_c$= 4.2 J/m$^2$ and $G_c$= 44.7 J/m$^2$ for the lower and upper lines. (**G**) Adhesion switching ratio ($SR$) as a function of indenter radius, where $F_{low}$ is data from positive to positive.

sliding and hydrostatic pressure that the membrane applies to the target object when it is wrapped around that object.

Another important parameter for manipulation is the adhesion switching ratio, $SR \equiv F_{high}/F_{low}$, where $F_{high}$ is the adhesive force in the "on" state (i.e. neutral to negative or positive to negative) and $F_{low}$ is the adhesive force in the "off" state (i.e. positive to positive). We calculate this for our system where the $F_{high}$ is the adhesive force for the adhesion and wrapping modes, while the $F_{low}$ is the adhesive force in the release condition. We find that the adhesion switching ratio increases with increasing indenter radii (Figure 3.1G), reaching a maximum value of 187 for the 12.5 mm indenter. Overall, the soft adhesive's ability to achieve a high force capacity ($\sim$ 50 N), rapid release ($<$ 0.1 s), and high switching ratio provides key properties for object manipulation.

### 3.2.2 Characterizing RISO's Soft Adhesives across Diverse Objects

In Section 3.2.1 we focused on idealized objects to explore the mechanics behind the soft adhesives. We next move towards diverse objects, and characterize how RISO's soft adhesive can grasp items as a function of their curvature, roughness, and surface porosity (see Figure 3.2). For each type of object we measured the gripper's force capacity when using the neutral to negative grasp (i.e., adhesion dominated) as well as the positive to negative grasp (i.e., combined adhesion and wrapping).

We start with curved indenters in Figure 3.2A-B. Here the soft adhesive's performance depended on the actuation strategy: in the neutral to negative case $F_c$ decreased as the curvature increased, while with the positive to negative pressure change $F_c$ was roughly constant. Intuitively, we might expect the force capacity to be lower for more curved items

because of a decreased surface area (i.e., the soft adhesive was only making contact with the tip of the indenter). The wrapping effect within the positive to negative condition mitigated this issue and enhanced the force capacity across all curvature values. We next tested target objects with engraved surfaces to create effective, controlled roughness (see Figure 3.2C-D). When the engraved lines were closer together the surface was more rough — leading to lower contact area $A$ and smaller $F_c$ values. Conversely, when the lines were far apart the surface was more smooth, resulting in larger contact area and gripper forces. Here we observed a small improvement of the positive to negative over the neutral to negative condition. Finally, we measured the adhesive force when grasping objects of different surface porosity (see Figure 3.2E-F). As the porosity increased the surface area decreased — this led to lower force capacity across both gripper conditions. Nonetheless, even with a surface porosity of nearly 80%, RISO's soft gripper was able to generate adhesion forces of up to 0.9 N. RISO's ability to grasp porous objects, as well as discrete objects of different size as seen in Figure 1.1C, contrasts with vacuum grippers. Vacuum gripper struggle to grasp and hold porous and discrete objects because they cannot maintain an airtight seal; by contrast, RISO takes advantage of its dynamic surface adhesion to grasp and release these challenging objects.

### 3.2.3 Comparing RISOs to Existing Grippers

Over the previous two experiments we isolated the soft component of RISO grippers under idealized conditions. Moving forward, we will unify these soft materials with rigid end-effectors to form RISO grippers. Our core insight is that RISOs *combine and decouple* the rigid and soft gripper mechanisms, enabling grasps along a spectrum from purely rigid, to purely soft, to rigid-soft. We hypothesize that this decoupling will fundamentally increase the range of objects that RISOs can pick up, hold, and release. To test this hypothesis, here

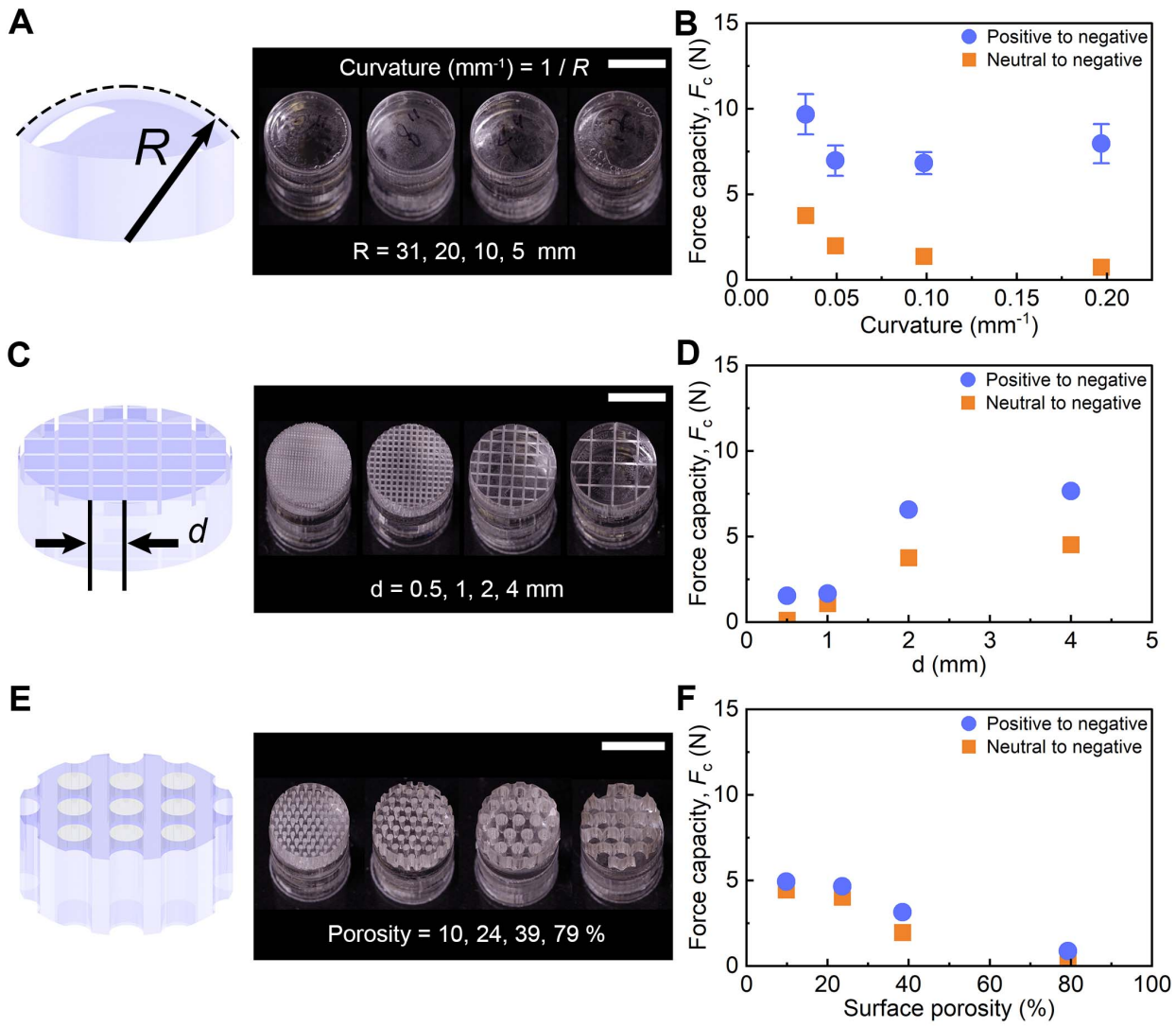


Figure 3.2: (**A**) Curved indenters with four different curvatures. (**B**) Force capacity $F_c$ vs. indenter curvature. (**C**) Rough indenters with lines etched at distance $d$ from one another. (**D**) Force capacity $F_c$ vs. different line distances. (**E**) Porous indenters with four levels of porosity. (**F**) Force capacity $F_c$ vs surface porosity. Across all plots the indenters have a radius of 7.5 mm and the scale bars are 10 mm.

we explore the range of objects that robot arms and human operators can grasp with RISO grippers and state-of-the-art alternatives.

**Independent Variables** We compared three different grippers: RISO, a industrial Soft-Gripper [1] and a granular jamming gripper [15] (see Figure 3.3B and Figure S5A). Each of these grippers were mounted at the end-effector of a 7-DoF FrankaEmika robot arm [2].

To understand how these different grippers performed in isolation — without any human guidance — we applied our autonomous controller from Section 3.1.2. Here the robot arm identified objects with a camera, and then autonomously moved its gripper to align with the detected object. Next, to test how the grippers performed with a human-in-the-loop, we applied the human controller from Section 3.1.2. Under this approach humans operated a joystick to remotely control the robot arm and attached grippers without any autonomous assistance. We recruited 12 participants (4 female, average age $22.9 \pm 2.73$) from the Virginia Tech community to take part in this study. All participants provided informed written consent following university guidelines (IRB #22-308). The order in which participants used the grippers was randomized: some started with RISO, others started with a SoftGripper, and others started with the granular jamming gripper.

**Dependent Variables** The gripper, robot arm, and human operator collaborated to pick up, carry, and then drop a dataset of 15 household objects (see Figure 3.3A and Figure S5B). During each interaction the system manipulated one item: the interaction was considered a success if the gripper picked up an object, carried it across the table, and dropped it in the bin. To measure the user's perception of each gripper, we also conducted a 7-point Likert scale survey within the human-in-the-loop condition. Our questions focused on how easy it was to use the gripper, and whether participants preferred one gripper over the alternatives

(see Figure 3.3E and Table S8).

**Autonomous Results** Figure 3.3C shows the results of the autonomous test. This experiment compared the performance of RISO, the SoftGripper, and a granular jamming gripper when the robot's behavior was fully automated. Across all objects and 10 autonomous trials, the manipulation success rates were SoftGripper: 56%, Granular: 51%, and RISO: 93% (see Table S9). These differences in performance were statistically significant. A repeated measures ANOVA revealed that the gripper type had a significant effect on the overall success rate across 10 trials ($F(2, 18) = 156.42$, $p < 0.05$), and post-hoc tests in Figure 3.3C confirmed that RISO had a higher success rate than either the pneumatic SoftGripper ($p < 0.05$) or the granular jamming gripper ($p < 0.05$).

**Human-in-the-Loop Results** Figure 3.3D summarizes our results across 12 human participants. This experiment compared the performance of RISO to state-of-the-art alternatives when the system was fully controlled by human operators. We again found that the gripper type had a significant effect on the grasping success rate ($F(2, 22) = 138.37$, $p < 0.05$). Participants successfully grasped and manipulated objects more often with RISO as compared to the pneumatic SoftGripper ($p < 0.05$) and the granular jamming gripper ($p < 0.05$). Across 12 users the success rates were SoftGripper: 58%, Granular: 41%, and RISO: 88% (see Table S11). When surveyed using a questionnaire of Likert scale items, participants also expressed a subjective preference for the RISO gripper (see Figure 3.3E and Table S10). Participants rated the the RISO gripper as easier to use than the granular jamming gripper ($p < 0.05$), and indicated that they would rather interact with the RISO gripper again in the future instead of either the pneumatic SoftGripper ($p < 0.05$) or granular jamming gripper ($p < 0.05$).

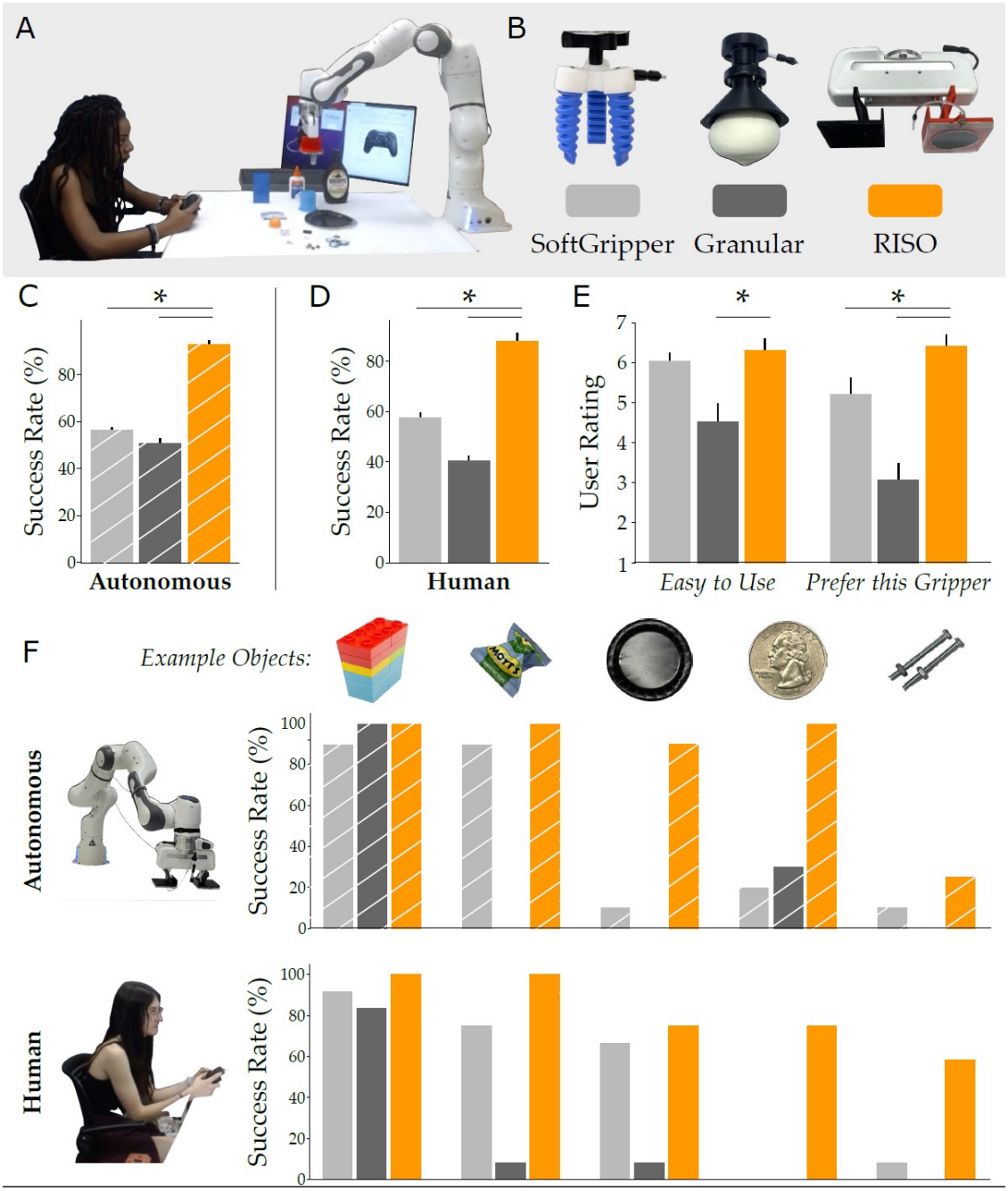


Figure 3.3: **Comparing RISOs to existing grippers.** (**A**) Experimental setup. Grippers were attached to a 7-DoF robot arm and used to grasp, move, and drop a dataset of 15 household objects. (**B**) We compared an industrial SoftGripper, a granular jamming gripper (Granular), and RISO. (**C**) Success rates for each gripper when the system was fully automated. (**D**) Success rates for each gripper with a human-in-the-loop. A total of 12 participants remotely controlled the robot arm and grippers using a joystick. (**E**) After working with each gripper users responded to a 7-point Likert scale survey. Users indicate how easy it was to use the gripper and which grippers they preferred. (**F**) Success rates for 5 sample objects where RISO outperformed SoftGripper and Granular.

**Comparing Grippers** Whether the grippers were controlled directly by humans or autonomously by the robot arm, RISO was able to grasp, carry, and drop a more diverse range of items than the SoftGripper or Granular jamming gripper. In Figure 3.3F we break down these results for some sample objects in the dataset (see all object success rates in Table S9). Across both human and autonomous control, the pneumatic SoftGripper failed to pick up small, numerous items (e.g., the nuts) or items that slip through the soft fingers (e.g., the quarter). Similarly, the granular jamming gripper struggles to grasp flat objects that the gripper cannot wrap around (e.g., the plate). RISO is able to overcome these limitations through its decoupled design: we can use the soft adhesive sheets to pick up small, numerous items, and the rigid end-effector to grasp large, heavy objects.

### 3.2.4 Reducing Effort with Shared Autonomy

When comparing RISO to state-of-the-art grippers in Section 3.2.3 we tested the extremes of our controls spectrum: fully autonomous or fully human controlled. Both of these control modes have advantages. On the one hand, an autonomous robot can optimize the low-level variables introduced by RISO grippers (e.g., the normal force and pneumatic pressure). On the other hand, a human can specify high-level targets and grasps (e.g., selecting whether to use the rigid, soft, or rigid-soft gripping mechanism). In Section 3.1.2 we combined the benefits of both approaches under a *shared autonomy* method for RISO grippers. This method integrates the human, robot arm, and RISO gripper: based on the human's joystick inputs, the robot and RISO infer the human's desired object, and then automate the arm and gripper behavior to help complete the task.

**Independent Variables** We compared our proposed shared autonomy method to systems completely controlled by the human. Twelve new participants from the Virginia Tech com-

munity (2 female, average age $24.1 \pm 4.5$ years) provided informed consent and took part in this user study (IRB #22-308). These participants interacted with a joystick to remotely control the 7-DoF FrankaEmika robot arm [2] and its attached RISO gripper. Within the *human* condition the robot directly executed the user's commands without providing any assistance. By contrast, under *shared autonomy* the robot and RISO provided partial assistance based on the inferred object and grasp type. The order of these conditions was counterbalanced: half of the users started with shared autonomy, and the other half started with human control.

**Dependent Variables** Participants operated the robot and RISO to pick up, carry, and then drop the same 15 household items as in Section 3.2.3 (also see Figure S5B). Our underlying hypothesis was that shared autonomy would make it easier for humans to leverage the RISO gripper. To measure changes in efficiency, we recorded the amount of time users actively controlled the robot with joystick inputs, and the total length of the robot's trajectory. Grippers that are easier to use should complete manipulation tasks with as little human guidance as necessary (e.g., fewer joystick inputs and shorter trajectory length). We also administered a 7-point Likert scale survey to assess the participants' subjective outcomes. Our questions are listed in Table S10, and ask about how helpful, easy to use, and intuitive the system was.

**Shared Autonomy Results** In Figure 3.4B-C we present the results of this user study. Paired t-tests revealed that the overall grasping success rates were not significantly different for either human control or shared autonomy ($t(11) = -0.62$, $p = .55$, also see Table S11). The main difference between conditions was the amount of human effort. When working with shared autonomy, participants were able to complete the manipulation tasks with fewer joystick inputs ($t(11) = 13.65$, $p < .05$), and the shared autonomy system moved more

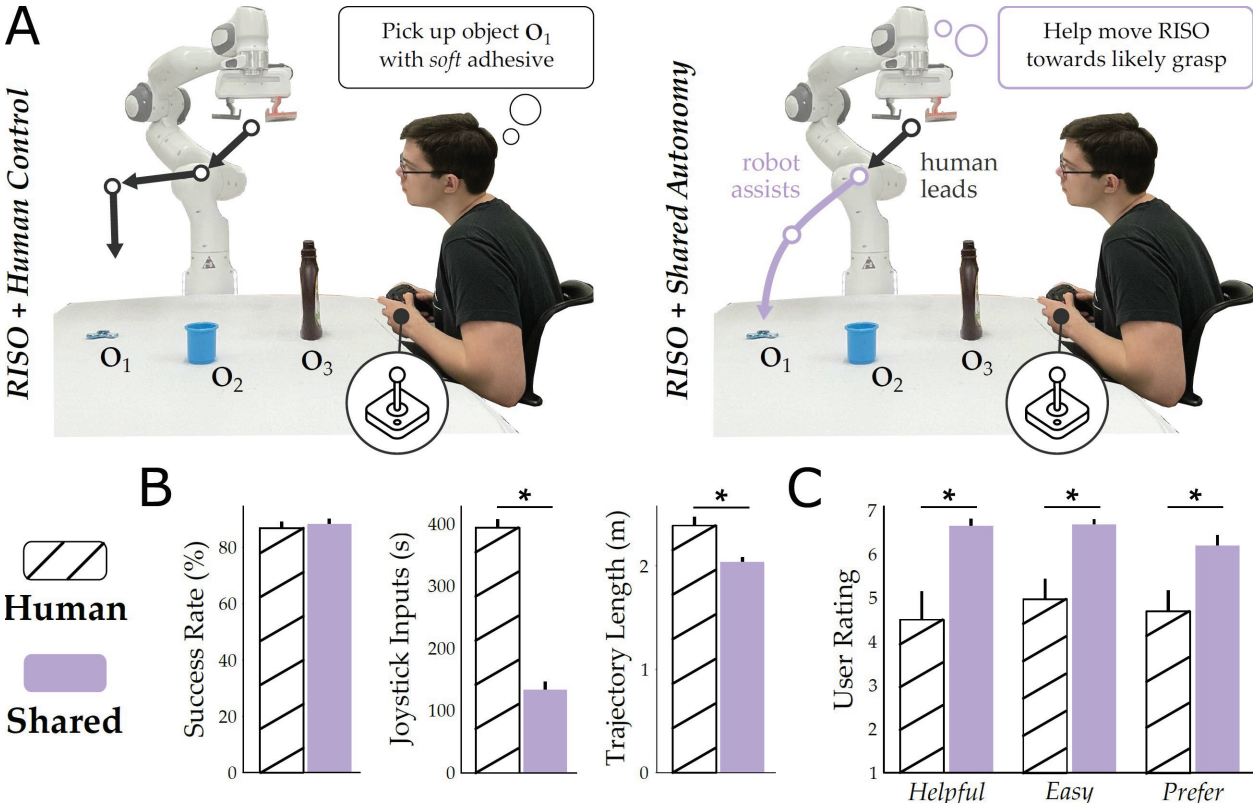


Figure 3.4: **Making it easier for humans to utilize RISOs.** (**A**) Overview of human control and shared autonomy. In human control the user teleoperates the robot and RISO throughout the entire manipulation task. By contrast, in shared autonomy the system uses the human's inputs to infer their desired object and grasp type. The system then partially automates the robot arm and RISO to help complete that grasp. (**B**) Objective results from a user study with 12 participants. With shared autonomy users were able to complete grasps with fewer joystick inputs and shorter robot trajectories. (**C**) Users responded to a 7-point Likert scale survey to indicate how *helpful* the controller was, how *easy* it was to use the gripper, and which control approach they *prefer* to use. Higher scores indicate agreement (e.g., more helpful), and an $*$ denotes statistical significance.

efficiently to complete each grasp ($t(11) = 4.58$, $p < .05$). This reduced the average time taken to manipulate objects: without shared control users needed 28.4 seconds to grasp each item, and with shared control this average dropped to 24.7 seconds. In support of these objective results, users indicated a subjective preference for working with RISO under the shared autonomy framework (Figure 3.4C and Table S10). Post-hoc tests show that participants perceived the shared autonomy approach to be more helpful ($p < .05$), easier to use ($p < .05$), and overall preferable to the human controller ($p < .05$). Viewed together, these objective and subjective results suggest that RISO grippers are not only capable of picking up a diverse range of objects, but also that we can reduce the human's effort when leveraging these RISO grippers.

## 3.3 Discussion and Conclusion

In this work we covered the surfaces of rigid end-effectors with a novel class of soft adhesives to form RISOs: RIgid-SOft grippers. Our underlying hypothesis was that RISOs would enhance grasping capabilities by both combining and decoupling rigid and soft mechanisms. Because the rigid and soft components were *combined*, RISO could perform rigid-soft manipulation, and because the components were *decoupled*, RISO could also perform purely rigid or purely soft grasps. We experimentally found that this combination enabled robots to overcome the fundamental limitations of each individual component. In our user studies robot arms and human operators successfully utilized RISOs to pick up, move, and release a wide range of objects: from flat items to 3D objects, from single items to multiple objects, and from small items to large objects. These enhanced grasping capabilities are practically useful in settings such as food processing, parts manufacturing, and assistive caregiving. We demonstrate one practical application in Figure 3.5, where a human operator utilized our RISO gripper

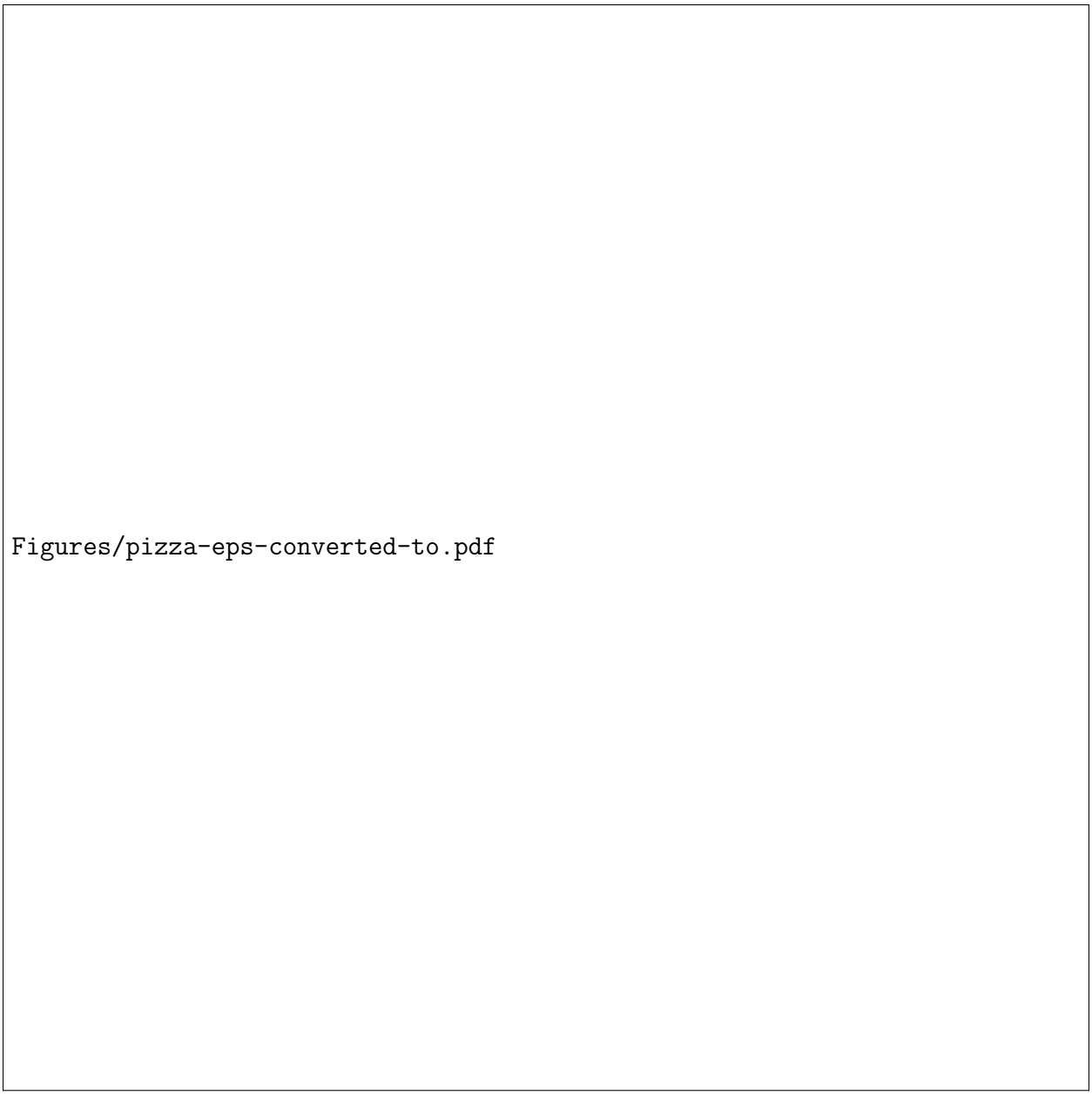


Figure 3.5: **RISO grasps and manipulates multiple food items to assemble a pizza.** A human teleoperated the robot arm and attached RISO gripper. Here we show snapshots of the resulting task from a side view (top row) and an overhead view (bottom row). The RISO used purely rigid grasps to manipulate the crust, spread the sauce, and pour the cheese. For small and numerous toppings the RISO used purely soft grasps: picking up, transporting, and releasing the pepperoni, peppers, and olives with the soft materials. See movie S12 for the overall task.

to assemble a pizza. This required grasping large, flat objects (the crust), manipulating tools (spreading the sauce and cheese), and picking up, transporting, and releasing small, irregular food items (the pepperoni, peppers, and olives). Because RISO can perform grasps along a spectrum from purely rigid to purely soft, the robot completed each of these diverse manipulation tasks with a single gripper. Moreover, we have grasped a 2.9 kg plastic cooking oil bottle with the soft adhesive (Figure S7). Overall, we have demonstrated that RISOs provide exceptional gripping range to rapidly manipulate small lightweight objects (2 mg) to heavy, complex items (2.9 kg) (over a 1.5 million times range in mass), and that robots and humans can effectively utilize these grippers in unstructured environments (with higher grasping success and user ratings as compared to state-of-the-art alternatives).

Another outcome of our studies was that the control scheme impacts the objective and subjective performance of the RISO gripper. This demonstrates that the way the human and robot are integrated with the gripper can have an effect on gripper outcomes. In particular, adhesion effectiveness is often characterized in controlled environments (i.e. static loading with precisely controlled alignment on testing machines) and considered to be a function of the adhesive alone [21, 22, 41]. However, when the adhesive or gripper is integrated with a robot arm and human user, this system now experiences variable inputs and motions that can significantly impact the functional adhesion capabilities. From the soft material viewpoint, this signifies the importance of designing in tolerance to misalignment and applied forces, consideration of adhesion switching speed and the ability to maintain high forces during the full object manipulation process, and integration of soft adhesives into larger robotic systems.

# Chapter 4

# Kiri-Spoon

## 4.1 Kiri-Spoon Design

In this section we present our design for Kiri-Spoon[1]. Here we apply our fundamental hypothesis: utensils for assistive feeding should be similar to traditional utensils in form, and similar to soft grippers in functionality. By leveraging this hypothesis we ultimately reach a novel utensil with a spoon's form factor that utilizes an actuated kirigami structure to encapsulate and release food items (see Figure 2.1). To ensure that this design is comfortable and meets the needs of users, we collaborate with stakeholders. To ensure that this design is food-safe and effective at grasping diverse morsels, we engineer a morphing bowl with controllable curvature. In what follows we describe our specific problem setting (Section 4.1.1), how stakeholders were involved in the iterative design process (Section 4.1.2), and the individual components of our resulting Kiri-Spoon (Section 4.1.3).

### 4.1.1 Problem Statement

We consider settings where a human with mobility limitations is leveraging an assistive robot arm to eat their everyday meal. This meal is placed on a table in front of the user. Next to the user — either attached to their wheelchair or mounted on the table — is an assistive

[1]The design files for Kiri-Spoon are available at: https://github.com/VT-Collab/Kiri-Spoon

robot arm. This robot is equipped with cameras to perceive the environment, as well as a utensil to manipulate food items. Consistent with standard practices for assistive eating, we assume that the foods are already in bite-sized morsels: i.e., the robot does not need to cut any items [13]. At each iteration the human specifies which food item they want to eat, and the robot attempts to pick up that morsel, carry it to the human, and then help transfer it into the human's mouth. From the robot's perspective, the system should successfully grasp, hold, and deliver the desired foods without spilling or dropping them. From the human's perspective, the system should be safe, comfortable, and intuitive.

### 4.1.2 Stakeholder-driven Iterative Design

In order for robot-assisted feeding to be successful, it is critical that these systems are designed with and by the stakeholders. Prior works have therefore integrated caregivers and adults with disabilities into the design process [13, 56, 59, 68, 99]. Here we similarly adopt a stakeholder-centric approach. Specifically, we interacted with occupational therapists and residents at The Virginia Home, a community for adults living with physical disabilities [93].

After collecting informal interviews about the types of assistive utensils that would be helpful and practical, we first developed an early iteration of Kiri-Spoon [50]. We then brought this iteration to The Virginia Home: here a set of $N = 4$ users compared our initial Kiri-Spoon design to a standard plastic spoon. Both spoons were held and manipulated by an Obi robot — see Section 4.4 for more details on the experimental setup and protocol. Overall, we leveraged Likert scale surveys and forced-choice questions to assess the user's perception of the utensil. We also recorded objective measures for the amount of food transferred to the human's mouth and the number of times food items were unintentionally dropped. Through this back-and-forth process we identified design steps needed for improved efficiency and

comfort. For example, our initial version of the Kiri-Spoon incorporated a rigid metal hoop to support the kirigami sheet. Stakeholders indicated that this rigid hoop was uncomfortable when eating, and recommended a more compliant structure so that they could manipulate the utensil and foods within their mouth. More generally, each of the key elements of our device — including its geometry, materials, and functionality — were reviewed or suggested by multiple stakeholders. We therefore present the Kiri-Spoon as a stakeholder-led system, created in collaboration with members of our target population.

### 4.1.3 Kiri-Spoon Components

Our resulting design for Kiri-Spoon is outlined in Figure 2.1. This design consists of three essential elements: a **kirigami sheet** that forms the spoon, a **flexible hoop** that holds one end of the kirigami sheet, and a **linear actuator** that displaces the other end of the kirigami sheet. Below we separately discuss each Kiri-Spoon component.

**Kirigami Sheet** The main component of Kiri-Spoon is a shape-morphing kirigami sheet. This sheet is composed of multiple discrete ribbons (which form the center of the spoon), a boundary ribbon (which acts as the edge of the spoon), and a pattern of mesh ribbons (which create an interwoven base). In its low-energy state our kirigami sheet is a flat, 2D ellipse with discrete ribbons parallel to the minor axis. When the boundary ribbon is pulled orthogonally to these discrete ribbons, the discrete ribbons *buckle* and the 2D sheet morphs into a 3D bowl. The resulting structure resembles a spoon, but with two important distinctions. First, the kirigami sheet is soft and deformable. Second, by pulling or releasing the boundary layer we can control the curvature of our kirigami structure along a continuous spectrum.

In practice, the resulting kirigami sheet undergoes significant shape changes. To achieve these changes we must manufacture the kirigami out of isotropic materials that deform uniformly

when pulled. Similarly, the materials should be ductile enough to extend when actuated, while also elastic enough to return to their original shape when released. We therefore fabricate our kirigami structures with thermoplastic polyurethane (TPU), an inexpensive and *food-safe* plastic that exhibits the desired material properties. The sheets are 3D printed to customize the geometry of the boundary ribbon, discrete ribbons, and mesh ribbons. We note that these mesh ribbons can be discrete (as shown in Figure 4.1, Top) or one continuous structure (as shown in Figure 4.1, Bottom). Using a continuous structure prevents liquid foods from falling out of the base of Kiri-Spoon.

**Flexible Hoop** The distal end of the kirigami sheet is mounted to a supporting hoop. When the human eats from the Kiri-Spoon, this hoop often enters their mouth; and when Kiri-Spoon is actuated, this hoop applies axial forces to extend the kirigami sheet. Correctly designing this hoop is therefore challenging, because the hoop must be a) flexible for the user's comfort, and also b) rigid enough to hold one end of the kirigami sheet in place. In collaboration with our stakeholders, we found an effective trade-off between these goals by leveraging nickel titanium (i.e., nitinol) wire. In our final design the flexible hoop is formed from a 1mm diameter nitinol wire coated by a soft, food-safe plastic wrapper. As shown in Figure 4.2, the resulting hoop bends when pressed against plates, bowls, or the human's

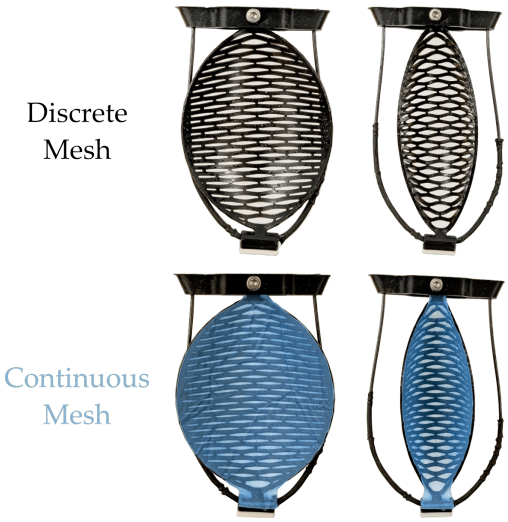


Figure 4.1: Two variations of Kiri-Spoon's mesh. (Top) For most foods a discrete mesh is sufficient. (Bottom) However, for liquid foods such as soups, a thin membrane can be mounted to the kirigami sheet. The resulting continuous mesh prevents liquids from falling out of the bottom of Kiri-Spoon.

mouth, and then reverts to its original shape after the contact ends. This compliance is particularly useful when Kiri-Spoon is deployed as a fork: if pressed against a plate, the hoop bends so that the kirigami sheet is parallel to the desired food morsel.

**Linear Actuator** The proximal end of the kirigami sheet is attached to the output of a 1-DoF linear actuator. This actuator applies controlled forces to extend or retract the boundary ribbon. We construct the actuator out of a rotatory 12V motor with an integrated encoder, and then connect that motor to a linear screw. Rotating the motor in one direction applies tension to the kirigami sheet, and rotating the motor in the opposite direction releases this tension. The actuator housing contains ball bearings for smooth, constrained motion; the system can fully extend or retract the kirigami sheet in under 2 s.

Figure 4.2: Demonstration of the flexible hoop. This flexibility is not only comfortable for users, but it also enables Kiri-Spoon to bend along the surface of plates and bowls. We leverage this flexibility to deploy Kiri-Spoon like a fork and pinch foods that are directly beneath the kirigami structure.

**Integration** By combining the kirigami sheet, flexible hoop, and linear actuator, we reach our Kiri-Spoon design. Kiri-Spoon can autonomously adjust the curvature of its spoon-like bowl to mechanically enclose or release food items. The specific kirigami sheet actuated by Kiri-Spoon is modular; caregivers can replace this sheet with new 3D printed designs for different users or for different sets of foods. For practical purposes, we emphasize that the flexible hoop and kirigami sheet are both *washable* and *food-safe*. The total weight of the Kiri-Spoon used in our tests is 85 g, and its volume at 15 mm displacement is $\approx$ 8 mL.

The life-cycle of the kirigami sheet depends on its materials and geometry: for example, in all our experiments we have not had TPU sheet A break. However, we did notice some minor effects of repeated use. After roughly 30 min of repeated actuation, the semi-major axis of the kirigami sheet extends less than 3 mm. Even after long-term usage we have not experienced a permanent displacement of more than 6 mm.

Once manufactured, Kiri-Spoon is then mounted at the end-effector using custom 3D printed attachments included in our online repository. In the following experiments we connect Kiri-Spoon to robot arms — e.g., FrankaEmika [28], UR5 [97] — and an assistive feeding device — e.g., Obi [63]. The algorithm used to control that system must account for Kiri-Spoon in two ways: the timing when Kiri-Spoon is opened or closed, and the amount of curvature of the kirigami structure. Similar to the geometry of the sheet, these control parameters can be adjusted for the specific user or food item. In Section 4.2 we will present a mechanics model of Kiri-Spoon. Then, in Sections 4.3–4.5, we will integrate the mechanical system with robot arms and assistive feedings algorithms.

## 4.2 Mechanics Model

In this section we develop a theoretical model of the kirigami sheet that forms the basis of Kiri-Spoon. During feeding, this kirigami sheet is pulled perpendicular to the discrete ribbons in order to create a spoon-shaped structure (see Figure 2.1 and Figure 4.1). Intuitively, the force required to deform the kirigami sheet depends on its geometry and material properties. Here we seek to better understand this intuition — specifically, we quantify the amount of tensile force needed to actuate Kiri-Spoon.

As shown in Figure 2.1, our kirigami structure is composed of three different types of interconnected ribbons that buckle and deform. Hence, to reach an overall model, we must

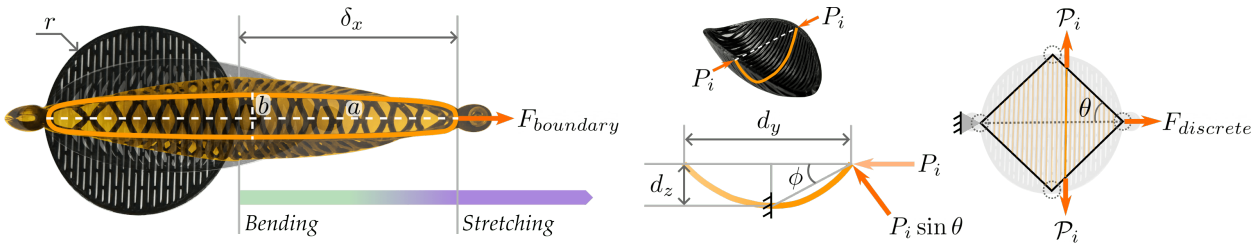


(a) Deformation of boundary ribbon

(b) Bending of discrete ribbon

Figure 4.3: Mechanics of the boundary and discrete ribbons under tensile load. (a) $F_{boundary}$ is the tensile force component needed to bend the boundary ribbon. $\delta_x$ is the total displacement from its undeformed position. The boundary starts as a circle of radius $r$ and bends into an ellipse with semi-major axis $a$ and semi-minor axis $b$. As the ellipse becomes flat, the boundary begins to stretch. (b) The boundary applies a compressive force $P$ on the discrete ribbons, bending them into an arch. $\phi$ is the angle between $P$ and the bent discrete ribbons. In response to the boundary compression, each ribbon exerts an equal opposing force on the boundary. $F_{discrete}$ is the tensile force component needed to overcome this opposing force.

consider each component. We individually analyze: (i) the force required to deform the boundary ribbon ($F_{boundary}$), (ii) the force needed to bend the discrete ribbons ($F_{discrete}$), and (iii) the force due to resistance from the mesh ribbons ($F_{mesh}$). By combining each of these components, we ultimately reach a lower bound on the force applied to the kirigami sheet as a function of its shape. Designers can leverage this mechanics model to select the materials, geometry, and actuator for their own Kiri-Spoons.

### 4.2.1 Boundary Ribbon Deformation

We start with the outer boundary ribbon that surrounds the kirigami sheet. In its equilibrium state this boundary ribbon is a circle with radius $r$. When tensile force is applied to the boundary, it deforms into an ellipse where its major axis is aligned with the direction of the applied force. We show this process in Figure 4.3(a) — let $a$ and $b$ denote the lengths of the semi-major and semi-minor axes, respectively.

**Geometry** We first calculate the dimensions of the boundary ribbon. These dimensions are practically important because food enters and exits the kirigami structure through this boundary ribbon — and we can even utilize the boundary ribbon to pinch morsels. For a displacement of $\delta_x$ in the direction of the tensile force, the length of the semi-major axis $a$ becomes $a = r + (\delta_x/2)$. To compute the semi-minor axis $b$, we assume that the length of the boundary ribbon (i.e., the perimeter) remains roughly constant during deformation. This enables us to leverage a standard formula for the dimensions of an ellipse:

$$\pi \left( 3(a+b) - \sqrt{(3a+b)(a+3b)} \right) = 2\pi r \tag{4.1}$$

The left side of Equation 4.1 is the perimeter of the deformed ellipse, while the right side is the circumference of the initially circular boundary. Solving this formula for $b$ completes the geometry of the boundary ribbon.

**Force** Given the geometry, we next compute the tensile force needed to deform the boundary ribbon. We denote this overall force as $F_{boundary}$. Intuitively, $F_{boundary}$ is what the actuator must apply in order to extend the semi-major axis in Figure 4.3(a). As we will show, there are two components of this force: bending (at low displacement) and stretching (at high displacement). Let $F_{bend}$ denote the bending component. Applying bending theory for circular rings [95], we reach:

$$F_{bend} = \frac{4EI\delta_x}{r^3} \left( \pi - \frac{8}{\pi} \right)^{-1} \tag{4.2}$$

where $E$ is the Young's modulus and $I$ is the second moment of area of the boundary cross-section. We set the initial radius of curvature for the ring to be $r$, since $r$ is the radius of the initially circular boundary. But the boundary ribbon does not remain circular throughout

deformation; hence, 4.2 is only accurate for small $\delta_x$ values. As the displacement $\delta_x$ grows the boundary ellipse becomes flat, increasing its aspect ratio $a/b$ and decreasing the radius of curvature at the ends of its major axis. As such, the actual bending force required to deform the boundary is higher than the force estimated by 4.2 (see our simulations in Appendix B.0.1).

In order to account for the inaccuracy of 4.2 at large displacement values, we next introduce the stretching force $F_{stretch}$. Consider the ellipse when fully extended. At this extreme the semi-minor axis converges to zero (i.e., $b \to 0$), and the boundary ribbon becomes two straight, parallel ribbons with length $\pi r$. Increasing $\delta_x$ any further must cause the ribbons to stretch — they are already fully extended. Accordingly, when displacement $\delta_x > r(\pi - 2)$, we set the bending force $F_{bend} = 0$ and compute the stretching force for the ribbons using Hooke's law:

$$F_{stretch} = \frac{2EA\delta_l}{\pi r} \tag{4.3}$$

Here $A$ is the area of cross-section and the change in length $\delta_l = \delta_x - r(\pi - 2)$.

Our final step for the mechanics of the boundary ribbon is to combine the bending and stretching forces. In practice, the boundary is pulled using a rigid attachment of width $2b_{min}$; hence, once the semi-major axis $b$ is equal to $b_{min}$, the boundary ribbon can no longer bend. We leverage this critical point to determine whether to apply 4.2 or 4.3. Overall, we model the total force required to deform the boundary ribbon as:

$$F_{boundary} = \begin{cases} F_{bend} & b \leq b_{min} \\ F_{stretch} & b > b_{min} \end{cases} \tag{4.4}$$

We note that 4.4 is necessarily a *lower bound* on the actual force. In practice, the boundary may start stretching even before it flattens to $b_{min}$, and the effective radius of the boundary

ribbon is not consistently $r$.

### 4.2.2 Discrete Ribbons Bending

The boundary ribbon forms the edge of the spoon, and is critical for pinching behaviors. But the base of the spoon is composed of multiple discrete ribbons — and these ribbons have an essential role in the shape of Kiri-Spoon. Interestingly, the discrete ribbons oppose the deformation of the boundary ribbon. Referring to Figure 2.1 and Figure 4.1, we note that the discrete ribbons are parallel to the minor axis of the boundary layer. When the kirigami sheet is actuated, these discrete ribbons must *bend* in order for the boundary ribbon to elongate. Consider Figure 4.3(a) and Figure 4.3(b): increasing displacement $\delta_x$ decreases the semi-minor axis $b$. This in turn compresses the discrete ribbons axially, causing each ribbon to bend into an arch. Below we derive the shape of these arches, as well as the forces the boundary ribbon applies to the discrete ribbons.

**Geometry** Building on our early work [50], we model the arch formed by a discrete ribbon as a catenary:

$$l_{ribbon} = 2\alpha \sinh(d_y/2\alpha) \tag{4.5}$$

$$d_z^2 + 2\alpha d_z - (l_{ribbon}/2)^2 = 0 \tag{4.6}$$

Here $l_{ribbon}$ is the undeformed length of the discrete ribbon, $d_y$ is the distance between its endpoints, $d_z$ is the maximum depth at its center, and $\alpha$ is a parameter that defines its shape. Because each discrete ribbon has a different length, these values will vary along the kirigami structure.

**Force** Equipped with this geometry, we next seek to determine how much tensile force is required to bend the discrete ribbons (i.e., $F_{discrete}$). Modeling $F_{discrete}$ is necessary to determine the overall force required to actuate Kiri-Spoon: in order to elongate the kirigami sheet, we must overcome the resistance of the discrete ribbons. For the $i$-th discrete ribbon, let $P_i$ be the axial force exerted by the boundary ribbon. Similarly, let $\mathcal{P}_i = -P_i$ be the equal and opposite force that $i$-th discrete ribbon applies back to the boundary. As shown in Figure 4.3(b), these forces lie in the same plane as the boundary layer.

We can compute the resistance force $\mathcal{P}_i$ as a function of the discrete ribbon's geometry and material properties. When the kirigami structure is actuated, the boundary ribbon applies a force at both ends of the $i$-th discrete ribbon. We estimate this force by treating each half of the discrete ribbon as a cantilever beam [31]:

$$P_i \sin\phi = \frac{3EId_z}{(l_{ribbon}/2)^3} \tag{4.7}$$

Within this equation the maximum deflection of the cantilever beam is set equal to the depth of the catenary. Here $\phi$ is the approximate angle between the applied force $P$ and the discrete ribbon:

$$\phi = \tan^{-1}\left(\frac{d_z}{d_y/2}\right) \tag{4.8}$$

Combining 4.7 and 4.8 enables us to solve for $P_i$, the compressive force applied by the boundary ribbon. The resistance force for the $i$-th discrete ribbon is simply the equal and opposite force: i.e., $\mathcal{P}_i = -P_i$.

We now have the resistance force from one discrete ribbon; our final step is to estimate the cumulative force $F_{discrete}$ needed to bend all the discrete ribbons. Let $n_d$ be the number of ribbons. We assume that these ribbons are spaced uniformly along the major axis of the kirigami sheet. As shown in Figure 4.3(b), the contribution of each discrete ribbon to

$F_{discrete}$ depends on the length of the ribbon (as described in 4.7), the distance between the discrete ribbon and the point of tensile load (i.e., the moment arm), and the angle $\theta$ between the tensile force direction and the boundary. As such, the force is directly proportional to the moment arm and inversely proportional to the ribbon length. For example, the discrete ribbon at the center (i.e., $i = \lceil n_d/2 \rceil$) has the greatest length, resulting in the smallest opposing force $\mathcal{P}_i$ but also the largest moment arm.

We provide detailed calculations for these effects in Appendix B.0.2. In conclusion, we find that the total tensile force due to resistance from all discrete ribbons is given by:

$$F_{discrete} = 2 \sum_{i=1}^{\lceil n_d/2 \rceil} \frac{P_i}{\tan\theta} \left( \frac{i}{\lfloor n_d/2 \rfloor + 1} \right) \tag{4.9}$$

Intuitively, in order to bend the discrete ribbons the actuator must apply a force greater than $F_{discrete}$.

### 4.2.3 Mesh Ribbons Resistance

So far we have derived the mechanics of the boundary ribbon and discrete ribbons. The only remaining element for our kirigami sheet is the mesh (see Figure 2.1 and Figure 4.1). Here we will only focus on the discrete mesh ribbons, since they are sufficient for most foods and can significantly impact kirigami mechanics. Within our design the mesh ribbons are used to interconnect the discrete ribbons. At alternating points a short mesh ribbon is placed between neighboring discrete ribbons, ultimately forming a grid-like pattern. In practice, the mesh ribbons help the Kiri-Spoon retain its shape while preventing small foods from slipping through the gaps. However, these mesh ribbons also increase the amount of force required to actuate our kirigami sheet.

**Force** We treat each of the mesh ribbons as an inextensible beam. Hence, we do not need to consider the geometry of these ribbons — just the effect that they have on actuator force. As shown in Figure 4.4, when the kirigami sheet is extended the mesh ribbons cause the attached discrete ribbons to bend. Specifically, each mesh ribbon bends a section of the discrete ribbon between prior and subsequent meshes. We consider these sections to be a simply supported beam with a center load of $Q$ [31]:

$$Q = \frac{48EI\delta_m}{l_m^3} \tag{4.10}$$

Here $l_m$ is the length of the section and $\delta_m$ is the maximum deflection of that section. The length $l_m$ is determined by the sheet's geometry (and therefore known). On the other hand, the deflection $\delta_m$ is unknown, and must be calculated as described below. Intuitively, computing $Q$ is important because it captures how tensile force is propagated along the mesh. Suppose that the first discrete ribbon ($i = 1$) is connected to the boundary layer via one central mesh (as shown in Figure 4.4). Then the overall resistance force caused by the mesh ribbons is equal to $Q_{i=1}$, i.e., 4.10 evaluated for the first discrete ribbon. We therefore set $F_{mesh} = Q_1$, where $F_{mesh}$ is the total tensile force caused by the mesh ribbons.

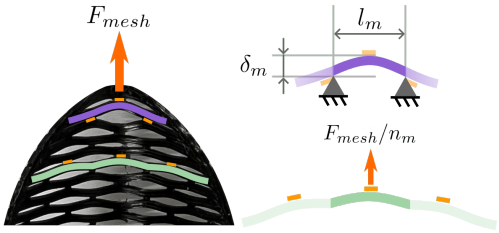


Figure 4.4: Dynamics of the mesh and discrete ribbons under tensile load. $F_{mesh}$ is the additional tensile force component needed to deform the kirigami sheet due to the mesh ribbons. The tensile force is equally divided into the mesh ribbons. Each mesh ribbon bends a section of the discrete ribbon. For example, the green ribbon is connected to three mesh ribbons. Therefore, the load on its central section is $F_{mesh}/3$ and the corresponding deflection is $\delta_{m,1}/3$. The total deflections along the central ribbon must equal the total displacement $\delta_x$.

Unfortunately, in order to apply 4.10 and find $Q_1$ we must identify the deflection $\delta_{m,1}$ of the first section. Because this first section is connected by mesh ribbons to a second section, and so on, finding $\delta_{m,1}$ becomes a recursive process. Consider the connection between the second and third discrete ribbons. To compute the force exerted by the central ribbon on the second discrete ribbon, i.e., $Q_2$, we assume that $F_{mesh}$ is equally distributed into the mesh ribbons. More formally, if there are $n_{m,i=2}$ mesh ribbons connecting the second and third discrete ribbons, the tensile load on the central section is $Q_{i=2} = F_{mesh}/n_{m,i=2}$ and the deflection in the second discrete ribbon is $\delta_{m,i=2} = \delta_{m,i=1}/n_{m,i=2}$. More generally, the deflection in the $i$-th discrete ribbon becomes:

$$\delta_{m,i} = \frac{\delta_{m,1}}{n_{m,i}} \tag{4.11}$$

We also recognize that the total deflection along the center for all discrete ribbons must equal the total deformation of the kirigami sheet in the direction of the tensile force:

$$\delta_x = \sum_{i}^{n_d} \delta_{m,i} = \delta_{m,1} \sum_{i}^{n_d} \frac{1}{n_{m,i}} \tag{4.12}$$

By leveraging 4.12 we can complete our recursive reasoning and calculate $\delta_{m,1}$. For any $\delta_x$, we first obtain $\delta_{m,1}$ using 4.12, and then apply $\delta_{m,1}$ to calculate $Q_1$ using 4.10. To overcome the resistance of the mesh ribbons and extend the kirigami sheet, the actuator must apply a force greater than $F_{mesh} = Q_1$.

### 4.2.4 Summary

We conclude our mechanics analysis by combining each of the effects covered in Sections 4.2.1, 4.2.2, 4.2.3. By adding the forces applied by the boundary ribbon, discrete ribbons, and

Table 4.1: Kirigami sheet properties

| Sheet | Material | Radius (mm) | Thickness (mm) | Ribbon width (mm) |
|---|---|---|---|---|
| **A** | TPU | 22.24 | 1 | 1 |
| B | TPU | 22.24 | 1.5 | 1 |
| C | TPU | 16.68 | 1 | 0.75 |
| D | PET | 22.14 | 0.25 | 0.8 |

mesh ribbons, we reach a lower bound on the total tensile force $F_{tensile}$ needed to actuate Kiri-Spoon.

$$F_{tensile} = F_{boundary} + F_{discrete} + F_{mesh} \tag{4.13}$$

The force $F_{tensile}$ is a lower bound because of the approximations necessary to capture interconnected ribbon mechanics. As we will show in the following validation tests, however, this is a *tight* lower bound with errors less than 1 N across different kirigami materials and geometries. Typical micro linear actuators that apply forces up to 50 N can easily compensate for this error.

### 4.2.5 Validation Experiments

Our theoretical model simplifies the calculation of the force required to actuate the kirigami sheet and the dimensions of the resulting kirigami structure. We now test this model to validate whether our approximations hold in practice, and to see if other designers can apply our model to develop their own Kiri-Spoons. For validation experiments we created four kirigami sheets with varying geometries and material properties (see Table 4.1), and compared our model predictions to the actual forces and sheet dimensions during testing.

We designed sheet A based on stakeholder feedback, using a soft TPU material and a radius tuned for user comfort while eating. To investigate how the thickness of the kirigami sheet affects the actuation force, we increased its thickness to create sheet B. Next, we varied the

radius of sheet A while maintaining the same sheet thickness and the number of discrete ribbons to produce sheet C. Finally, we fabricated sheet D using the PET material which has been used in previous kirigami-based grippers [105]. This PET material was described by our stakeholders as "too stiff" to be comfortable for eating.

We tested each of these sheets by attaching one end to a calibrated force sensor, and the opposite end to a linear screw. The screw was initially set to the undeformed length of the sheet and then actuated in increments of $\delta_x = 5$ millimeters (mm). Moving the screw displaced the boundary ribbon perpendicular to the discrete ribbons, causing the kirigami structure to deform into a 3D bowl. For each increment of displacement, we recorded the force measured by the sensor and the width of the deformed boundary ribbon.

Figure 4.5 summarizes our results. On the left, we illustrate our model predictions for sheet A. Using 4.1, we can accurately estimate the half-width (i.e., the semi-minor axis $b$) of the boundary up to $\delta_x = 20$ mm. For larger displacements, the boundary starts to stretch, increasing its length and causing our model — which assumes a constant boundary perimeter — to underestimate the width. Our model also closely approximates the tensile force needed to deform the kirigami sheet. The predicted force within our results is lower than the measured force primarily because we do not account for stretching until the boundary reaches its minimum width, as defined in 4.4.

On the right of Figure 4.5 we plot the mean absolute error in the model predictions for each different kirigami sheet. The average error in the predicted half-widths is only 2 mm for all sheets except B. Our rational here is that — as the thickness of the sheet increases — the discrete ribbons apply a greater opposing force on the boundary, increasing its width. However, our model does not account for this force when estimating the boundary dimensions. We also find that the average error in the predicted forces is less than 1 Newton (N) for all sheets except D. This is because sheet D is made of PET, which has a Young's modulus ($E$)

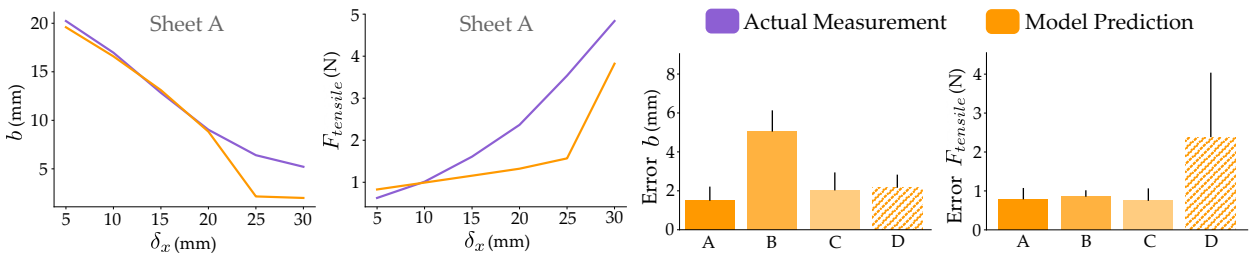


Figure 4.5: Results of validation experiments in Section 4.2.5. (Left) The half-width $b$ (semi-minor axis) and total tensile forces $F_{tensile}$ predicted by our model for sheet A. The predicted and measured widths closely align up to a displacement of $\delta_x = 20$, while the predicted forces underestimate the actual tensile force required to deform the kirigami sheet. Our predictions deviate from the actual measurements because we do not account for the torsion or stretching of the boundary ribbon before reaching the minimum width of $b_{min}$. (Right) For all sheets except B, the mean absolute error in the predicted half-width is approximately 2 millimeters (mm). Moreover, the mean absolute error in the predicted forces is less than 1 Newton (N) for all sheets except D. Note that sheet D has a significantly higher Young's modulus, leading to larger deformation forces. We use sheet A in our robot experiments.

of 3.57 GPa — approximately 200 times that of 3-D printed TPU — which has $E = 14.77$ MPa. As a result, the forces required to deform sheet D are significantly higher than the TPU sheets, leading to higher absolute prediction errors. Yet, across all sheets, the average error in our predictions is less than 25% of the maximum force required to actuate the sheets fully.

**Summary and Personalization** Our validation tests suggest that the proposed mechanics model is an accurate lower bound (i.e., $<$ 1N error) for the tensile force required to actuate kirigami sheets of varying thicknesses, sizes, and materials. In the subsequent experiments — including Sections 4.3, 4.4, and 4.5 — we will apply a Kiri-Spoon with sheet A. This particular sheet was designed based on the subjective feedback of our stakeholders, and we applied the theoretical forces calculated for this sheet to choose a suitable lead screw and motor for actuating our Kiri-Spoon.

However, we recognize that each individual user may prefer kirigami sheets of different size,

thickness, or material, and this preference may vary based on the types of foods that user consumes. To account for this personalization, designers can manufacture a customized sheet by starting with our CAD models and then modifying the dimensions according to their end-user's needs. For example, a wider kirigami sheet may be more suitable for stakeholders who prefer to take bigger bites of food — but this change would also require higher actuation forces. Designers can leverage our mechanics model to compute the maximum force required to actuate the kirigami sheet fully, and then select a linear actuator that reliably supplies that force.

## 4.3 Autonomous Acquisition

We have presented our design for Kiri-Spoon, and modeled the mechanics of this kirigami utensil. Next, we begin to test Kiri-Spoon's capabilities: can our utensil created specifically for robot arms effectively and easily acquire a wide range of bite-sized foods? In this section we compare a robot arm equipped with traditional forks and spoons to the same robot using a Kiri-Spoon. To measure the best-case performance of each system, we autonomously control the robot arm using a state-of-the-art algorithm for robot-assisted feeding. Our objective is to evaluate the mechanical advantage offered by Kiri-Spoon; i.e., whether adding Kiri-Spoon will make the overall system more effective at picking up diverse foods such as carrots, peas, tofu, cereal, jello, and soup. We hypothesize that Kiri-Spoon's ability to encapsulate the bites will enable it to more successfully pick soft and slippery foods, which often slide off spoons and forks. Moreover, while regular forks need to be precisely oriented for successful acquisition, we expect the Kiri-Spoon to be equally effective while maintaining a constant orientation because of its compliant structure.

**Task and Experimental Setup** Images of the attached Kiri-Spoon and target foods are shown in Figure 4.6. We mounted each feeding utensil in place of the end-effector for a 7-DoF Franka Emika robot arm [28], To detect foods, we also mounted an Intel RealSense D435 camera on the robot's wrist. The robot used its utensil and camera to autonomously perform two types of acquisition tasks: (i) *picking* food off a plate and (ii) *scooping* food from a bowl.

For *picking*, we autonomously controlled the acquisition motion using a pre-trained *Skewering-Position-Action Network (SPANet)* [25, 33]. This network outputs the target position $(x, y, z)$, roll $\gamma$, and pitch $\beta$ of robot's fork based on the location and orientation of the detected food. Similar to prior work, we discretized the pitch into three angles: $-45°$ (*tilted backward*), $0°$ (*vertical*), and $+45°$ (*tilted forward*). While we adjusted the pitch of the traditional fork based on the SPANet output, we maintained a constant pitch of $\beta = 45°$ for the Kiri-Spoon (see Figure 4.6, Left). For *scooping*, we pre-programmed a fixed motion pattern for both the traditional spoon and the Kiri-Spoon. This motion pattern was tuned in offline experiments to maximize the success rate of the traditional spoon. In addition to controlling the robot's motion, we used an Arduino Uno board to autonomously actuate Kiri-Spoon to a pre-defined spoon-like shape in the scooping task and to a high curvature state in the picking task after reaching the food.

**Independent Variables** We compared the acquisition performance of the Kiri-Spoon to a traditional fork in the picking task and to a traditional spoon in the scooping task. Inspired by related works [25, 55, 87], we selected five foods of varying size, shape, hardness, and consistency for each task to test the Kiri-Spoon in acquiring diverse foods. The robot manipulated its traditional fork to try to pick up carrots, cherry tomatoes, peas, silken tofu, and lettuce bites (Figure 4.6, Top). Similarly, the robot leveraged its traditional spoon to try

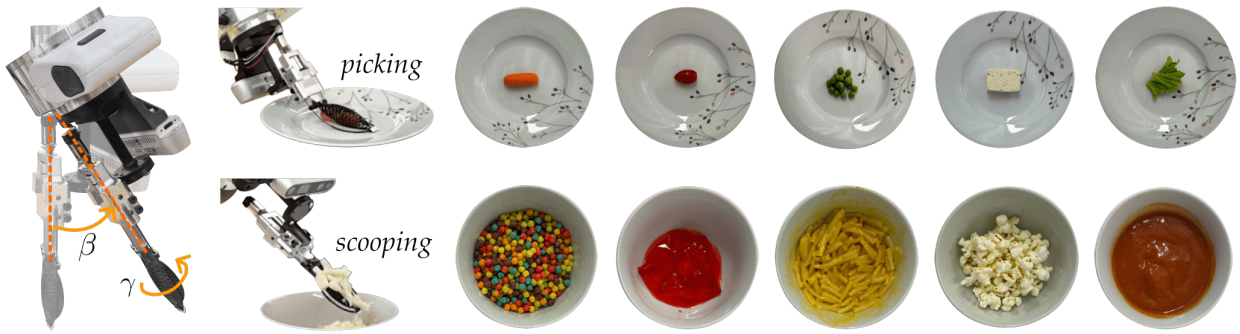


Figure 4.6: Experimental setup for the autonomous tests in Section 4.3. (Left) Position and orientation of Kiri-Spoon during autonomous acquisition. When picking foods from a plate, the flexible hoop and kirigami sheet bend to align with the orientation of that plate. Upon reaching the target position, we rapidly increase the curvature of the kirigami sheet to firmly grasp the desired food. In contrast, Kiri-Spoon maintains a spoon-like curvature when scooping food from a bowl. (Right) Foods used in our acquisition experiments. For picking, we include round foods of different sizes, i.e., carrots, cherry tomatoes, and peas. We also test with soft and slippery foods like silken tofu and flat foods like lettuce. For scooping, we include dry foods like cereal and popcorn, sticky foods like macaroni and cheese, slippery foods like jello, and liquid foods like tomato soup.

to scoop cereal, macaroni and cheese, jello, popcorn, and tomato soup (Figure 4.6, Bottom). After completing trials with the traditional utensils, the robot then attempted to iteratively acquire, carry, and release all of these foods using a single Kiri-Spoon and its food-safe kirigami sheet. The robot's control algorithm remained constant across the experiment.

**Dependent Variables** The robot arm attempted to pick or scoop each food 10 times using both the traditional utensils and the Kiri-Spoon. In the picking task we recorded the percentage of **successful attempts**, while in the scooping task we measured the total **weight of food** collected over 10 attempts. We considered an individual acquisition attempt to be successful if the food stayed on the utensil for 5 seconds after it was picked. For a fair comparison of the weight of food acquired, we ensured that the spoon and Kiri-Spoon had similar volumes.

### 4.3.1 Results

Our experimental results are summarized in Figure 4.7. These results should be viewed as the current *best case* performance for robot arms using forks and spoons; we applied assistive eating algorithms specifically designed for these utensils, and tuned the experimental setup to maximize their performance. But even in this best-case setting, we found that Kiri-Spoon matched or outperformed the traditional utensils across most foods. Kiri-Spoon picked up all types of foods besides lettuce with a success rate of more than 80%. Lettuce was a failure case for Kiri-Spoon: its flat, thin surface stuck to the plate, and Kiri-Spoon was unable to get purchase to pinch the morsel. On the other hand, the robot was usually able to pick up lettuce with a traditional fork. Fundamentally, Kiri-Spoon employs a different grasping mechanism than standard forks — while the fork skewers the food to hold it using friction, Kiri-Spoon encapsulates the food within its kirigami bowl. It is therefore challenging for Kiri-Spoon to pick up items that lay flat on the plate, as well as foods that are larger than the radius of its kirigami sheet.

By contrast, Kiri-Spoon's mechanical intelligence enables the robot to successfully grasp a diverse set of foods without ever changing end-effector orientation. When robots use standard forks, prior works and our results demonstrate that the fork's orientation and manipulation is crucial for acquisition [25, 33, 55, 90]. For example, to pick up round and cylindrical foods like carrots, tomatoes, and peas, the traditional fork needs to have a pitch $\beta = 0°$ so that its tines enter the food vertically and the item does not roll away. But when the robot is using a fork to pick up soft and slippery foods like silken tofu, the tines need to be angled to ensure that the food stays on the fork. In contrast to the fork — which the robot arm needs to carefully manipulate — the robot can hold Kiri-Spoon at a constant orientation. In Figure 4.7 Kiri-Spoon successfully encapsulates and carries both food types while keeping a constant pitch of $\beta = 45°$. This capability can especially be useful in

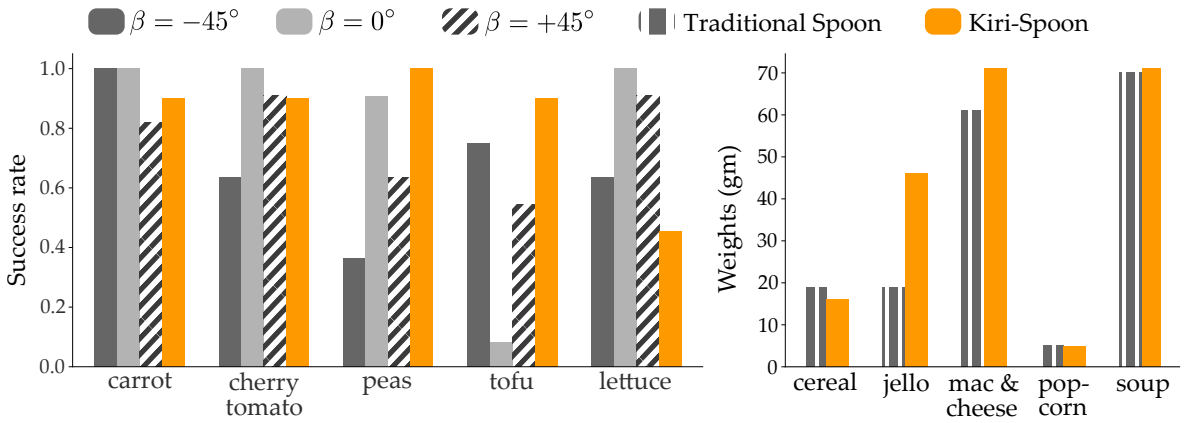


Figure 4.7: Results for autonomous acquisition tests in Section 4.3. (Left) Kiri-Spoon successfully picks round foods such as carrots, tomatoes, peas, and tofu, but struggles to pick flat foods like lettuce as compared to a traditional fork. While the pitch of the fork needs to be changed according to the shape and hardness of the food, Kiri-Spoon is easier to control because it does not require any pitch adjustment. (Right) Kiri-Spoon scoops the same amount of dry and sticky foods as a traditional spoon. Across both tasks, Kiri-Spoon outperforms the traditional utensils in acquiring slippery foods like jello and tofu.

constrained environments where reaching the desired angle for a fork can cause collisions with objects on the dining table. In such scenarios, a robot leveraging Kiri-Spoon can move to an orientation that avoids collisions and use its flexible hoop to reach and successfully acquire the food.

Now focusing on the scooping task, we find that Kiri-Spoon functions similar to traditional spoons for both dry foods, such as cereal and popcorn, and sticky foods, like macaroni and cheese. However, the two utensils perform differently for slippery foods (e.g, jello). When handling slippery foods with traditional spoons the jello can easily slide off the utensil, particularly if the robot moves quickly or with the wrong angle. Kiri-Spoon is more effective here because it encapsulates the slippery jello pieces within its kirigami structure, preventing them from accidentally falling. We note that for all the foods except soup we leveraged a kirigami sheet with a discrete mesh (see Figure 4.1, Top). This was sufficient to acquire and carry foods with solid or viscous components. But for the soup — which was a liquid — we applied a kirigami sheet with a continuous mesh (see Figure 4.1, Bottom). This continuous

mesh was necessary to keep the soup from flowing out of the bottom of Kiri-Spoon. Across autonomous testing we did not find that the type of mesh had a noticeable affect on our Kiri-Spoon performance; both mesh types can be used interchangeably. We typically prefer the discrete mesh because it is easier to manufacture and actuate. While kirigami sheets with a discrete mesh can be directly 3D printed, manufacturing the continuous mesh requires using an ellipsoidal mold to shape the membrane before the sheet can be printed onto it.

**Summary** Our autonomous tests highlight three mechanical advantages of Kiri-Spoon. First, Kiri-Spoon is a single feeding utensil that can function both as a fork (picking carrots from a plate) and as a spoon (scooping soup from a bowl). This utility is practically important for assistive feeding scenarios since changing utensils means that the robot arm must switch its end-effector. Instead of detaching a fork to mount a spoon — or *vice versa* — here the robot arm can stick with just a single utensil. Second, we find that the robot arm can effectively leverage Kiri-Spoon like a fork without needing to change its orientation. This makes the arm's manipulation task easier: the system does not need to tune the end-effector angle to pick up different types of foods. Finally, while the Kiri-Spoon struggles to consistently pick large and flat foods like lettuce, it outperforms traditional utensils in handling slippery foods such as jello and tofu. This matches our expectations — Kiri-Spoon can enclose foods within its kirigami structure, thereby preventing morsels from unintentionally falling during interaction.

## 4.4 User Studies with Participants with Disabilities

Our autonomous study in Section 4.3 demonstrated that Kiri-Spoon can effectively acquire, carry, and release a diverse set of bite-sized foods. This functionality suggests that —

from the robot's perspective — Kiri-Spoon is an advantageous utensil. But what about the human's perspective? In this section we interact with stakeholders who require assistance during eating to assess the comfort and performance of Kiri-Spoon. The purpose of these studies is to determine whether Kiri-Spoon addresses the needs of its intended users.

We performed this experiment across two sessions at The Virginia Home [93]. During both sessions the Kiri-Spoon was attached to an Obi [63], a table-top robot arm and bowl system that is commercially available for assistive feeding (see Figure 4.8, Left). By default, the Obi is equipped with a traditional spoon that it employs to scoop foods from the bowl and carry them to the user's mouth. We compared this default setup to an Obi with our Kiri-Spoon mounted in place of the standard spoon. Our first experimental session focused on identifying the design characteristics necessary for a comfortable Kiri-Spoon (also see Section 4.1). Given this guidance from the stakeholders, in our second experimental session we returned with a finalized Kiri-Spoon. Here occupational therapists and $N = 4$ residents with mobility limitations compared our finalized Kiri-Spoon to the traditional spoon, and we collected objective and subjective results from their interactions. Both of these user studies followed the same general procedure. We have already discussed the design considerations (i.e., the outcomes of the first session) in Section 4.1. Accordingly, here we will focus on our experimental procedure and results from the second visit with stakeholders[2].

**Experimental Setup** In both visits we tested the Kiri-Spoon attached to an [63], a medical device specifically designed for assistive feeding. The Obi consists of a 6-DoF robot arm and utensil with four bowls for storing food (see Figure 4.8, Left). Participants were able to control Obi using two switches: one to change which bowl the robot will scoop from, and the other to scoop food from that bowl and bring it to the human's mouth. The simplicity of the

[2]For videos of this study and our other experiments, please see https://youtu.be/ZJpQREdTz80

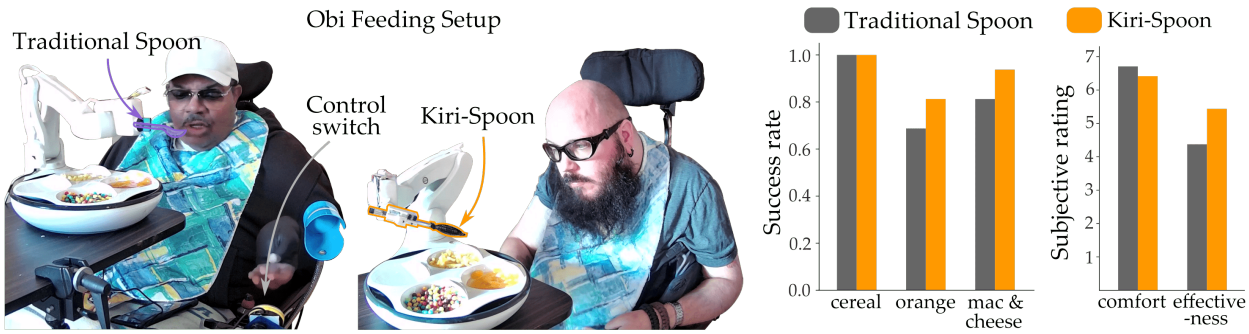


Figure 4.8: Experimental setup and results from our second round of stakeholder tests in Section 4.4. (Left) Residents of The Virginia Home interacting with the Obi feeding device and scooping food using a traditional spoon and Kiri-Spoon. (Right) Objective and subjective results across $N = 4$ adults who require assistance when eating. Kiri-Spoon had a slightly higher success rate than the traditional spoon when picking canned oranges (i.e., a slippery food) and macaroni and cheese (i.e., a sticky food). Both utensils were equally effective at picking cereal (i.e., a dry food). Overall, users perceived the Kiri-Spoon to be almost as comfortable as the traditional spoon while being more effective in picking and securely carrying the food to their mouth.

control interface enables users with mobility impairments to feed themselves independently. We positioned the control switches according to the mobility range of each participant. In addition, we integrated Kiri-Spoon within the robot's control circuit so that it automatically closed its kirigami sheet when scooping the food, and then opened that kirigami sheet after the morsel was brought to the human's mouth. The additional weight of the Kiri-Spoon had no discernable impact on Obi's ability to scoop and lift the food to the user's mouth.

**Participants** During both visits to [93], we interacted with $N = 4$ residents living with upper-limb mobility impairments. Three of these residents participated in both sessions but the fourth participant was different in each session. All participants were adult men aged $40 \pm 10.5$ years, and they each provided informed consent in accordance with Virginia Tech University guidelines (IRB #22-308). Three of the participants identified themselves as quadriplegic, and the two other participants self-identified as having limited arm mobility or arm spasms. All of these users reported that they depend upon a caregiver everyday in order

to eat their meals. The leading occupational therapist from The Virginia Home supervised the sessions to ensure the participant's safety.

**Independent Variables** The Obi is pre-programmed to execute scooping motions using a fixed trajectory, and this system cannot perform picking tasks. Therefore, in this study we only compared **Kiri-Spoon** to a **traditional spoon**. Participants used the Obi equipped with both utensils to scoop and eat three different types of foods. In accordance with the participant's preferences, we tested a dry food (cereal), a sticky food (macaroni and cheese), and a slippery food (canned oranges). The experiments followed a within-subjects design: all participants attempted to scoop and eat each type of food four times with the traditional spoon, and four times with Kiri-Spoon. The order of presentation was balanced so that half of the participants started with Kiri-Spoon.

**Dependent Variables** We collected objective and subjective measures for each utensil. To assess objective performance, we recorded the number of scooping attempts where the Obi successfully acquired food. We report this metric as *Success Rate*, defined as the number of successful acquisitions divided by the number of attempted acquisitions. To better assess the stakeholder's subjective perception of the system, we asked each participant to answer a survey after using both utensils. The survey items are listed in Table 4.2. We grouped these items into two scales: **Comfort** and **Effectiveness**. Items in the comfort scale assessed the perceived comfort, intuitiveness, and safety of each feeding utensil. Items in the effectiveness scale measured the perceived ability of the utensils to successfully acquire, carry, and transfer morsels without spilling. Finally, at the end of each session we asked participants to indicate their preferred feeding utensil (forced-choice question), and provide open-ended responses about the advantages and limitations of Kiri-Spoon.

Table 4.2: Survey for participants living with physical disabilities (Likert scales with 7-options)

| |
|---|
| **Comfort:** |
| Q1. This utensil was comfortable to use. |
| Q2. This utensil was jarring to use and not comfortable. |
| Q3. This utensil was simple to figure out how to eat off of. |
| Q4. It was difficult to understand how to eat out of this utensil. |
| Q5. I felt safe and comfortable being fed using this utensil. |
| Q6. I felt apprehensive being fed by this utensil. |
| **Effectiveness:** |
| Q7. The utensil picked up the desired food consistently. |
| Q8. This utensil was unable to get a lot of food. |
| Q9. I felt like this utensil kept the food secure until it reached me. |
| Q10. I was often worried the food would fall off the utensil. |

### 4.4.1 Results

Our results from experiments with the finalized Kiri-Spoon are summarized in Figure 4.8 (Right). For these results, we note that the sample size ($N = 4$) was not sufficient to reliably perform statistical tests.

Objectively, both utensils had similar success rates. The spoon and Kiri-Spoon acquired cereal in all trials, and the Kiri-Spoon was marginally better at scooping slippery oranges as well as sticky macaroni and cheese. Subjectively, users perceived the regular spoon to be comfortable to use and eat from. This outcome was expected given people's familiarity with traditional spoons. Interestingly, participants rated the Kiri-Spoon to be almost as comfortable as the regular spoon despite their lack of familiarity with this device. We also found that stakeholders perceived the Kiri-Spoon to be more effective: they felt that the quantity of food acquired by the Kiri-Spoon — and the security with which the Kiri-Spoon

held that food — made it more reliable.

Overall, half of the participants said that they preferred eating from the Kiri-Spoon while the other half preferred the regular spoon. Participants who liked using the Kiri-Spoon said that it was "more secure when it came to picking up food" and that "the spoon was not better than the Kiri-Spoon in any way." Participants who preferred the regular spoon did not provide any specific reason for their choice and stated that there was "nothing worse about the Kiri-Spoon."

**Summary** By including stakeholders in the design process we were able to arrive at a Kiri-Spoon that participants found as comfortable as a traditional spoon. Consistent with our results from Section 4.3, stakeholders also perceived Kiri-Spoon to be more effective than a standard utensil — and this stakeholder viewpoint is critical as we develop assistive systems for real-world users. However, we recognize that our results are necessarily limited because of the $N = 4$ sample size. As such, in the next section we conduct a follow-up study on users without disabilities to more precisely test the benefits of Kiri-Spoon. We wish to evaluate the comfort and effectiveness of Kiri-Spoon in both scooping and picking tasks with a larger number of participants.

## 4.5 User Study with Participants without Disabilities

To more precisely analyze the role of Kiri-Spoon within robot-assisted feeding, we conducted a final user study on participants without disabilities. A variety of related works have developed *algorithmic intelligence* that enables robot arms to dexterously manipulate utensils and feed users. By contrast, in this paper we propose to leverage *mechanical intelligence* to make assistive eating easier. For this final study we therefore explore the independent

and complementary effects of both directions. Participants interact with a 6-DoF UR5 [97] robot arm to grasp, carry, and eat diverse foods. We vary the *algorithm* that controls the robot arm: in one condition users teleoperate the robot throughout the task, and in the other condition the robot leverages state-of-the-art methods to autonomously acquire and transfer foods. We also vary the *utensil* that the robot manipulates: similar to Section 4.3, we compare Kiri-Spoon to traditional forks and spoons. Overall, the goal of this section is to measure how algorithmic and mechanical advances *separately* contribute to robot-assisted feeding, as well as how the *combination* of control software and utensil hardware improves system performance.

**Independent Variables** We varied the robot along two axes: (a) its *feeding utensil* and (b) its *control algorithm*. For feeding utensils, we compared **traditional utensils** to **Kiri-Spoon**. When the desired food required stabbing (i.e., grapes), the robot used the fork, and when the desired food needed scooping (i.e., cereal), the robot used the spoon. By contrast, in the Kiri-Spoon condition the robot applied our utensil across all foods. For the control algorithm, we compared manual teleoperation (**manual**) to autonomous food acquisition (**auto**). During manual teleoperation participants used a joystick to modulate the position and orientation of the end-effector when acquiring the food. On the other hand, in the autonomous mode the robot used SPANet [25, 33] to detect the food item and choose the appropriate acquisition strategy. After acquiring the food, participants teleoperated the robot to bring the food to their mouths. The robot maintained a speed of 0.15 meters/second during teleoperation across all conditions.

**Participants** We recruited 16 adults without mobility limitations (4 female, 3 non-binary, ages $22.5 \pm 2.5$ years) from the Virginia Tech community. All participants provided informed written consent as per the university guidelines (IRB #22-308). The study followed a within-

subjects design: each participant used both control algorithms (**manual** and **auto**) and interacted with both feeding utensils (**traditional** and **Kiri-Spoon**). We balanced the order of control algorithms and feeding utensils using a Latin square design to account for ordering effects. Put another way, the same number of participants started with **manual**, **traditional** as started with **auto**, **Kiri-Spoon**.

**Study Procedure** Images of our experimental setup are shown in Figure 4.9. Participants interacted with a 6-DoF UR5 robot arm [97] that had utensils attached to its end-effector. Using this assistive arm, participants fed themselves four different bite-sized foods. The selected foods were a subset of the items tested in our previous experiments, but were tailored to be more appetizing for the participants. Specifically, the foods included grapes, orange slices, cereal and canned oranges. We selected these foods in order to test morsels with different shapes, sizes, and textures. To acquire the grapes and orange slices the robot needed to use picking motions (i.e., leveraging a plate and fork). Alternatively, to acquire the cereal and canned oranges — which included the juice from the can — the robot had to perform scooping motions (i.e., leveraging a bowl and spoon). Once the food had been picked or scooped the participants brought it to their mouths and ate the morsels.

After the participants were introduced to the system they had five minutes to practice manipulating the joystick and utensils. The participants then attempted to eat each of the foods under every combination of control strategy and feeding utensil. For a given trial, participants were allowed a maximum of three attempts. If the user was unable to acquire, carry, and transfer the desired morsel to the mouth across all three attempts, that trial was marked as a failure and the user moved on to the next trial.

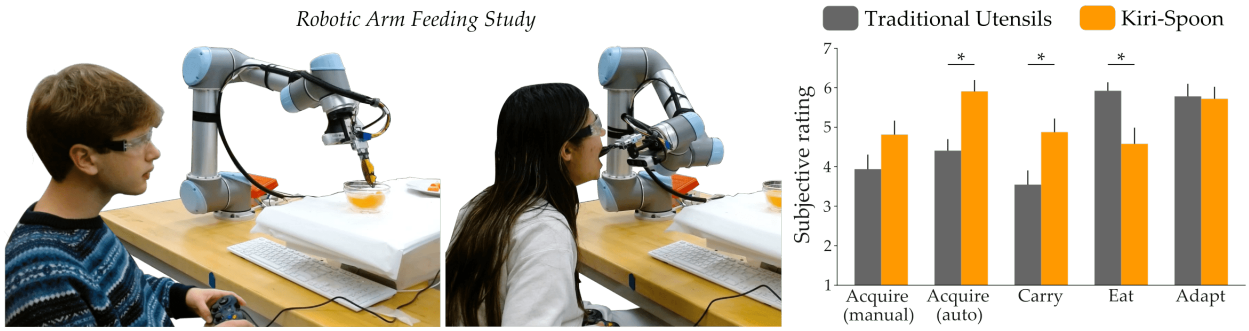


Figure 4.9: Experimental setup for our comparison of mechanical and algorithmic intelligence in Section 4.5. We varied the robot's control algorithm and the feeding utensil, and explored the effects of both variables. (Left) Users teleoperating the robot arm to scoop food from the bowl and then eating that food from the feeding utensil. (Right) Subjective results. While users found it equally difficult to manually acquire food using traditional utensils and Kiri-Spoon, they perceived Kiri-Spoon to be significantly more effective than the traditional utensils when acquiring food autonomously. Users also rated the Kiri-Spoon to be more secure and easier to control when carrying the acquired food to their mouths. On the contrary — perhaps because of their familiarity with spoons and forks — users found it more comfortable to eat morsels from traditional utensils as compared to Kiri-Spoon. The error bars indicate standard error.

**Dependent Variables** We recorded both objective and subjective measures to assess the independent and combined effects of control algorithm and feeding utensil.

**Objective Metrics** For each condition we found the number of *attempts* required to successfully acquire food, the *amount* of food acquired after all attempts, and the *total time* required to eat all four foods using each feeding utensil and acquisition strategy. While the spoon and Kiri-Spoon had similar volumes, every type of food had a different size and weight. To account for this variation, we measured *amount* by counting the number of items acquired in each attempt — e.g., the number of orange slices or cereal particles — and normalizing the counts across food types. We also measured the complexity of operating each feeding utensil by recording the total *position* and *rotation* joystick inputs provided by users.

Table 4.3: Survey for participants without physical disabilities (Likert scales with 7-options)

| |
|---|
| **Acquire (Manual):** |
| Q1. It was effective and easy to pick up food manually. |
| Q2. I struggled to pick up food when controlling the robot manually. |
| **Acquire (Autonomous):** |
| Q3. It was effective and easy to pick up food autonomously. |
| Q4. I struggled to pick up food when controlling the robot autonomously. |
| **Carry:** |
| Q5. It was easy to carry food using the utensil with minimal spills. |
| Q6. It was difficult to carry food with the utensil without dropping it. |
| Q7. I was not worried about dropping food when bringing it to my mouth. |
| Q8. I had to be precise to not drop the food when bringing it to my mouth. |
| **Eat:** |
| Q9. It was easy to get the food off of the utensil and into my mouth. |
| Q10. It was difficult to get the food off of the utensil to feed myself. |
| Q11. This utensil was comfortable to eat off of. |
| Q12. This utensil was jarring to eat off of and not comfortable. |
| **Adapt:** |
| Q13. I was able to understand and adapt to the utensil with little effort. |
| Q14. I was not sure how to use the utensil throughout the trial. |

**Subjective Metrics** After participants completed each individual condition we administered a 7-point Likert scale survey [77]. The items from this survey are listed in Table 4.3. Overall, the survey is divided into five scales: how easy it was to *acquire* the food manually versus autonomously, how easy it was to *carry* the food securely to the human's mouth, how comfortable it was to *eat* the food from the utensil, and whether users were able to *adapt* to that utensil. Additionally, after users completed the experiment we asked them to indicate their preferred utensil and control algorithm using a forced-choice paradigm.

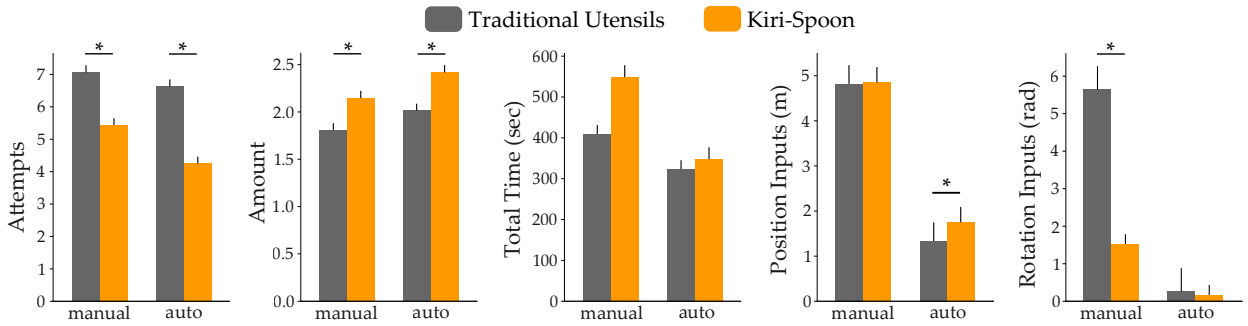


Figure 4.10: Objective results from our study in Section 4.5. Participants interacted with a robot arm using two control algorithms: either manual teleoperation or autonomous acquisition. For each control option, we tested robots equipped with traditional utensils (i.e., forks and spoons) or Kiri-Spoon. Our results show that Kiri-Spoon reduces the number of attempts required to pick up foods, and increases the amount of food acquired. Importantly, this trend is consistent regardless of the control algorithm, suggesting that Kiri-Spoon offers a fundamental mechanical advantage. Kiri-Spoon increased the amount of time required to eat in the manual condition, likely because users were unsure how to teleoperate Kiri-Spoon. Finally, Kiri-Spoon does not require precise orientation to acquire foods, leading to fewer rotation inputs during feeding task. The error bars indicate standard error.

### 4.5.1 Objective Results

Figure 4.10 summarizes our objective results. We performed a two-way ANOVA with repeated measures to evaluate the effects of *feeding utensil* and *control algorithm* on each of the dependent variables.

First, we observed that users required the least number of *attempts* and acquired the largest *amount* of food when using Kiri-Spoon with autonomous acquisition. Our results indicated significant main effects for **feeding utensil** ($p < 0.001$) and **control algorithm** ($p < 0.05$) on the number of *attempts*. We also found significant main effects for **feeding utensil** ($p < 0.01$) and marginal significance for **control algorithm** ($p = 0.057$) on the *amount* of food acquired. There was no significant interaction between the two independent variables for either attempts or amount. Interestingly, on average, *users acquired more food and needed fewer attempts when controlling the Kiri-Spoon manually as compared to using*

*traditional utensils with autonomous control*. This suggests Kiri-Spoon can contribute to assistive feeding independent of the control algorithm used by the robot arm. Overall, we find that both the mechanical advantages of Kiri-Spoon and the algorithmic advancements of recent autonomous approaches enhance efficiency and success of food acquisition.

Next, we observed that while users required fewer attempts with Kiri-Spoon, they took more *total time* using this utensil. Our results indicated no significant main effect for **feeding utensil** ($p = 0.305$) but a significant main effect for **control algorithm** ($p < 0.05$) on the *total time*, with a marginally significant interaction between these two independent variables ($p = 0.059$). Put another way, we found that the time efficiency of Kiri-Spoon was dependent on the choice of acquisition strategy. When participants had to teleoperate the robot arm, Kiri-Spoon added additional time; we suspect that this may have occurred because users were unfamiliar with how to manipulate Kiri-Spoon. By contrast, when Kiri-Spoon was controlled autonomously, the total time was comparable to traditional utensils.

Lastly, we investigated the number of *joystick inputs* that users needed to control the *position* and *orientation* of the feeding utensils. As a reminder, in the manual condition participants used a joystick to teleoperate the robot arm throughout the entire task. In the autonomous condition the robot acquired foods without any assistance — but users still needed to leverage the joystick at the end of the task to safely move the robot closer to their mouth. Hence, we would expect that autonomous acquisition leads to fewer inputs than manual teleoperation; and indeed, **control algorithm** had a significant main effect for both position ($p < 0.001$) and rotation ($p < 0.001$). When comparing Kiri-Spoon to traditional utensils, users applied roughly the same number of inputs for position ($p = 0.138$). On the other hand, **feeding utensil** had a significant effect on the number of orientation inputs ($p < 0.01$). In Section 4.3 we found that Kiri-Spoon could leverage its flexible structure to acquire foods without changing orientation; this trend continued here, where participants

picked and scooped foods without having to tune the angle of Kiri-Spoon.

**Summary** Our objective results demonstrate the complementary benefits of using the mechanically superior Kiri-Spoon design with recent autonomous approaches for food acquisition. When controlled autonomously, Kiri-Spoon was able to acquire the most amount of food in the least number of attempts. It also needed fewer rotational inputs than standard utensils when being controlled manually. However, the additional step of having to actuate the kirigami sheet negatively impacted its time efficiency, especially during user teleoperation. We suggest that this effect may have been caused by the novelty of our system, and perhaps users more familiar with Kiri-Spoon will not require added time.

### 4.5.2 Subjective Results

Given our objective results, we now change gears to focus on how users subjectively perceived the assistive robot. Our overall subjective results are displayed in Figure 4.9, Right.

Participants thought it was easier to acquire and carry foods using Kiri-Spoon as compared to traditional utensils. A paired t-test indicated a significant difference between traditional utensils and Kiri-Spoon when acquiring the food autonomously ($p < 0.01$), and for carrying that food without spilling ($p < 0.05$). However, users provided a higher rating ($p < 0.05$) for the comfort of traditional utensils. This is not unexpected; forks and spoons have been optimized for human comfort over thousands of years [27].

Despite the lack of comfort, 10 out of 16 users stated that they would prefer to use Kiri-Spoon over traditional utensils. In addition, 2 of the remaining 6 users felt that both utensils were equal. Participants explained their preference by stating that "the Kiri-Spoon was much more versatile than the traditional utensils, and excelled at picking up every type of

food" even though it was "bit less comfortable." One of the users also mentioned that they "enjoyed the flexibility of the Kiri-Spoon" which "made picking up food easy and intuitive", whereas the "traditional utensils were difficult to control due to their rigid nature." Users who preferred the traditional utensils said that they "enjoyed the traditional utensil because it was stagnant in their mouth." These comments indicate that — at least for some users — the mechanical advantages offered by the Kiri-Spoon outweigh its lack of comfort as compared to traditional utensils. Lastly, when asked about their preferred control approach, 10 out of 16 users chose autonomous acquisition, stating that "autonomous feeding saves more effort."

**Future Improvements** Some users also provided comments that present directions for improving the Kiri-Spoon in future work. For instance, one user stated that they wished to have "more control options over the Kiri-Spoon" such as the ability to "flip it upside down to press it down on the food and close it" for all tasks. Another user stated that "the Kiri-Spoon with lots of practice would be ideal in combination with a fork." Based on these comments, in future work, we intend to equip Kiri-Spoon with soft fork-like tines that can skewer flat foods, and then evaluate user perceptions of Kiri-Spoon after long-term use. We hypothesize that once people get familiar with using the Kiri-Spoon — as they are with traditional utensils — they could feel more comfortable eating from a deformable feeding utensil.

## 4.6 Discussion and Conclusion

Assistive robot arms have the potential to improve the lives of adults with mobility limitations. To achieve this potential, we believe that both *algorithmic* and *mechanical* intelligence

are necessary. In this work we therefore collaborated with stakeholders to develop a mechanical utensil specifically for robot-assisted feeding. Our resulting mechanism (which we named Kiri-Spoon) consists of a soft kirigami sheet and a compact 1-DoF linear actuator. At equilibrium, the kirigami sheet is a spoon-like 2D ellipse; but when we extend this sheet, the structure deforms into a 3D bowl that encapsulates food items. We highlight that our design has several attractive features for adoption — the key materials are food safe, inexpensive to manufacture, interchangeable, and washable. Moreover, Kiri-Spoon can be deployed as both a spoon (scooping foods like cereal or soup) and as a fork (pinching foods like carrots or oranges).

To analyze Kiri-Spoon, we developed a mechanics model that relates the amount of applied force to the geometry of the kirigami sheet. This model is challenging because the kirigami sheet consists of multiple deformable ribbons — a boundary ribbon, discrete ribbons, and mesh ribbons. Our theoretical model integrated each of these ribbons to provide a lower bound on the combined interaction. Designers can leverage this model to select the correct material, geometry, and actuation for their own Kiri-Spoon.

Next, we conducted three separate experiments to evaluate how Kiri-Spoon advances robot-assisted feeding. (1) We first compared Kiri-Spoon to traditional forks and spoons in a fully autonomous setting: here the robot arm used a state-of-the-art assistive feeding algorithm to control each utensil and acquire diverse foods. We found that Kiri-Spoon led to higher acquisition rates for small and soft items (e.g., peas, tofu, jello) and similar acquisition rates for larger morsels (e.g., carrots, mac & cheese). (2) In our second experiment we attached Kiri-Spoon to a commercial assistive eating device, and brought the resulting system to a local center for adults with physical disabilities. A caregiver and $N = 4$ participants compared the device with and without Kiri-Spoon; their results suggest that users perceive Kiri-Spoon to be about as comfortable as a traditional spoon, but more effective at acquiring

and transferring foods. (3) To better analyze these results we conducted a follow-up study on users without physical disabilities. For this final study we attached the Kiri-Spoon to a UR5 robot arm, and varied two separate factors: the algorithm the robot used to control the utensil, and the utensil the robot was equipped with. Our results suggest that both algorithm and utensil have an impact on performance. Interestingly, the improvements caused by Kiri-Spoon in efficiently acquiring the foods were larger than the improvements caused by using an autonomous feeding algorithm — indicating the importance of mechanical intelligence. Overall, the combination of both state-of-the-art algorithms and our Kiri-Spoon utensil led to the most effective robot-assisted feeding.

**Limitations** Taken together, our theoretical and experimental results suggest that Kiri-Spoon can meaningfully advance robot-assisted feeding by making the process of acquiring, carrying, and transferring foods more robust. However, we also identified some areas for improvement. Specifically, we found that Kiri-Spoon sometimes failed to grasp foods that had a large, flat geometry (e.g., lettuce). Kiri-Spoon fell short here because it was unable to scoop or pinch the lettuce without the food slipping away — whereas a traditional fork could just skewer this morsel. Inspired by sporks, in our future work we will explore adding soft fork-like tines to Kiri-Spoon to better handle these edge cases. We are also interested in using Kiri-Spoon on more complex plates with multiple different morsels. If the food types are separated on the same plate, then our current approach is sufficient — for instance, in Section 4.4 participants ate from multiple bowls each with different items. But future work should focus on settings where these foods are mixed together — i.e., noodles with meatballs — and the utensil needs to handle this combination.

# Bibliography


[1] Dobot Magician SoftGripper - 3 Fingers. https://www.soft-gripping.shop/en/dobot-magician-softgripper-3-fingers.html.

[2] Franka Emika - Next Generation Robotics. https://www.franka.de/.

[3] Products: Grippers, Camera and Force Torque Sensors - Robotiq. https://robotiq.com/products.

[4] Vahid Alizadehyazdi, Michael Bonthron, and Matthew Spenko. An electrostatic/gecko-inspired adhesives soft robotic gripper. *IEEE Robotics and Automation Letters*, 5(3): 4679–4686, 2020.

[5] Ansys. *Ansys Mechanical*, 2024. https://www.ansys.com/products/structures/ansys-mechanical.

[6] Brenna D Argall. Autonomy in rehabilitation robotics: An intersection. *Annual Review of Control, Robotics, and Autonomous Systems*, 1:441–463, 2018.

[7] Kellar Autumn, Metin Sitti, Yiching A Liang, Anne M Peattie, Wendy R Hansen, Simon Sponberg, Thomas W Kenny, Ronald Fearing, Jacob N Israelachvili, and Robert J Full. Evidence for van der Waals adhesion in gecko setae. *Proceedings of the National Academy of Sciences*, 99(19):12252–12256, 2002.

[8] Edward J Barron III, Ella T Williams, Ravi Tutika, Nathan Lazarus, and Michael D Bartlett. A unified understanding of magnetorheological elastomers for rapid and extreme stiffness tuning. *RSC Applied Polymers*, 2023.

[9] Michael D Bartlett, Andrew B Croll, Daniel R King, Beth M Paret, Duncan J Irschick, and Alfred J Crosby. Looking beyond fibrillar features to scale gecko-like adhesion. *Advanced Materials*, 24(8):1078–1083, 2012.

[10] Michael D Bartlett, Scott W Case, Anthony J Kinloch, and David A Dillard. Peel tests for quantifying adhesion and toughness: A review. *Progress in Materials Science*, 137:101086, 2023.

[11] Suneel Belkhale, Ethan K Gordon, Yuxiao Chen, Siddhartha Srinivasa, Tapomayukh Bhattacharjee, and Dorsa Sadigh. Balancing efficiency and comfort in robot-assisted bite transfer. In *IEEE International Conference on Robotics and Automation*, pages 4757–4763, 2022.

[12] Amisha Bhaskar, Rui Liu, Vishnu D Sharma, Guangyao Shi, and Pratap Tokekar. LAVA: Long-horizon visual action based food acquisition. *arXiv preprint arXiv:2403.12876*, 2024.

[13] Tapomayukh Bhattacharjee, Ethan K Gordon, Rosario Scalise, Maria E Cabrera, Anat Caspi, Maya Cakmak, and Siddhartha S Srinivasa. Is more autonomy always better? Exploring preferences of users with mobility impairments in robot-assisted feeding. In *ACM/IEEE International Conference on Human-Robot Interaction*, pages 181–190, 2020.

[14] Lionel Birglen and Thomas Schlicht. A statistical review of industrial robotic grippers. *Robotics and Computer-Integrated Manufacturing*, 49:88–97, 2018.

[15] Eric Brown, Nicholas Rodenberg, John Amend, Annan Mozeika, Erik Steltz, Mitchell R Zakin, Hod Lipson, and Heinrich M Jaeger. Universal robotic gripper based on the jamming of granular material. *Proceedings of the National Academy of Sciences*, 107 (44):18809–18814, 2010.

[16] Joao Buzzatto, Haodan Jiang, Junbang Liang, Bryan Busby, Angus Lynch, Ricardo V Godoy, Saori Matsunaga, Rintaro Haraguchi, Toshisada Mariyama, Bruce A Macdonald, and Minas Liarokapis. Multi-layer, sensorised kirigami grippers for delicate yet robust robot grasping and single-grasp object identification. *IEEE Access*, 2024.

[17] Vito Cacucciolo, Herbert Shea, and Giuseppe Carbone. Peeling in electroadhesion soft grippers. *Extreme Mechanics Letters*, 50:101529, 2022.

[18] Gerard Canal, Guillem Alenyà, and Carme Torras. Personalization framework for adaptive robotic feeding assistance. In *International Conference on Social Robotics*, pages 22–31, 2016.

[19] Han Chen, JiaQi Zhu, Yu Cao, ZhiSheng Xia, ZhiPing Chai, Han Ding, and ZhiGang Wu. Soft-rigid coupling grippers: Collaboration strategies and integrated fabrication methods. *Science China Technological Sciences*, 2023.

[20] Ryan Coulson, Christopher J Stabile, Kevin T Turner, and Carmel Majidi. Versatile soft robot gripper enabled by stiffness and adhesion tuning via thermoplastic composite. *Soft Robotics*, 9(2):189–200, 2022.

[21] Costantino Creton and Matteo Ciccotti. Fracture and adhesion of soft materials: a review. *Reports on Progress in Physics*, 79(4):046601, 2016.

[22] Andrew B Croll, Nasibeh Hosseini, and Michael D Bartlett. Switchable adhesives for multifunctional interfaces. *Advanced Materials Technologies*, 4(8), 2019.

[23] ELISpoon. *Independent Eating*, 2024. https://elispoon.com/.

[24] Qinyuan Fang, Maria Kyrarini, Danijela Ristic-Durrant, and Axel Gräser. RGB-D camera based 3D human mouth detection and tracking towards robotic feeding assis-

tance. In *Pervasive Technologies Related to Assistive Environments Conference*, pages 391–396, 2018.

[25] Ryan Feng, Youngsun Kim, Gilwoo Lee, Ethan K Gordon, Matt Schmittle, Shivaum Kumar, Tapomayukh Bhattacharjee, and Siddhartha S Srinivasa. Robot-assisted feeding: Generalizing skewering strategies across food items on a plate. In *The International Symposium of Robotics Research*, pages 427–442, 2019.

[26] Kevin C Fleming, Jonathan M Evans, and Darryl S Chutka. Caregiver and clinician shortages in an aging nation. In *Mayo Clinic Proceedings*, volume 78, pages 1026–1040, 2003.

[27] Helen S Foote. Spoons: Past and present. *The Bulletin of the Cleveland Museum of Art*, 21(4):53–63, 1934.

[28] Franka Robotics. *Franka Research 3*, 2024. https://franka.de/products.

[29] A Gafer, D Heymans, Domenico Prattichizzo, and Gionata Salvietti. The quad-spatula gripper: A novel soft-rigid gripper for food handling. In *IEEE International Conference on Soft Robotics*, pages 39–45, 2020.

[30] Daniel Gallenberger, Tapomayukh Bhattacharjee, Youngsun Kim, and Siddhartha S Srinivasa. Transfer depends on acquisition: Analyzing manipulation strategies for robotic feeding. In *ACM/IEEE International Conference on Human-Robot Interaction*, pages 267–276, 2019.

[31] James M Gere and Barry J Goodno. *Mechanics of Materials*. Cengange Learning, 2009.

[32] Paul Glick, Srinivasan A Suresh, Donald Ruffatto, Mark Cutkosky, Michael T Tolley,

and Aaron Parness. A soft robotic gripper with gecko-inspired adhesive. *IEEE Robotics and Automation Letters*, 3(2):903–910, 2018.

[33] Ethan Kroll Gordon, Amal Nanavati, Ramya Challa, Bernie Hao Zhu, Taylor Annette Kessler Faulkner, and Siddhartha Srinivasa. Towards general single-utensil food acquisition with human-informed actions. In *Conference on Robot Learning*, pages 2414–2428, 2023.

[34] Jennifer Grannen, Yilin Wu, Suneel Belkhale, and Dorsa Sadigh. Learning bimanual scooping policies for food acquisition. In *Conference on Robot Learning*, 2022.

[35] Xin-Yu Guo, Wen-Bo Li, Qiu-Hua Gao, Han Yan, Yan-Qiong Fei, and Wen-Ming Zhang. Self-locking mechanism for variable stiffness rigid–soft gripper. *Smart Materials and Structures*, 29(3), 2020.

[36] Nayoung Ha, Ruolin Ye, Ziang Liu, Shubhangi Sinha, and Tapomayukh Bhattacharjee. REPeat: A real2sim2real approach for pre-acquisition of soft food items in robot-assisted feeding. In *IEEE/RSJ International Conference on Intelligent Robots and Systems*, 2024.

[37] Yufei Hao, Shantonu Biswas, Elliot Wright Hawkes, Tianmiao Wang, Mengjia Zhu, Li Wen, and Yon Visell. A multimodal, enveloping soft gripper: Shape conformation, bioinspired adhesion, and expansion-driven suction. *IEEE Transactions on Robotics*, 37(2):350–362, 2020.

[38] Jaime Hernandez, Md Samiul Haque Sunny, Javier Sanjuan, Ivan Rulik, Md Ishrak Islam Zarif, Sheikh Iqbal Ahamed, Helal Uddin Ahmed, and Mohammad H Rahman. Current designs of robotic arm grippers: A comprehensive systematic review. *Robotics*, 12(1):5, 2023.

[39] Qiqiang Hu, Erbao Dong, and Dong Sun. Soft gripper design based on the integration of flat dry adhesive, soft actuator, and microspine. *IEEE Transactions on Robotics*, 37 (4):1065–1080, 2021.

[40] Catrine Jacobsson, Karin Axelsson, Per Olov Österlind, and Astrid Norberg. How people with stroke and healthy older people experience the eating process. *Journal of Clinical Nursing*, 9(2):255–264, 2000.

[41] Anand Jagota and Chung-Yuen Hui. Adhesion, friction, and compliance of bio-mimetic and bio-inspired structured interfaces. *Materials Science and Engineering: R: Reports*, 72(12):253–292, 2011.

[42] Siddarth Jain and Brenna Argall. Probabilistic human intent recognition for shared autonomy in assistive robotics. *ACM Transactions on Human-Robot Interaction*, 9(1): 1–23, 2019.

[43] Shervin Javdani, Henny Admoni, Stefania Pellegrinelli, Siddhartha S Srinivasa, and J Andrew Bagnell. Shared autonomy via hindsight optimization for teleoperation and teaming. *The International Journal of Robotics Research*, 37(7):717–742, 2018.

[44] Rajat Kumar Jenamani, Daniel Stabile, Ziang Liu, Abrar Anwar, Katherine Dimitropoulou, and Tapomayukh Bhattacharjee. Feel the bite: Robot-assisted inside-mouth bite transfer using robust mouth perception and physical interaction-aware control. In *ACM/IEEE International Conference on Human-Robot Interaction*, pages 313–322, 2024.

[45] Rajat Kumar Jenamani, Priya Sundaresan, Maram Sakr, Tapomayukh Bhattacharjee, and Dorsa Sadigh. FLAIR: Feeding via long-horizon acquisition of realistic dishes. *arXiv preprint arXiv:2407.07561*, 2024.

[46] Hong Jun Jeon, Smitha Milli, and Anca Dragan. Reward-rational (implicit) choice: A unifying formalism for reward learning. *Advances in Neural Information Processing Systems*, pages 4415–4426, 2020.

[47] Peiyuan Jiang, Daji Ergu, Fangyao Liu, Ying Cai, and Bo Ma. A review of Yolo algorithm developments. *Procedia Computer Science*, 199:1066–1073, 2022.

[48] Ananth Jonnavittula, Shaunak A Mehta, and Dylan P Losey. SARI: Shared autonomy across repeated interaction. *ACM Transactions on Human-Robot Interaction*, 2024.

[49] Maya Keely, Yeunhee Kim, Shaunak A Mehta, Joshua Hoegerman, Robert Ramirez Sanchez, Emily Paul, Camryn Mills, Dylan P Losey, and Michael D Bartlett. Combining and decoupling rigid and soft grippers to enhance robotic manipulation. *Soft Robotics*, 2024.

[50] Maya N Keely, Heramb Nemlekar, and Dylan P Losey. Kiri-Spoon: A soft shape-changing utensil for robot-assisted feeding. In *IEEE/RSJ International Conference on Intelligent Robots and Systems*, 2024.

[51] Kinova. *Gain Autonomy*, 2024. https://assistive.kinovarobotics.com/.

[52] Chanhong Lee, Huiqi Shi, Jiyoung Jung, Bowen Zheng, Kan Wang, Ravi Tutika, Rong Long, Bruce P Lee, Grace X Gu, and Michael D Bartlett. Bioinspired materials for underwater adhesion with pathways to switchability. *Cell Reports Physical Science*, 4 (10), 2023.

[53] Long Li, Fengming Xie, Tianhong Wang, Guopeng Wang, Yingzhong Tian, Tao Jin, and Quan Zhang. Stiffness-tunable soft gripper with soft-rigid hybrid actuation for versatile manipulations. *Soft Robotics*, 9(6):1108–1119, 2022.

[54] Shuguang Li, John J Stampfli, Helen J Xu, Elian Malkin, Evelin Villegas Diaz, Daniela Rus, and Robert J Wood. A vacuum-driven origami "magic-ball" soft gripper. In *IEEE International Conference on Robotics and Automation*, pages 7401–7408, 2019.

[55] Rui Liu, Zahiruddin Mahammad, Amisha Bhaskar, and Pratap Tokekar. IMRL: Integrating visual, physical, temporal, and geometric representations for enhanced food acquisition. *arXiv preprint arXiv:2409.12092*, 2024.

[56] Sara Ljungblad. Applying "designerly framing" to understand assisted feeding as social aesthetic bodily experiences. *ACM Transactions on Human-Robot Interaction*, 12(2): 1–23, 2023.

[57] Dylan P Losey, Hong Jun Jeon, Mengxi Li, Krishnan Srinivasan, Ajay Mandlekar, Animesh Garg, Jeannette Bohg, and Dorsa Sadigh. Learning latent actions to control assistive robots. *Autonomous Robots*, 46(1):115–147, 2022.

[58] Shaunak A Mehta, Yeunhee Kim, Joshua Hoegerman, Michael D Bartlett, and Dylan P Losey. Riso: Combining rigid grippers with soft switchable adhesives. In *IEEE International Conference on Soft Robotics*, 2023.

[59] Amal Nanavati, Patricia Alves-Oliveira, Tyler Schrenk, Ethan K Gordon, Maya Cakmak, and Siddhartha S Srinivasa. Design principles for robot-assisted feeding in social contexts. In *ACM/IEEE International Conference on Human-Robot Interaction*, pages 24–33, 2023.

[60] Amal Nanavati, Vinitha Ranganeni, and Maya Cakmak. Physically assistive robots: A systematic review of mobile and manipulator robots that physically assist people with disabilities. *Annual Review of Control, Robotics, and Autonomous Systems*, 7, 2023.

[61] Isira Naotunna, Chamika Janith Perera, Chameera Sandaruwan, RARC Gopura, and

Thilina Dulantha Lalitharatne. Meal assistance robots: A review on current status, challenges and future directions. In *IEEE/SICE International Symposium on System Integration*, pages 211–216, 2015.

[62] Amir Mohammadi Nasab, Amin Sabzehzar, Milad Tatari, Carmel Majidi, and Wanliang Shan. A soft gripper with rigidity tunable elastomer strips as ligaments. *Soft robotics*, 4(4):411–420, 2017.

[63] Obi. *Meet Obi: The Adaptive Eating Device - Eat Independently!*, 2024. https://meetobi.com/.

[64] Jan Ondras, Abrar Anwar, Tong Wu, Fanjun Bu, Malte Jung, Jorge Jose Ortiz, and Tapomayukh Bhattacharjee. Human-robot commensality: Bite timing prediction for robot-assisted feeding in groups. In *Conference on Robot Learning*, pages 921–933, 2023.

[65] Akhil Padmanabha, Jessie Yuan, Janavi Gupta, Zulekha Karachiwalla, Carmel Majidi, Henny Admoni, and Zackory Erickson. Voicepilot: Harnessing LLMs as speech interfaces for physically assistive robots. In *ACM Symposium on User Interface Software and Technology*, pages 1–18, 2024.

[66] Daehyung Park, Hokeun Kim, Yuuna Hoshi, Zackory Erickson, Ariel Kapusta, and Charles C Kemp. A multimodal execution monitor with anomaly classification for robot-assisted feeding. In *IEEE/RSJ International Conference on Intelligent Robots and Systems*, pages 5406–5413, 2017.

[67] Wookeun Park, Seongmin Seo, and Joonbum Bae. A hybrid gripper with soft material and rigid structures. *IEEE Robotics and Automation Letters*, 4(1):65–72, 2018.

[68] Max Pascher, Annalies Baumeister, Stefan Schneegass, Barbara Klein, and Jens

Gerken. Recommendations for the development of a robotic drinking and eating aid- an ethnographic study. In *Human-Computer Interaction – INTERACT 2021*, pages 331–351, 2021.

[69] Zhikang Peng, Dongli Liu, Xiaoyun Song, Meihua Wang, Yiwen Rao, Yanjie Guo, and Jun Peng. The enhanced adaptive grasping of a soft robotic gripper using rigid supports. *Applied System Innovation*, 7(1):15, 2024.

[70] Guy N Phillips. Feasibility study for assistive feeder. *Southwest Research Institute*, page 1–130, 1987.

[71] C Piazza, G Grioli, MG Catalano, and Bicchi. A century of robotic hands. *Annual Review of Control, Robotics, and Autonomous Systems*, 2:1–32, 2019.

[72] Daniel J Rea and Stela H Seo. Still not solved: A call for renewed focus on user-centered teleoperation interfaces. *Frontiers in Robotics and AI*, 9:704225, 2022.

[73] Gustavo Alfonso Garcia Ricardez, Jun Takamatsu, Tsukasa Ogasawara, and Jorge Solis Alfaro. Quantitative comfort evaluation of eating assistive devices based on interaction forces estimation using an accelerometer. In *IEEE International Symposium on Robot and Human Interactive Communication*, pages 909–914, 2018.

[74] Nicolas Rojas, Raymond R Ma, and Aaron M Dollar. The GR2 gripper: An underactuated hand for open-loop in-hand planar manipulation. *IEEE Transactions on Robotics*, 32(3):763–770, 2016.

[75] Wilson Ruotolo, Dane Brouwer, and Mark R Cutkosky. From grasping to manipulation with gecko-inspired adhesives on a multifinger gripper. *Science Robotics*, 6(61): eabi9773, 2021.

[76] Lindsay Sanneman, Christopher Fourie, and Julie A Shah. The state of industrial robotics: Emerging technologies, challenges, and key research directions. *Foundations and Trends in Robotics*, 8(3):225–306, 2021.

[77] Mariah L Schrum, Michael Johnson, Muyleng Ghuy, and Matthew C Gombolay. Four years in review: Statistical practices of likert scales in human-robot interaction studies. In *ACM/IEEE International Conference on Human-Robot Interaction*, pages 43–52, 2020.

[78] W Seamone and G Schmeisser. Early clinical evaluation of a robot arm/worktable system for spinal-cord-injured persons. *Journal of Rehabilitation Research and Development*, 22(1):38–57, 1985.

[79] Lorenzo Shaikewitz, Yilin Wu, Suneel Belkhale, Jennifer Grannen, Priya Sundaresan, and Dorsa Sadigh. In-mouth robotic bite transfer with visual and haptic sensing. In *IEEE International Conference on Robotics and Automation*, pages 9885–9895, 2023.

[80] Jun Shintake, Samuel Rosset, Bryan Schubert, Dario Floreano, and Herbert Shea. Versatile soft grippers with intrinsic electroadhesion based on multifunctional polymer actuators. *Advanced Materials*, 28(2):231–238, 2016.

[81] Jun Shintake, Vito Cacucciolo, Dario Floreano, and Herbert Shea. Soft robotic grippers. *Advanced Materials*, 30(29), 2018.

[82] Samantha E Shune. An altered eating experience: Attitudes toward feeding assistance among younger and older adults. *Rehabilitation Nursing Journal*, 45(2):97–105, 2020.

[83] Sukho Song and Metin Sitti. Soft grippers using micro-fibrillar adhesives for transfer printing. *Advanced Materials*, 26(28):4901–4906, 2014.

[84] Sukho Song, Carmel Majidi, and Metin Sitti. Geckogripper: A soft, inflatable robotic gripper using gecko-inspired elastomer micro-fiber adhesives. In *IEEE/RSJ International Conference on Intelligent Robots and Systems*, pages 4624–4629, 2014.

[85] Sukho Song, Dirk-Michael Drotlef, Carmel Majidi, and Metin Sitti. Controllable load sharing for soft adhesive interfaces on three-dimensional surfaces. *Proceedings of the National Academy of Sciences*, 114(22):E4344–E4353, 2017.

[86] Anthony Staros and Edward Peizer. Veterans administration prosthetics center research report. *Bulletin of Prosthetics Research*, 1977.

[87] Priya Sundaresan, Suneel Belkhale, and Dorsa Sadigh. Learning visuo-haptic skewering strategies for robot-assisted feeding. In *Conference on Robot Learning*, pages 332–341, 2023.

[88] Priya Sundaresan, Jiajun Wu, and Dorsa Sadigh. Learning sequential acquisition policies for robot-assisted feeding. In *Conference on Robot Learning*, 2023.

[89] Matthew D Swift, Cole B Haverkamp, Christopher J Stabile, Dohgyu Hwang, Raymond H Plaut, Kevin T Turner, David A Dillard, and Michael D Bartlett. Active membranes on rigidity tunable foundations for programmable, rapidly switchable adhesion. *Advanced Materials Technologies*, 5(11):2000676, 2020.

[90] Yen-Ling Tai, Yu Chien Chiu, Yu-Wei Chao, and Yi-Ting Chen. Scone: A food scooping robot learning framework with active perception. In *Conference on Robot Learning*, pages 849–865, 2023.

[91] Milad Tatari, Amir Mohammadi Nasab, Kevin T Turner, and Wanliang Shan. Dynamically tunable dry adhesion via subsurface stiffness modulation. *Advanced Materials Interfaces*, 5(18):1800321, 2018.

[92] Danielle M Taylor. *Americans With Disabilities: 2014*. US Census Bureau, 2018.

[93] The Virginia Home. *A Rich Tradition of Compassion*, 2024. https://thevirginiahome.org/.

[94] Hongmiao Tian, Xiangming Li, Jinyou Shao, Chao Wang, Yan Wang, Yazhou Tian, and Haoran Liu. Gecko-effect inspired soft gripper with high and switchable adhesion for rough surfaces. *Advanced Materials Interfaces*, 6(18):1900875, 2019.

[95] Stephen P Timoshenko and James M Gere. *Theory of Elastic Stability*. Courier Corporation, 2012.

[96] Mike Topping. An overview of the development of Handy 1, a rehabilitation robot to assist the severely disabled. *Artificial Life and Robotics*, 2000.

[97] Universal Robotics. *UR5e: Lightweight, Versatile Cobot*, 2024. https://www.universal-robots.com/products/ur5e/.

[98] Kirstin van Dam, Marieke Gielissen, Ruth Bles, Agnes van der Poel, and Brigitte Boon. The impact of assistive living technology on perceived independence of people with a physical disability in executing daily activities: A systematic literature review. *Disability and Rehabilitation: Assistive Technology*, 19(4):1262–1271, 2024.

[99] Sasha Wald, Kavya Puthuveetil, and Zackory Erickson. Do mistakes matter? Comparing trust responses of different age groups to errors made by physically assistive robots. In *IEEE International Conference on Robot and Human Interactive Communication*, pages 373–380, 2024.

[100] Guangchao Wan, Yanbing Tang, Kevin T Turner, Teng Zhang, and Wanliang Shan. Tunable dry adhesion of soft hollow pillars through sidewall buckling under low pressure. *Advanced Functional Materials*, 33(2):2209905, 2023.

[101] Zhongkui Wang, Yuuki Torigoe, and Shinichi Hirai. A prestressed soft gripper: Design, modeling, fabrication, and tests for food handling. *IEEE Robotics and Automation Letters*, 2(4):1909–1916, 2017.

[102] Zhongkui Wang, Shinichi Hirai, and Sadao Kawamura. Challenges and opportunities in robotic food handling: A review. *Frontiers in Robotics and AI*, 8:789107, 2022.

[103] Hayden Webb, Podshara Chanrungmaneekul, Shenli Yuan, and Kaiyu Hang. Wearable roller rings to enable robot dexterous in-hand manipulation through active surfaces. *arXiv preprint arXiv:2403.13132*, 2024.

[104] Ying Wei, Yonghua Chen, Tao Ren, Qiao Chen, Changxin Yan, Yang Yang, and Yingtian Li. A novel, variable stiffness robotic gripper based on integrated soft actuating and particle jamming. *Soft Robotics*, 3(3):134–143, 2016.

[105] Yi Yang, Katherine Vella, and Douglas P Holmes. Grasping with kirigami shells. *Science Robotics*, 6(54):eabd6426, 2021.

[106] Rachel Zenker, Connor Pardell, Andrea Gilmore-Bykovskyi, Amy JH Kind, and Nicole Werner. Exploring workload among informal caregivers of persons with dementia. In *Proceedings of the Human Factors and Ergonomics Society Annual Meeting*, volume 61, pages 1297–1297, 2017.

[107] Baohua Zhang, Yuanxin Xie, Jun Zhou, Kai Wang, and Zhen Zhang. State-of-the-art robotic grippers, grasping and control strategies, as well as their applications in agricultural robots: A review. *Computers and Electronics in Agriculture*, 177:105694, 2020.

# Appendices

# Appendix A

# RISO Supplementary Material

## Combining and Decoupling Rigid and Soft Grippers to Enhance Robotic Manipulation

Maya Keely[†,1], Yeunhee Kim[†,2], Shaunak A. Mehta[1], Joshua Hoegerman[1], Robert Ramirez Sanchez[1], Emily Paul[1], Camryn Mills[2], Dylan P. Losey[*,1], and Michael D. Bartlett[*,2,3]

[1]Department of Mechanical Engineering, Collaborative Robotics Lab, Virginia Tech, Blacksburg, VA 24061, USA
[2]Department of Mechanical Engineering, Soft Materials and Structures Lab, Virginia Tech, Blacksburg, VA 24061, USA
[3]Macromolecules Innovation Institute, Virginia Tech, Blacksburg, VA 24061, USA.

[†]These authors contributed equally to this work
[*]To whom correspondence should be addressed: losey@vt.edu, mbartlett@vt.edu

Table S9. Grasping success rates with RISO and other state-of-the-art grippers.

Table S10. Questionnaire items and user responses with shared autonomy.

Table S11. Grasping success rates with human control and shared autonomy.

Movie S12. Summary video that visualizes the methods and experiments from the paper.

Site S13. Link to an online repository with the code for controlling RISOs.

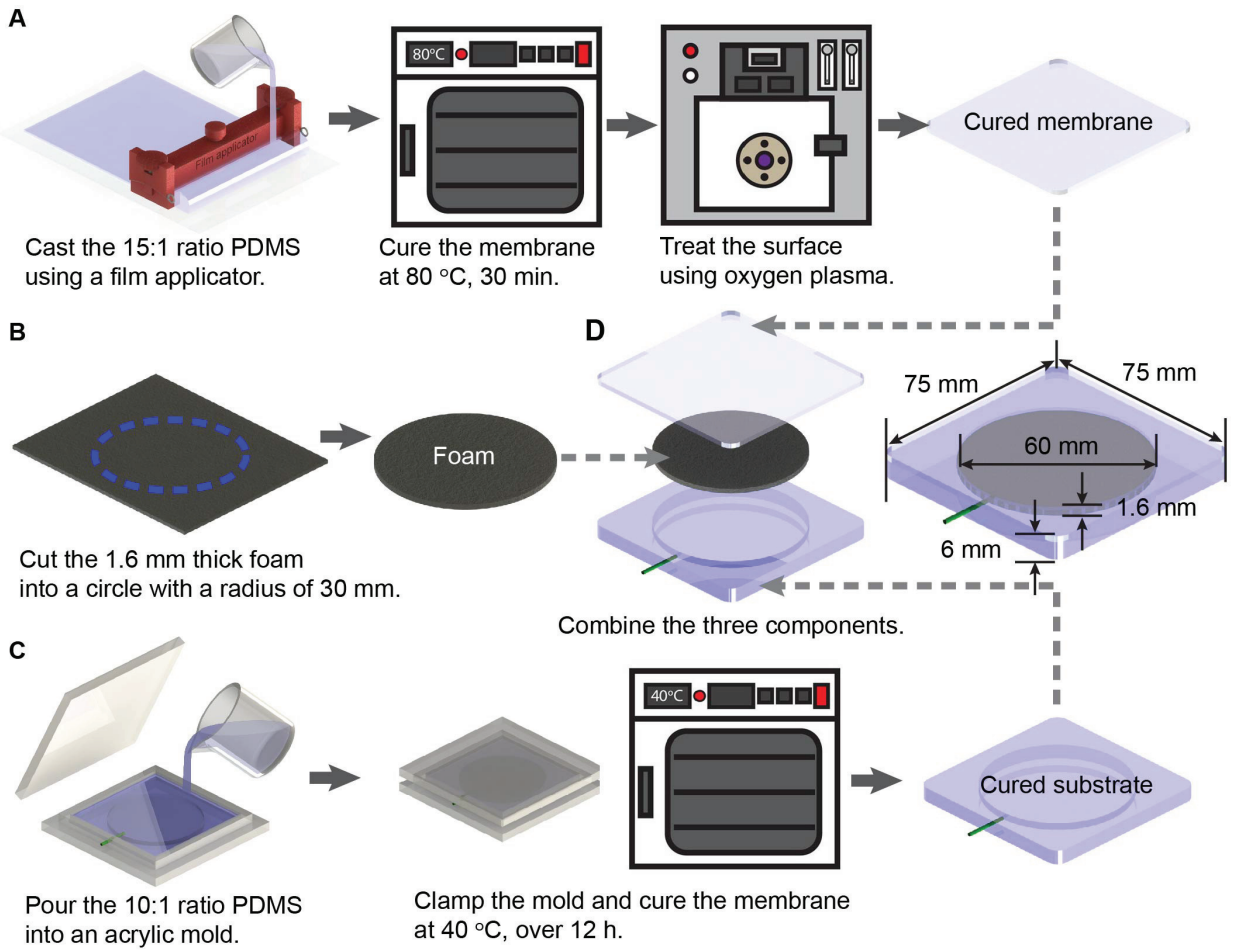


Figure S1: Figure S1: **Fabrication flow for the soft adhesive.** Fabrication process for the (**A**) membrane, (**B**) foam, (**C**) underlying substrate, and (**D**) integrated soft adhesive. The soft switchable adhesive has three subcomponents: a soft elastomeric Polydimethylsiloxane membrane (PDMS, Sylgard 184, Dow), 1.6 mm polyurethane foam foundation (Poron Very Soft 20 pcf Microcellular Polyurethane, Rogers Corporation), and an underlying PDMS substrate (PDMS, Sylgard 184, Dow).

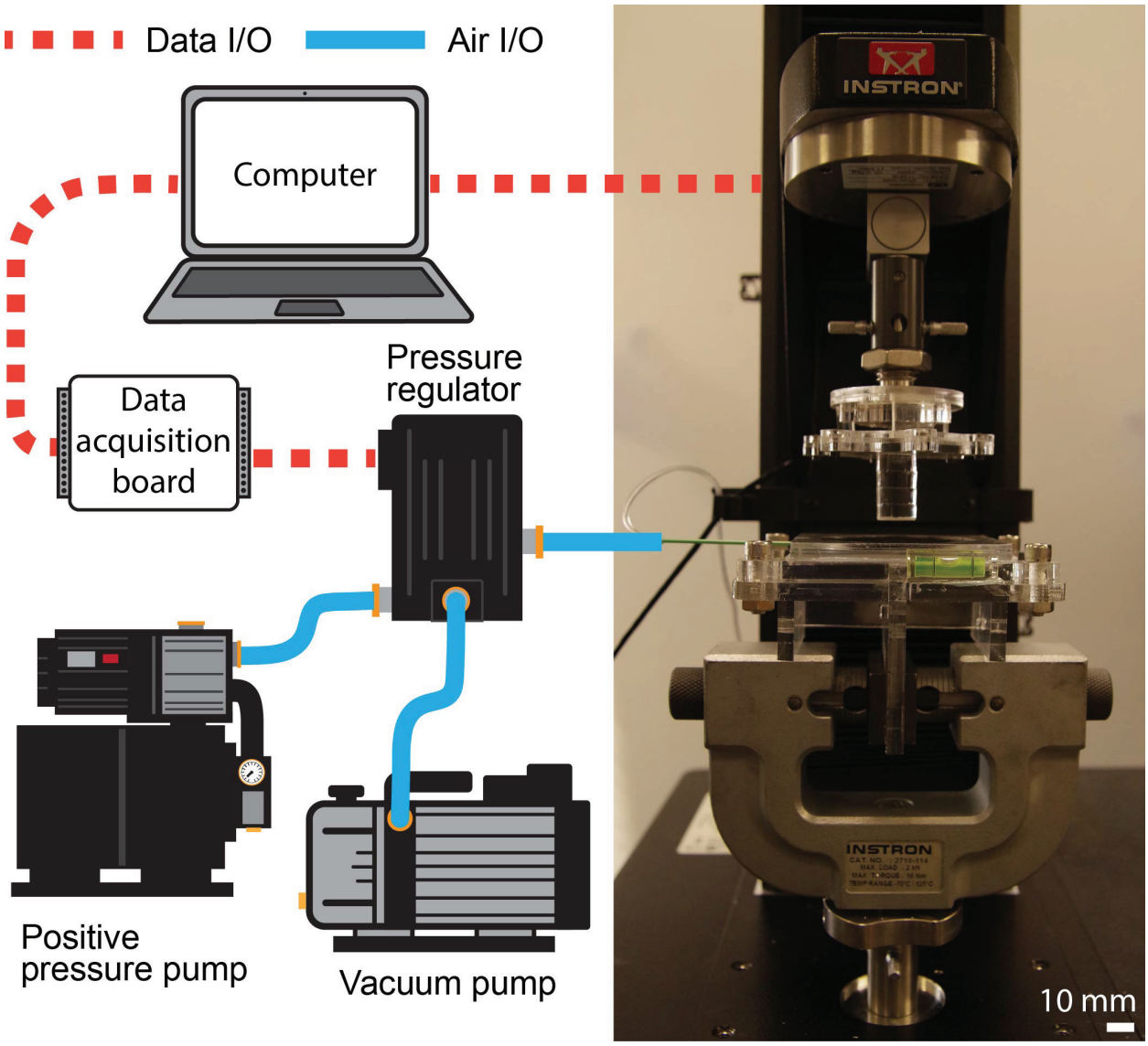


Figure S2: Figure S2: **Experimental setup for adhesion characterization.** The indentation experiment utilizes a pressure regulator to control the positive (1.5 kPa), neutral, or negative pneumatic pressure (-85 kPa) which is synchronized to the mechanical testing machine through a data acquisition board controlled by a computer. Tests are performed by displacing the sample until a preload of 25 kPa is reached, the preload is held for 5 seconds, and then the sample is retracted with a detachment speed of 10 mm/min. All substrates in Figures 3.1 and 3.2 are acrylic and are manufactured by laser cutting. Indenters with different curvatures in Figure 3.2A are cut from a hemispherical acrylic structure with a radius of 7.5 mm, and the indenters with different line distances are engraved with a power and speed of 30% (PLS 6150, Universal Laser Systems).

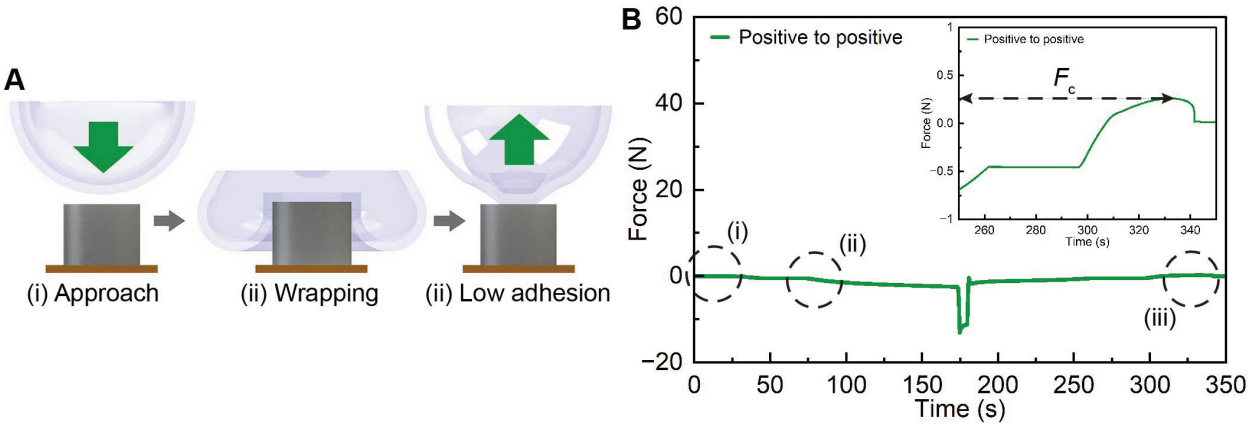


Figure S3: Figure S3: **Release mechanism of the soft adhesive.** (**A**) Schematics showing the approach, wrapping, and low adhesion state using an inflated membrane. (**B**) Force vs time plot from an indentation experiment where the inset shows the point where $F_c$ is measured.

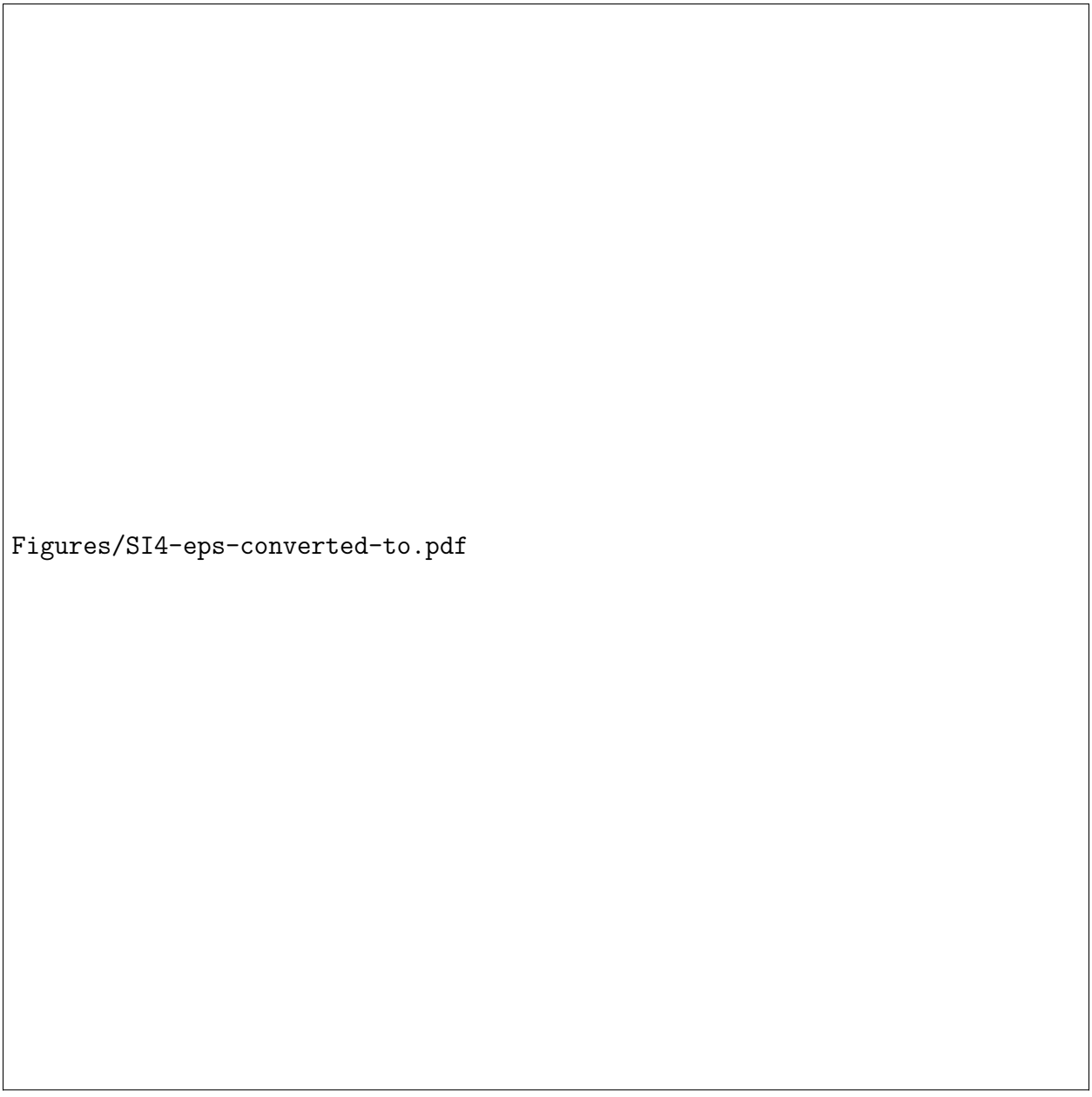


Figure S4: Figure S4: **Adhesion testing procedure.** (**A**) Images and schematics showing a sequence of the adhesion testing procedure of the neutral to negative condition and the (**B**) positive to negative condition. The scale bar is 10 mm.


Figure S5: Figure S5: **Comparison of grippers and the dataset of objects. (A)** The SoftGripper [1], the granular jamming gripper [15], and our RISO Gripper. **(B)** The 15 objects used in our experiments from Section 3.2.3 and Section 3.2.4. For both images, a marker indicates the relative size of the items.


Figure S6: Figure S6: RISO gripper grasping and releasing a 2 mg object (a piece of pencil lead). The lead is highlighted in orange. To grasp the lead we actuate the soft adhesive with a negative pressure, and to release the lead on command we apply a positive pressure.

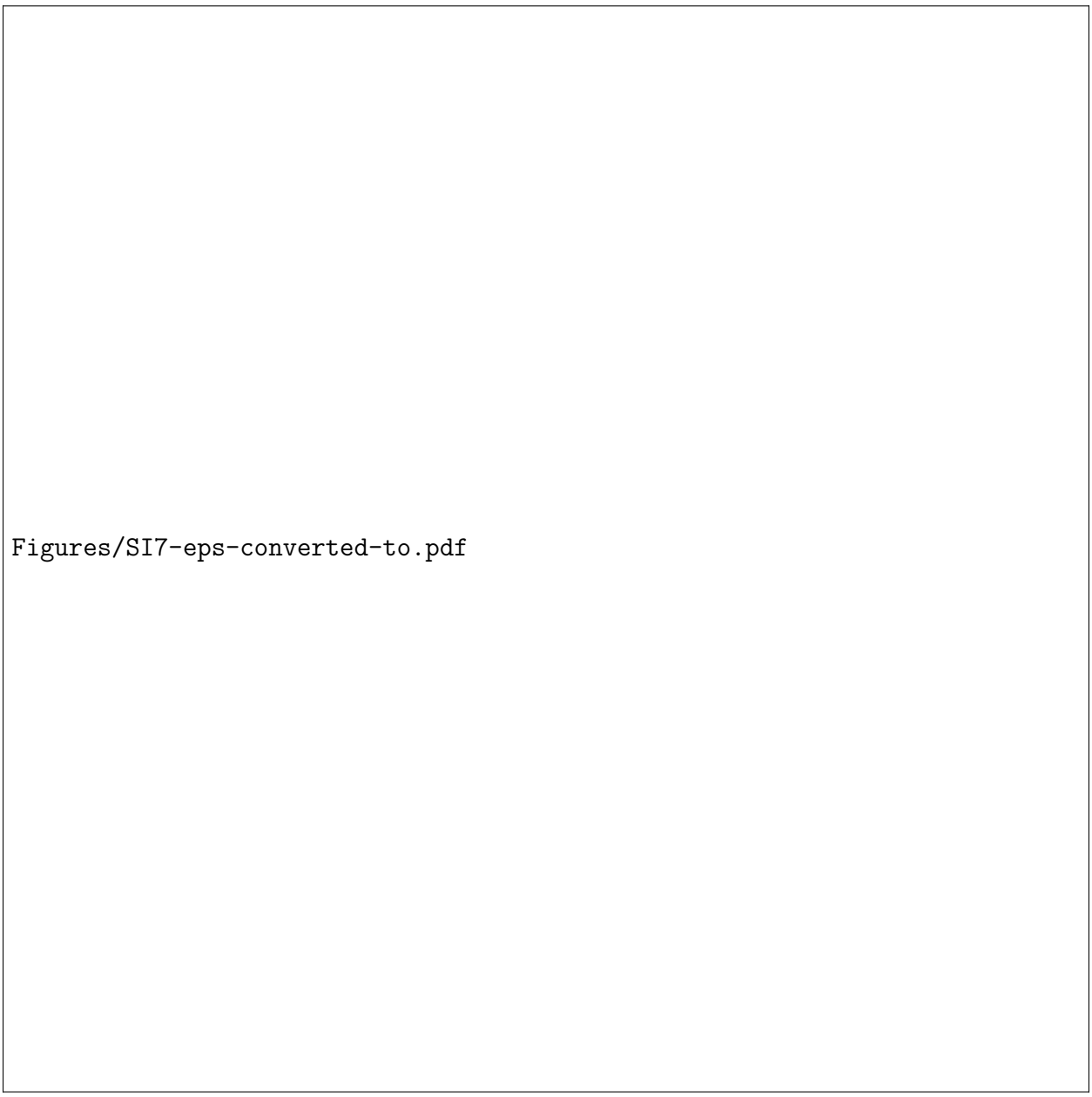


Figure S7: Figure S7: A RISO gripper lifting and controllably releasing a 2.9 kg bottle of cooking oil with the soft adhesive mounted on a robot.

Table S8: **Questionnaire items and responses from our Likert scale survey comparing each type of gripper**. In Section 3.2.3 participants teleoperated the SoftGripper, the granular jamming gripper, and RISO to pickup a dataset of items. We used this survey to assess the user's subjective response to each different gripper. (Left) The questionnaire items listed below explore whether the robot picked up all the objects, whether it was easy to control the gripper, if the user could predict a successful grasp, and if they would prefer to use this gripper again in the future. (Right) After collecting all the responses, we first confirmed that the participants' answers to these questions were consistent using Cronbach's $\alpha$ (reliability $> 0.7$). We then used post-hoc analysis to see if the scores for RISO were higher than the scores for the SoftGripper or Granular gripper. Here a $p$-value of less than 0.05 indicates that the participants scored RISO more highly (e.g., better at picking up objects), and that these differences in scores were statistically significant.

| 2***Questionnaire Item** | 2***Reliability** | 2***F(2, 22)** | **p-value** | |
|---|---|---|---|---|
| | | | SoftGripper | Granular |
| The gripper picked up all the objects I wanted.<br>The gripper did not do a good job of picking up objects. | 2*0.859 | 2*33.754 | 2*p <0.05* | 2*p <0.05* |
| I found it easy and intuitive to control the gripper.<br>I had trouble controlling the gripper to do what I wanted. | 2*0.809 | 2*8.075 | 2*0.482 | 2*p <0.05* |
| I could easily predict whether the gripper would pick up an object.<br>It was hard to guess if the gripper would pick up or drop an object. | 2*0.896 | 2*8.052 | 2*p <0.05* | 2*p <0.05* |
| If I had to use this robot, I would like to use this gripper again.<br>I would not want to use this gripper in the future. | 2*0.967 | 2*18.395 | 2*p <0.05* | 2*p <0.05* |

Table S9: **Grasping success rate per object with RISO and other state-of-the-art grippers.** In a successful grasp the robot picks up, carries, and then releases the object(s). The success percentage is reported for three grippers: SoftGripper [1], granular jamming gripper [15], and our RISO (see Section 3.2.3). In autonomous control the robot arm and gripper perform the task without a human-in-the-loop. By contrast, in human control a participant teleoperated the robot and gripper without autonomous assistance. We observe that the robot and human were able to successfully pick up and manipulate more objects with RISO as compared to the SoftGripper or granular jamming gripper.

| 3*Objects | Autonomous Control | | | Human Control | | |
|---|---|---|---|---|---|---|
| | **SoftGripper** Success [%] | **Granular** Success [%] | **RISO** Success [%] | **SoftGripper** Success [%] | **Granular** Success [%] | **RISO** Success [%] |
| Glue | 50.00% | 0.00% | 100.00% | 25.00% | 41.67% | 100.00% |
| Lego Tower | 90.00% | 100.00% | 100.00% | 91.67% | 83.33% | 100.00% |
| Syrup Bottle | 100.00% | 20.00% | 100.00% | 100.00% | 16.67% | 83.33% |
| Bearings | 3.75% | 0.00% | 97.50% | 9.79% | 0.00% | 89.58% |
| Cup | 100.00% | 100.00% | 100.00% | 100.00% | 100.00% | 75.00% |
| Dice | 80.00% | 95.00% | 100.00% | 100.00% | 66.67% | 100.00% |
| Fidget Spinner | 90.00% | 100.00% | 100.00% | 66.67% | 91.67% | 100.00% |
| Fruit Snacks | 90.00% | 0.00% | 100.00% | 75.00% | 8.33% | 100.00% |
| Hemisphere | 100.00% | 100.00% | 100.00% | 100.00% | 100.00% | 100.00% |
| Nuts | 75.00% | 95.00% | 90.00% | 95.83% | 54.17% | 79.17% |
| Paper Plate | 10.00% | 0.00% | 90.00% | 66.67% | 8.33% | 75.00% |
| Quarter | 20.00% | 30.00% | 100.00% | 0.00% | 0.00% | 75.00% |
| Screws | 10.00% | 0.00% | 25.00% | 8.33% | 0.00% | 58.33% |
| Skittles | 30.00% | 22.50% | 95.00% | 31.25% | 8.33% | 97.92% |
| Weight | 0.00% | 100.00% | 100.00% | 0.00% | 33.33% | 91.67% |

Table S10: **Questionnaire items and responses from the Likert scale survey with shared autonomy**. In Section 3.2.4 participants teleoperated a robot and attached RISO to manipulate 15 household items. They either controlled the robot directly (using human control) or with some assistance (shared autonomy). After completing the manipulation task with each control strategy the participants answered the following questions. (Left) The questionnaire items explored whether the robot helped users to complete the task, if it was intuitive to control the robot and the RISO gripper, if the robot recognized the user's intent, if it was easy to leverage the RISO, and if the participants preferred using that control approach. (Right) To analyze these results we first grouped the items into five scales and tested their reliability using Cronbach's $\alpha$. If the responses were reliable (i.e., if $\alpha > 0.7$) then we proceeded to use paired t-tests to compare the means. The $p$-values indicate if the users preferred shared autonomy over human control, and an $*$ denotes statistical significance. Participants perceived the RISO with shared autonomy as more helpful, better at recognizing their intent, easier to use, and preferable to the alternative. The participants responses to questions about intuitiveness were not consistent (i.e., not reliable enough to analyze).

| **Questionnaire Item** | **Reliability** | **t(11)** | **p-value** |
|---|---|---|---|
| The robot helped me to pick up objects.<br>The robot did not help me do the task. | 2*0.943 | 2*-3.115 | 2*p <0.05* |
| I found it intuitive to control the robot arm and gripper.<br>I was not sure how the robot would respond to my inputs. | 2*-0.401 | 2*- | 2*- |
| The robot recognized what I was trying to do.<br>The robot did not seem to learn my intent. | 2*0.904 | 2*-3.872 | 2*p <0.05* |
| This control mode made it easy to use the gripper.<br>It was hard to use the gripper the way I wanted. | 2*0.878 | 2*-3.83 | 2*p <0.05* |
| I preferred controlling the robot and gripper using this mode. | - | -2.681 | p <0.05* |

Table S11: **Grasping success rate per object with human control and shared autonomy.** In Section 3.2.4 we compared how effectively participants were able to utilize RISO with human control and shared autonomy. Below we report the grasping success percentage per each object across all 12 participants. Users were instructed to grasp the glue, Lego tower, and syrup bottle with RISO's rigid gripper, and participants used RISO's soft adhesive to grasp the remaining objects. We found that users had a similar success rate when working with human control and shared autonomy.

| 2*Objects | Human Success [%] | Shared Success [%] |
|---|---|---|
| Glue | 100.00% | 100.00% |
| Lego Tower | 100.00% | 100.00% |
| Syrup Bottle | 100.00% | 100.00% |
| Bearings | 91.67% | 93.75% |
| Cup | 75.00% | 58.33% |
| Dice | 91.67% | 100.00% |
| Fidget Spinner | 75.00% | 83.33% |
| Fruit Snacks | 100.00% | 100.00% |
| Hemisphere | 100.00% | 100.00% |
| Nuts | 100.00% | 91.67% |
| Paper Plate | 75.00% | 75.00% |
| Quarter | 50.00% | 66.67% |
| Screws | 58.33% | 70.83% |
| Skittles | 87.50% | 87.50% |
| Weight | 100.00% | 100.00% |

**SM12:** [Attached] Summary video that visualizes the methods and experiments from the paper. This same video is available online at: https://youtu.be/du085R0gPFI

**SM13:** Link to an online repository with the code for a robot arm and attached RISO. This includes the parameters used in autonomous control, human control, and our shared autonomy method:
https://github.com/VT-Collab/RISO_Gripper

# Appendix B

# Kiri-Spoon Appendix

### B.0.1 Simulation of Boundary Deformation

In Section 4.2 we propose a theoretical model for tensile force required to actuate the kirigami structure of Kiri-Spoon. One component of this tensile force is the force required to bend the *boundary* of the kirigami sheet. We compute this force, $F_{bend}$, using 4.2 based on the bending theory of circular rings. In order to apply this theory we assume that the radius of curvature of the boundary ring is equal to the initial radius $r$ of the kirigami sheet at its equilibrium.

As the boundary deforms into an ellipse, however, its radius of curvature changes. In particular, the radius of curvature decreases at the ends of the major axis along which we apply the tensile force. Based on 4.2 we know that the $F_{bend}$ is inversely proportional to the radius of curvature. Therefore, the actual force required to bend the elliptical boundary should be higher than the force computed using the initial radius of the circular kirigami sheet $r$. In other words, our theoretic model provides a lower bound on the actual bending force. Here we present physics simulation results to validate this claim.

We simulate the bending of a circular ring in ANSYS Mechanical [5], a finite element analysis software for structural deformations. A visualization of this simulation is shown in Figure S1. For our testing we use a 3D model of a ring with the same material properties and dimensions as kirigami sheet A in Table 4.1. We define one end of the circular ring as a fixed support,

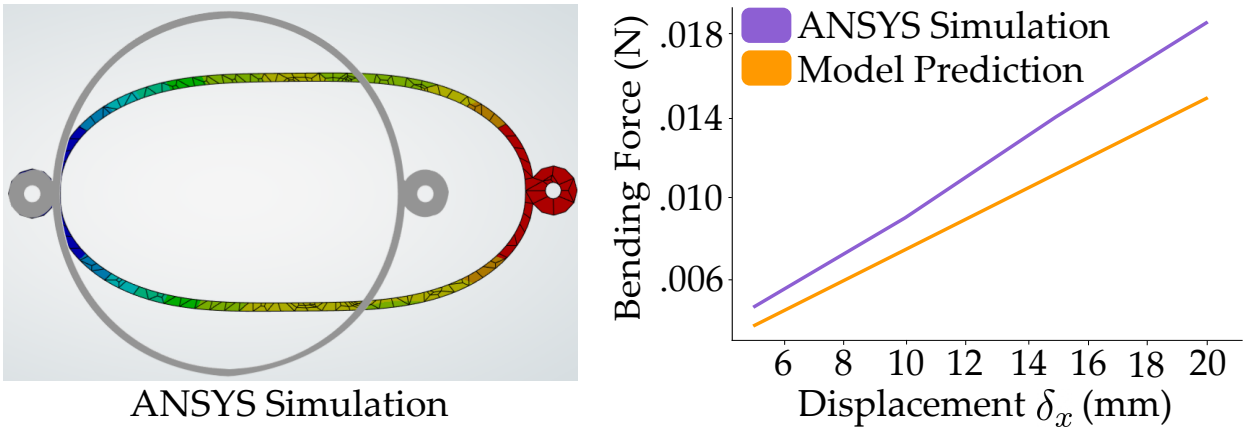


Figure S1: Physics simulation in support of 4.2. (Left) ANSYS simulation environment. The initial circular boundary is shown in grey, while the colored ellipse depicts the deformed elliptical boundary for a displacement of 20 millimeters. (Right) Simulation results showing that the force predicted by our model in 4.2 is a lower bound on the actual tensile force required to bend the boundary ribbon.

and apply an incremental tensile load on the opposite end. As the ring deforms, we measure the displacement along the major axis. We then compare the force applied in simulation to the force computed by our model using 4.2. Our results are shown in Figure S1, Right. From this test we find that the force required to deform the boundary in simulation is higher than the force estimated by our model; this result aligns with our claim that $F_{bend}$ is a *lower bound* on the bending force.

### B.0.2 Derivation for Discrete Ribbons Bending

When the kirigami sheet is actuated, the boundary bends and pushes on the enclosed discrete ribbons. These discrete ribbons oppose the deformation of the boundary, and so we must apply an additional tensile force $F_{discrete}$ to overcome their resistance. In Section 4.2.2 we outlined our derivation for $F_{discrete}$. Here we provide additional details and analysis for computing this tensile force.

We will first compute the tensile force needed to overcome a single discrete ribbon. Consider

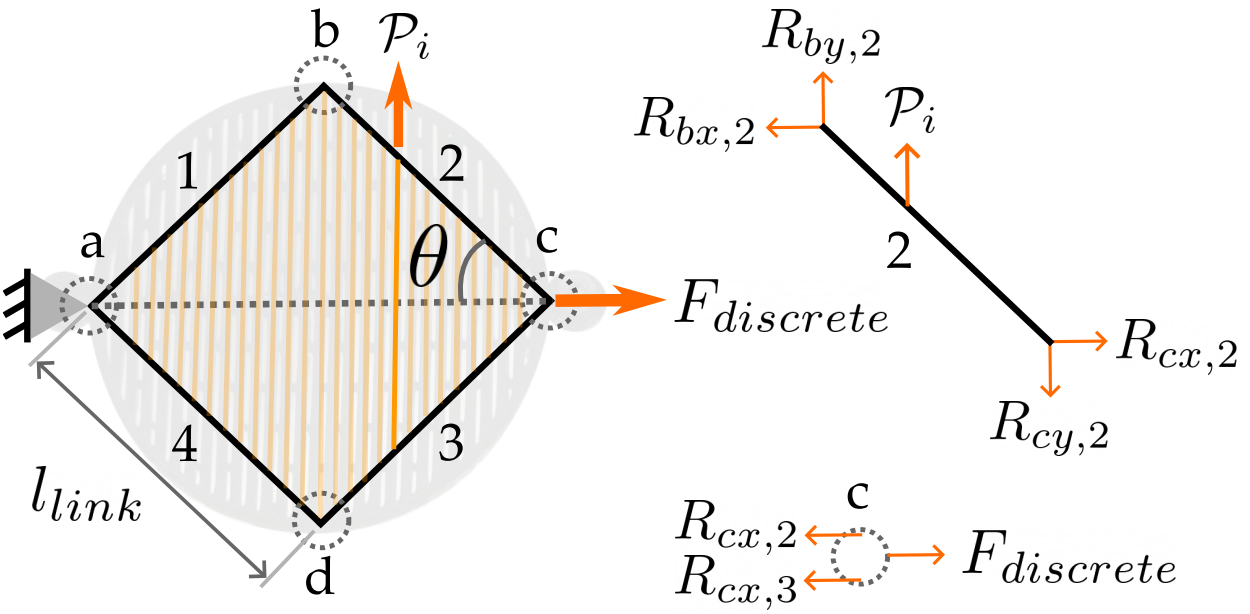


Figure S2: Finding the resistance force caused by the discrete ribbons. (Left) Four-bar linkage model. Joints $a$ and $c$ specify the ends of the major axis of the elliptical boundary layer, while joints $b$ and $d$ specify its minor axis. The joints are connected by rigid links 1, 2, 3 and 4. When joint $c$ is pulled along the major axis by a tensile force $F_{discrete}$, the links bring joints $b$ and $c$ closer, reducing the width of the boundary along the minor axis. This deforms the discrete ribbons which exert an opposing force $\mathcal{P}$ on the links. (Right) Free body diagrams of link 2 and joint $c$.

a kirigami sheet with $n_d$ discrete ribbons and let $\mathcal{P}_i$ be the opposing force exerted by the $i$-th discrete ribbon. We start by modeling the boundary as a four-bar linkage where joints $a$ and $c$ align with the ends of the major axis of the elliptical boundary, and joints $b$ and $d$ mark its minor axis (see Figure S2). As such, half of the discrete ribbons are to the left of joints $b$ and $d$, and the other half are to their right. The joints are sequentially connected by rigid links of length $l_{link}$. As shown in Figure S2, $F_{discrete}$ is applied at joint $c$ by keeping the position of joint $a$ fixed, while the opposing forces from the discrete ribbons act on the links between these joints.

Let the $i$-th discrete ribbon apply a force $\mathcal{P}_i$ on link 2. This force results in a clockwise

moment $M_{i,2}$ at joint $c$:

$$M_{i,2} = \mathcal{P}_i \cdot l_{link} \left( \frac{i}{\lfloor n_d/2 \rfloor + 1} \right) \cos\theta \tag{B.1}$$

Here $l_{link}\,(i/\lfloor n_d/2 \rfloor + 1)$ is the distance between joint $c$ and the point at which the force $\mathcal{P}_i$ acts on the link, and $\theta$ is the angle formed by the link with the tensile force direction.

B.1 calculates the moment due to a single discrete ribbon on link 2. To obtain the moment due to all discrete ribbons that act on link 2 we can compute their sum:

$$M_2 = \sum_{i=1}^{\lceil n_d/2 \rceil} \mathcal{P}_i \cdot l_{link} \left( \frac{i}{\lfloor n_d/2 \rfloor + 1} \right) \cos\theta \tag{B.2}$$

Next, we need to establish how this moment relates to the tensile force $F_{discrete}$. The combined moment $M_2$ is counteracted by the moment due to the reaction forces $R_{bx,2}$ and $R_{by,2}$ at the ends of the link. From Figure S2 we see that $R_{bx,2} = R_{cx,2}$, while $R_{by,2}$ can be computed by balancing the forces across all links. In this case $R_{by,2} = 0$. Therefore, the moment due to all discrete ribbons on link 2 is equal and opposite to the moment due to $R_{bx,2}$, yielding:

$$M_2 = R_{bx,2} \cdot l \sin\theta = R_{cx,2} \cdot l \sin\theta \tag{B.3}$$

We can now connect $R_{cx,2}$ to $F_{discrete}$ by balancing the forces at joint $c$. Joint $c$ is connected to two links, 2 and 3. Therefore, the tensile force applied at joint $c$ is equal to the sum of the reaction forces due to both the links: $F_{discrete} = R_{cx,2} + R_{cx,3}$. But because our four-bar linkage model is symmetric, $R_{cx,2} = R_{cx,3}$ and so:

$$F_{discrete} = 2R_{cx,2} \tag{B.4}$$

In summary, by combining the Equations (B.2), (B.3), and (B.4), we obtain the additional

tensile force due to the discrete ribbons. This result is 4.9 in Section 4.2.2.